HYDROGEOLOGICAL INVESTIGATION AND CHARACTERIZATION OF ALPU SECTOR-A COAL FIELD IN ESKISEHIR-TURKEY

A THESIS SUBMITTED TO
THE GRADUATE SCHOOL OF NATURAL AND APPLIED SCIENCES
OF
MIDDLE EAST TECHNICAL UNIVERSITY

BY

TEVFİK KAAN DÜZ

IN PARTIAL FULFILLMENT OF THE REQUIREMENTS
FOR
THE DEGREE OF MASTER OF SCIENCE
IN
GEOLOGICAL ENGINEERING

JULY 2018

Approval of the thesis:

HYDROGEOLOGICAL INVESTIGATION AND CHARACTERIZATION OF ALPU SECTOR-A COAL FIELD IN ESKISEHIR TURKEY

submitted by **TEVFİK KAAN DÜZ** in partial fulfillment of the requirements for the degree of **Master of Science in Geological Engineering Department, Middle East Technical University** by,

Prof. Dr. Halil Kalıpçılar
Dean, Graduate School of **Natural and Applied Science** ____________________

Prof. Dr. Erdin Bozkurt
Head of Department, **Geological Engineering** ____________________

Prof. Dr. Hasan Yazıcıgil
Supervisor, **Geological Engineering Dept., METU** ____________________

Examining Committee Members:

Prof. Dr. Mehmet Ekmekçi
Hydrogeological Engineering Dept., Hacettepe University ____________________

Prof. Dr. Hasan Yazıcıgil
Geological Engineering Dept., METU ____________________

Prof. Dr. M. Zeki Çamur
Geological Engineering Dept., METU ____________________

Assoc.Prof. Dr. Koray K. Yılmaz
Geological Engineering Dept., METU ____________________

Assoc. Prof. Dr. Özlem Yağbasan
Department of Geography Education, Gazi University ____________________

Date: 12.07.2018

I hereby declare that all information in this document has been obtained and presented in accordance with academic rules and ethical conduct. I also declare that, as required by these rules and conduct, I have fully cited and referenced all material and results that are not original to this work.

Name, Last Name: Tevfik Kaan DÜZ

Signature:

ABSTRACT

HYDROGEOLOGICAL INVESTIGATION AND CHARACTERIZATION OF ALPU SECTOR-A COAL FIELD IN ESKISEHIR-TURKEY

DÜZ, Tevfik Kaan
M.S., Department of Geological Engineering
Supervisor: Prof. Dr. Hasan YAZICIGİL
July 2018, 147 pages

The purpose of the study is to investigate and characterize the hydrogeological conditions at the Alpu Sector-A Coal Field which is located in the Eskisehir Province in Turkey. This is required to provide baseline hydrogeological information before environmental impact assessment of the planned mining operations can be done. The characterization studies included hydrogeological and hydrochemical analysis of groundwater and surface water. The spatial and temporal variations in groundwater levels are determined by measuring the groundwater levels in drilled observation and pumping wells and analyzing the pore pressure from the vibrating wire piezometers installed in different depths. The hydraulic parameters of the groundwater system are estimated by conducting aquifer tests in drilled pumping wells. The hydrochemical characteristics of the waters are based upon measured field water quality parameters and chemical analyses of the samples taken at periodic intervals from both surface and groundwater. The most prolific aquifer in the Sector-A is the alluvium aquifer which interacts with the Porsuk Stream. There is a vertical upward hydraulic gradient with excessive pore pressure beneath the coal seams. None of the waters in the study area are suitable for drinking and irrigation purposes.

Key Words: Alpu Sector-A Coal Field, Hydrogeological Characterization, Aquifer Tests, Vibrating Wire Piezometers, Hydrochemistry

ÖZ

ALPU A-SEKTÖRÜ KÖMÜR SAHASININ HİDROJEOLOJİK ETÜDÜ VE KARAKTERİZASYONU

Düz, Tevfik Kaan
Yüksek Lisans, Jeoloji Mühendisliği Bölümü
Tez Yöneticisi: Prof. Dr. Hasan YAZICIGİL
Temmuz 2018, 147 sayfa

Bu çalışma Türkiye'nin Eskişehir ilinde yer alan Alpu A-Sektörü Kömür Sahasının hidrojeolojik karakterizasyonunu ortaya koymayı amaçlamaktadır. Gerçekleştirilen çalışma, planlanan madencilik faaliyetleri için gereken Çevresel Etki Değerlendirme raporlarının hazırlanması için gerekli hidrojeolojik bilgilerin temelini oluşturmaktadır. Yapılan karakterizasyon çalışmaları bölgenin yüzey ve yeraltı sularının hidrojeolojik ve hidrokimyasal analizlerini içermektedir. Yeraltı su seviye değerlerindeki zamansal ve konumsal değişimler mevcut pompaj ve gözlem kuyularından yapılan ölçümlerle ve farklı derinliklere yerleştirilmiş titreşen tel piyezometrelerinin gözenek suyu basınç verilerinin analiz edilmesiyle belirlenmiştir. Yeraltısuyu sisteminin hidrolik parametre değerleri açılan pompaj kuyularında gerçekleştirilen akifer testleri ile saptanmıştır. Suların hidrokimyasal karakteristikleri sahada gerçekleştirilen su kalite parametre ölçümleri, yüzey ve yeraltı sularından periyodik olarak alınan örneklerin kimyasal analizlerinin yaptırılmasıyla belirlenmiştir. A-Sektöründeki en verimli akifer, Porsuk Çayı ile etkileşime giren alüvyon akiferidir. Kömür bantlarının altında yüksek gözenek basıncına sahip dikey yukarı yönlü hidrolik eğim vardır. Çalışma alanındaki suların hiçbiri içme ve sulama amacı için uygun değildir..

Anahtar Kelimeler: Alpu A-Sektörü Kömür Sahası, Hidrojeolojik Karakterizasyon, Akifer Testleri, Titreşen Tel Piyezometreleri, Hidrokimya

TO MY BELOVED FAMILY AND TEAMMATES...

ACKNOWLEDGEMENT

The author is grateful to the supervisor, Prof. Dr. Hasan Yazıcıgil, for giving an opportunity to work under his guidance. His theoretical support, guidance, criticism, trust and encouragement have continued at all stages of this study.

The author also would like to thank Prof. Dr. F. Bora Rojay, Prof. Dr. M. Zeki Çamur and Assoc. Prof. Dr. Koray K. Yılmaz for their valuable contributions to the project "Hydrogeological Investigation and Characterization of Alpu A-Sector Coal Field". Also, most sincere gratitude and appreciation are expressed to each manager and employee of Esan Eczacıbaşı Industrial Raw Materials Inc. (ESAN) and AECOM individually for their trust and support.

This master thesis had been conducted as part of the METU project no: 2016-03-09-2-00-15, entitled "Hydrogeological Investigation and Characterization of Alpu A-Sector Coal Field" supported by Esan Eczacıbaşı Industrial Raw Materials Inc.. Therefore, the support provided by Esan Eczacıbaşı Industrial Raw Materials Inc. is greatly appreciated.

The author would also like to wish deepest thanks to his colleagues and friends; Yusuf Can Güney, Nuri Erhan Ersoy, Elif Dilara Yapıcı, Cansu Kahraman, Osman Uludağ and Hatice Kılıç for their supports.

The author extends his gratitude to Mertcan Özbakır for his valuable support and encouragement at the initial steps of his career.

Finally, the author would like to express his sincere appreciation to his parents and METU Falcons American Football Team members for their patience, love and encouragement of a life time.

TABLE OF CONTENTS

LIST OF TABLES

LIST OF FIGURES

CHAPTER 1

INTRODUCTION

1.1. Purpose and Scope

Esan Eczacıbaşı Industrial Raw Materials Inc. (ESAN) has conducted coal exploration studies in the Sector-A coal field of Turkish Coal Enterprises (TKİ) which is located in the vicinity of Çavlum and Ağapınar villages in Alpu District in Eskişehir Province. The baseline studies are required before the environmental impact assessment and feasibility studies can be done. Hence, the purpose of this study is to investigate chemical, physical and hydraulic parameters of the groundwater system and to characterize it. The scope of the study included a review of the existing topographical, hydrological, hydrogeological and water quality data. Pumping, observation and vibrating wire piezometer wells were drilled in the study area to obtain data to characterize the groundwater system. The aquifer tests were conducted in these wells and groundwater levels were monitored on monthly basis. The field water quality parameters such as temperature (T), pH, electrical conductivity (EC) and dissolved oxygen (DO) were measured on monthly basis from all pre-defined water monitoring points to characterize the hydrochemistry and water quality. Some surface water monitoring points were also defined to establish the surface water runoff and evaluate the surface water flow potential in the study area. The water bearing units in the study area were identified. Spatial and temporal variations in groundwater levels and pore pressures as well as spatial and temporal variations in groundwater quality were determined.

1.2. Location of Study Area

The study area is located within the Eskişehir graben at the northwest of the Central Anatolia. The Sector-A is located approximately 12 km northeast of Eskişehir and 7 km northeast of Ankara-Eskişehir road. The study area is accessed via Eskişehir-Alpu road that passes through the southern part. Ağapınar, Çavlum, Sevinç and Yassıhöyük that belong to the Odunpazarı Municipality and Gökdere and Cumhuriyet that belong to Tepebaşı Municipality are located within and/or in close vicinity of the study area. The Sector-A which is located within the study area is approximately 18.9 km^2 and the longest distance from north to south is 4 km (UTM 4408000-4412000 North); from east to west is 9.7 km (UTM 299500-309150 East) (Figure 1.1).

The study area located in Alpu plain is drained by the Porsuk Stream which flows from west to east through the Central Part of Sector-A. The Porsuk Stream, which is the main tributary of the Sakarya River, starts from Kütahya, passes through Kütahya and Eskişehir plains and reaches to the Alpu plain.

Figure 1.1. Location Map of the Study Area

1.3. Previous Studies

The earliest geological study within and around the study area was conducted on behalf of General Directorate of Mineral Research and Exploration (MTA) by Siyako et al.,, in 1991. This study resulted with a geological report with the name of “Tertiary geology of the Bozüyük-İnönü Eskişehir-Beylikova-Sakarya regions and their coal potential”. To determine the distribution of Tertiary rocks in the field, geological maps of scale 1/100.000 for I23, I24, I25, I26 and I27 map sheets were prepared and the coal potential of the region was investigated. Following this study, a geological report entitled “Geology of the middle and southern part of the Sakarya Region” was prepared by Gözler et al. in 1997 for MTA. In this report, geological maps of scale 1/100.000 and 1/25.000 for I24, I25, I26 and I27 map sheets were developed. In a study conducted by Şengüler (2013), the geology and stratigraphy of Eskişehir–Alpu coal basin were published (Şengüler, 2013). In 2015, another study conducted by Toprak et al., for the same area focused on the petrographical properties and depositional environment of this basin. Two-dimensional high resolution seismic data has been collected by Turkish Petroleum Inc. (TPAO) in all coal sectors including Sector-A during 2016 and the faults in Sector-A have been interpreted (TPAO, 2016). A scoping study was completed by Palaris (2016) for the mining of the lignite resources in Sector-A. The coal exploration studies in all sectors that were conducted by MTA and ESAN on behalf of TKİ have been completed in 2017. In addition to all of these studies, 1/25.000 scale geological map of the study area and its vicinity is prepared by MTA.

In comparison to geological studies, limited hydrogeological studies have been carried out for the study area and its surrounding. In 1977, General Directorate of State Hydraulic Works (DSI) prepared “Hydrogeological Investigation Report for Eskişehir–Alpu Basin” to determine potential, quantity and quality of the groundwater in this basin and to specify areas suitable for groundwater exploitation. In 2010, DSI revised this report to recalculate the groundwater reserve in the basin. MTA conducted a pre-hydrogeological investigation of the coal inventory area in Alpu basin (Bayram, 2015). A hydrogeological investigation and characterization study was conducted by Yazıcıgil et al., in 2016 within the license area of ESAN in the southern part of Sector-A. In addition, Yazıcıgil et al., (2017) developed a 3-dimensional groundwater flow model for the license area of ESAN and predicted groundwater inflows to typical underground panels. A detailed hydrogeological investigation for Sector-A as well as whole sectors (A through E) have been conducted by Yazıcıgil et al., 2017 and 2018, respectively.

CHAPTER 2

DESCRIPTION OF THE STUDY AREA

2.1. Topography

Digital Elevation Model (DEM) of the study area is produced from the 1/25000 scale topographical maps (Figure 2.1). According to the model, the Sector-A located on both sides of the Porsuk Stream is almost flat with elevations ranging between 770 m in the south and 840 m in the Taşlı hill in the north. The highest elevations within the region are formed by the hills in the north and south of the plain area are formed by the alluvial deposits of the Porsuk Stream.

The hills forming the elevated points in Sector-A and its vicinity are shown in Figure 2.1. The Taşlı, Deveci and unnamed hills in Sector-A have elevations 818 m, 793 m and 784 m, respectively. The highest hill in the study area is however Çürüksu Hill in the south of Sector-A with an elevation of 977 m.

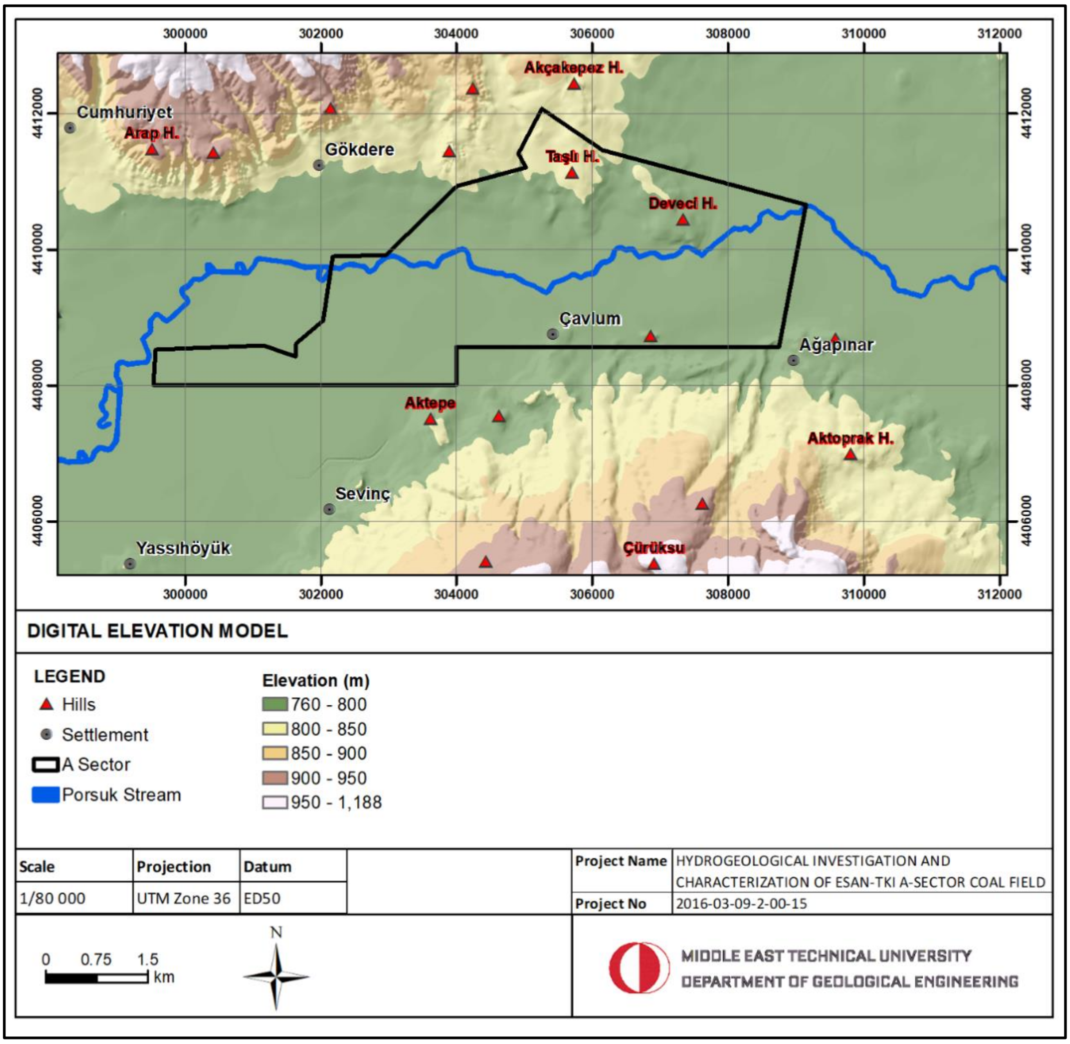

Figure 2.1. Digital elevation model of the study area and the surroundings (Yazıcıgil et al., 2017).

2.2. Settlements and Population

The most populated settlements that could be affected socio-culturally by mining activities within the study area are Odunpazarı and Tepebaşı Districts. According to the Address Based Population Registration System of TUİK (Turkish Statistical Institute) 2016 data, the populations of Odunpazarı and Tepebaşı districts are 391106 and 343701, respectively.

The settlements in the study area are those of Cumhuriyet and Gökdere villages of Tepebaşı Municipality and Çavlum, Sevinç, Yassıhöyük and Ağapınar villages of the Odunpazarı Municipality. The population statistics of the settlements were obtained from Address Based Population Registration System of TUİK (Turkish Statistical Institute) 2016 data and are shown in Figure 2.2. The total population of these villages listed above is 3008. The only village located in Sector-A is Çavlum with 136 people (TUİK, 2016).

The drinking and domestic water needs of Çavlum village are met from a captage developed in silicified limestone belonging to Miocene in the license area of ESAN in the south of Sector-A (Yazıcıgil et al.,, 2016). The water is delivered by gravity to the water depot in the south of the village and distributed from the depot to the village.

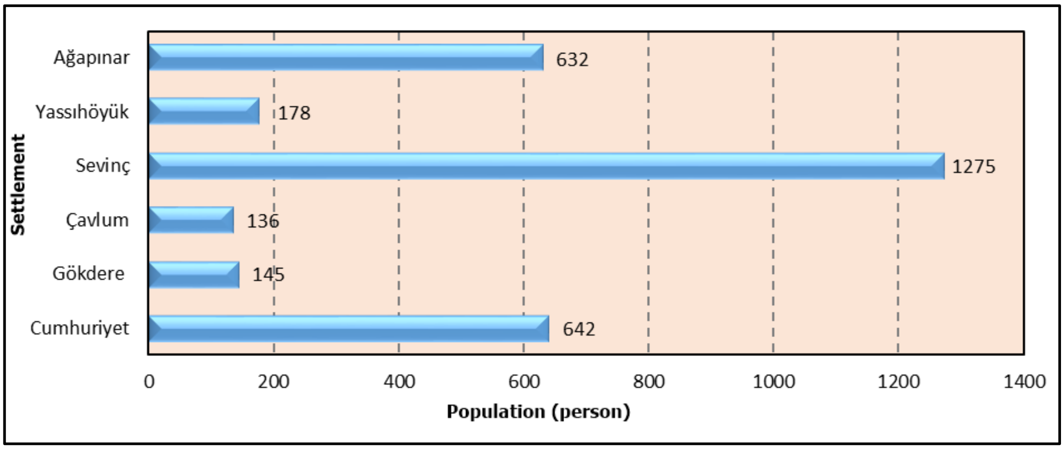

Figure 2.2. Population distributions of the settlement areas (TÜİK, 2016)

2.3. Climate and Meteorology

In the northwestern part of the Central Anatolia and in the Sakarya River basin region where the Sector-A is located, winters are cold and snowy, springs are moderately rainy and summers are dry, partly cloudy and clear due to the typical continental climate characteristics. In this region, the temperature differences are high between summer and winter months while icing events are usually seen in winter. According to Köppen climate classification, regional climate is represented by “CSB” climate code which is defined as warm winter, hot summer, arid but short climate (mid-latitude climate type); but according to Thornthwaite, it is represented by “DB’1db3” climate code which is defined as semi-arid, mild mesothermal, little or no water surplus, nearly continental conditions type of climate (Dönmez, 1979).

To reveal the meteorological characteristics within and in the vicinity of the study area, the data of meteorological stations operated/in operation by Turkish State Meteorological Service (MGM) has been investigated (Table 2.1, Figure 2.3).

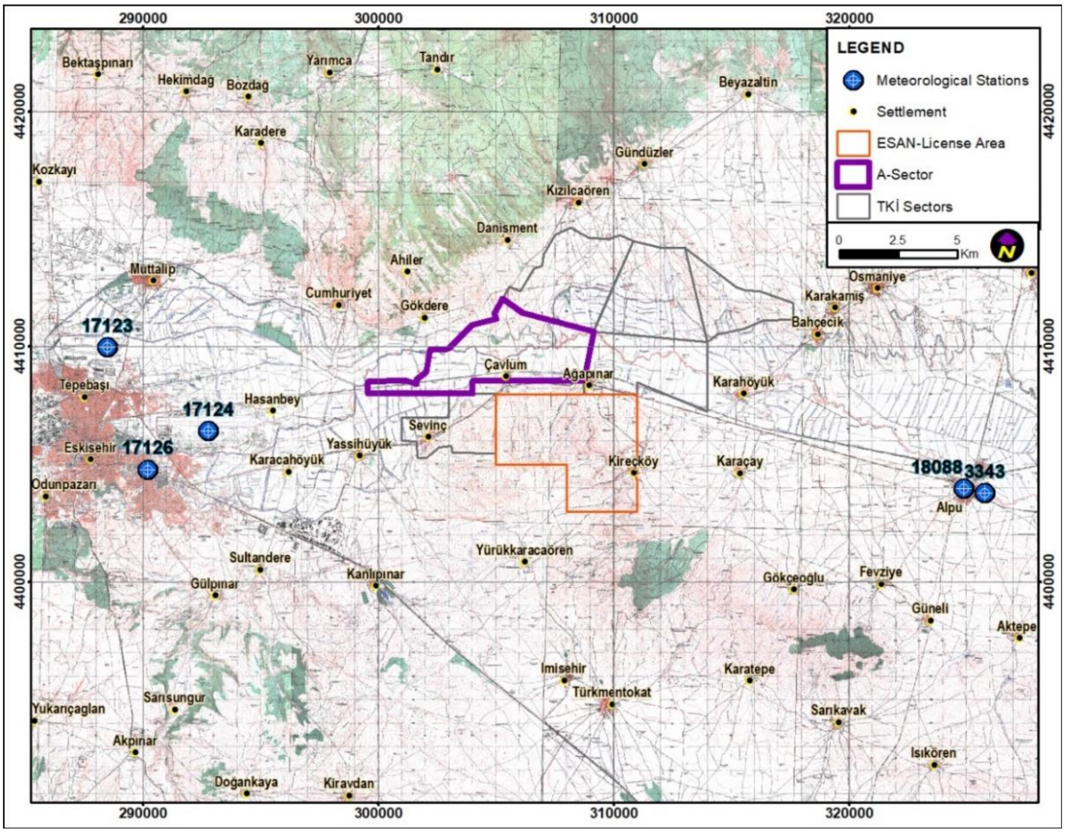

Figure 2.3. Locations of the meteorological stations around the study area

Table 2.1. Data inventory belonging to the meteorological stations (Yazıcıgil et al., 2017)

Institution	Station No.	Station Name	UTM Longitude	UTM Latitude	Elevation (m)	Distance to the Study Area (km)	Data Period
MGM	17126	Eskişehir Regional Directorate of Meteorology	290146	4404721	801	10	1929-1978, 1981-1990, 2007-2014
MGM	17124	Eskişehir Military Airport	293045	4406434	785	7	1978-1981
MGM	17123	Anadolu Civil Airport	287460	4410374	789	11	1990-2012
MGM	3343	Alpu	325815	4403788	765	17	1984-2002
MGM	18088	Alpu	324924	4403973	771	17	2013-to date

Among these stations, stations named Eskişehir Regional Directorate of Meteorology (No. 17126), Eskişehir Military Airport (No. 17124) and Eskişehir Anadolu Civil Airport (No.17123) represent the meteorological conditions of Eskişehir city center which is located 12 km southwest of Sector-A whereas stations 3343 and 18088 represent the rural conditions of Alpu which is located 17 km southeast of Sector-A. The Eskişehir Regional Directorate of Meteorology (No. 17126) station has the longest observation period. This station has been operated from 1929 until present, with loss of data between the years 1978-1981 and 1990-2006. Since the stations Military Airport (No. 17124) and Anadolu Civil Airport (No. 17123) have been operated for the time period during which station No. 17126 was closed, it is possible to create a near-continuous dataset for the Eskişehir city center from 1929 until present. In addition to these stations representing the city conditions, the Alpu meteorological station (No. 3343) is also used because Sector-A has a rural character and is located between Eskişehir and Alpu. The Alpu Meteorological Station No. 3343 has been operated between the years 1984-2002. After the closure of meteorological station (No. 3343) at Alpu, Turkish State Meteorological Services established a new station numbered as 18088 which has been operating from February 2013 to date. The data recorded at this station is also evaluated because its record overlaps with the study period. For the stations listed in Table 2.1, the total monthly precipitation, monthly average, minimum and maximum temperature, monthly average relative humidity and total monthly open surface evaporation values are discussed below, respectively.

2.3.1. Precipitation

To investigate the long-term precipitation regime of the study area, total annual precipitation and cumulative deviation from mean annual precipitation for the station named Eskişehir Regional Directorate of Meteorology (No. 17126) is presented in Figure 2.4 for the 1929-2016 periods. For the 1978-1981 and 1990-2006 years during which the data for station No. 17126 were missing, the data measured in stations 17124 and 17123 were used, respectively. Moreover, precipitation data for meteorological station No. 17126 was deemed inaccurate during 2007-2012 periods due to the extremely low precipitation values compared to other stations and other years and hence the precipitation data for the station No. 17123 were used during this period. As shown in Figure 2.4, for the 1929-2016 period, with 194 mm of rainfall the year 1932 was the driest year, and with 518 mm of rainfall the year 1963 was the wettest year. The long-term average annual rainfall in Eskişehir city center is 367 mm. During the study period (2016), total annual rainfall (348.8 mm) is %5 less than the long term annual rainfall. Investigation of cumulative deviation from mean annual rainfall graph shows that the 1929-1937, 1951-1956, 1982-1997 and 2002-2008 years correspond to the dry period and the 1938-1950, 1957-1981 and 2009-2012 years, generally correspond to the wet period. Looking at the general rainfall trend, 1957-1981 period is marked by a significantly wet period, and 1982-2016 period is marked by a significantly dry period.

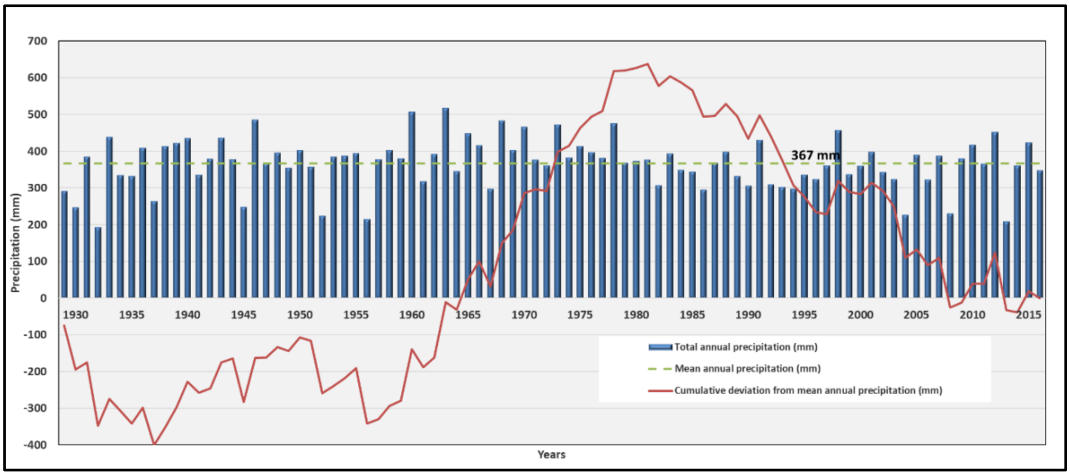

Figure 2.4. Eskişehir Regional Directorate of Meteorology Station total annual precipitation (mm) and cumulative deviation from mean annual precipitation (mm) graph (1929-2016) (Yazıcıgil et al., 2017).

Alpu meteorological station No. 3343 has been operated continuously between years 1985-2001 and represents the rural conditions. Total annual precipitation and cumulative deviation from mean annual precipitation graph for Alpu station No. 3343 is presented in Figure 2.5. As can be seen from this graph, for the 1985-2001 period, the year 1992 is the driest year with 288 mm of rainfall, whereas the year 1997 is the wettest year with 535 mm of rainfall. The long-term average total annual rainfall in Alpu station is 388 mm; which is 21 mm more than the Eskişehir city center. Investigation of the cumulative deviation from mean annual precipitation graph yields that, generally dry conditions prevailed between years 1985-1996, whereas generally wet conditions prevailed during 1997-2001. Dry and wet periods in Alpu and Eskişehir city center (Figure 2.4) are overlapping.

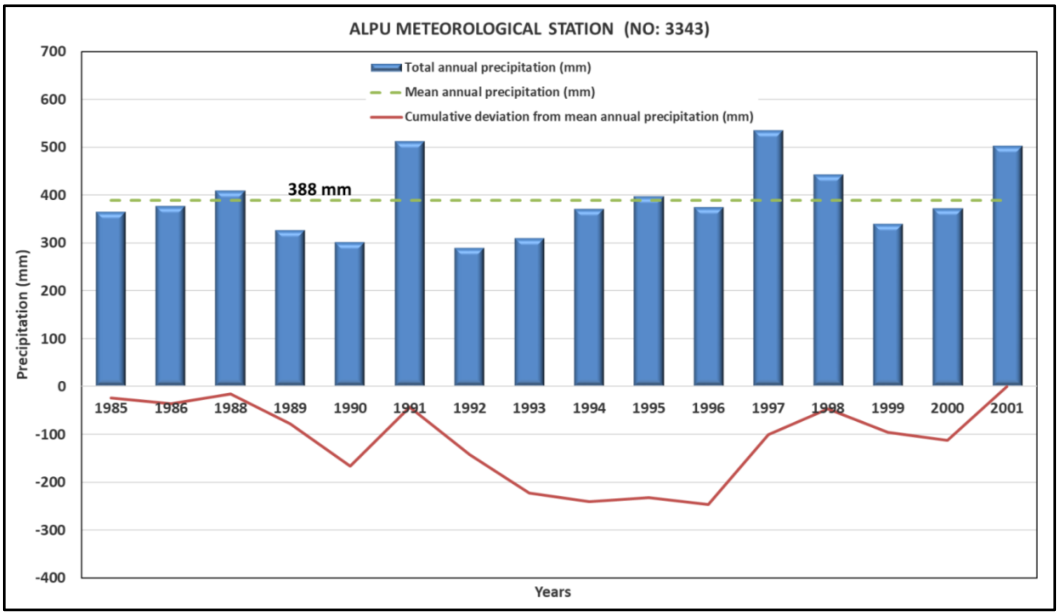

Figure 2.5. Total annual precipitation (mm) and cumulative deviation from mean annual precipitation (mm) graph for meteorological station No.3343 (1985-2001) (Yazıcıgil et al., 2017)

The Alpu meteorological station no. 18088, which has been in operation since February 2013, does not have a common operation period with station No. 3343. The station No. 17126, located in city center which has data since 1929, has only 4 years of common period with Station No. 18088; therefore, the short overlapping period between two stations will not yield statistically reliable results for correlating them. Therefore, average monthly precipitation values for stations 3343, 17126 and 18088 were calculated by using the values corresponding to the their operation periods and compared (Figure 2.6).

As can be seen from Figure 2.6, the data from station 18088 shows that June is the wettest month (64.4 mm/month), and July is the driest month (1.2 mm/month) in Alpu in the past few years. The highest rainfall observed in the month of June in the study area which has a typical continental climate is probably due to the convective precipitations commonly seen in spring and early summer months in central and eastern regions. The monthly rainfall is highest with values of 51.8 mm and 46.1 mm in December in stations 3343 and 17126, respectively. The lowest monthly precipitation at station 3343 is observed in September with a value of 11.7 mm whereas it is 8.7 mm in August at station 17126.

The monthly average rainfall data from stations 3343 and 18088 is compared (Figure 2.6). The aveage annual precipitation calculated for the period 2013-2016 at station no. 18088 is 354 mm which is 8.8 percent lower than the aveage annual rainfall for the 1984-2002 period at station 3343. This shows that the precpitation has decreased over the past few years in the region. Moreover, the latest annual average rainfall (354 mm/year) of the rural region being 3.5 percent lower than the long-term average annual rainfall at Eskişehir city center (367 mm/year) shows that the rainfall in the region has been decreased in recent years. Since the study area is situated in between Alpu and Eskişehir city center, the precipitation is expected to be in between the values measured at stations 18088 and 17126.

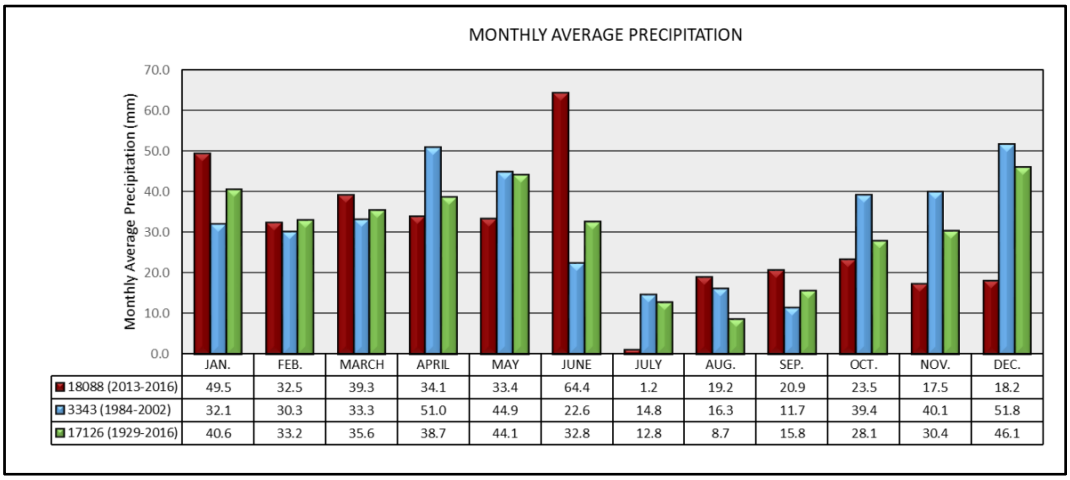

	JAN.	FEB.	MARCH	APRIL	MAY	JUNE	JULY	AUG.	SEP.	OCT.	NOV.	DEC.
18088 (2013-2016)	49.5	32.5	39.3	34.1	33.4	64.4	1.2	19.2	20.9	23.5	17.5	18.2
3343 (1984-2002)	32.1	30.3	33.3	51.0	44.9	22.6	14.8	16.3	11.7	39.4	40.1	51.8
17126 (1929-2016)	40.6	33.2	35.6	38.7	44.1	32.8	12.8	8.7	15.8	28.1	30.4	46.1

Figure 2.6. Monthly average precipitation data for No.18088 and No.3343 Alpu meteorological stations and No.17126 Eskişehir city center meteorological station (Yazıcıgil et al., 2017).

2.3.2. Temperature

Monthly average of the mean, minimum and maximum temperature values measured in Alpu station No. 3343 (years 1984-2002) and station No. 18088 (years 2013-2016) and Eskişehir city center Station No. 17126 (years 1929-2016) are presented in Figures 2.7-2.9, respectively. Examination of Figure 2.7 shows that the monthly average temperature values calculated from long-term data at Eskişehir city center are very similar to the monthly average values for Alpu 3343 and 18088 stations' values. However, monthly average values in all stations show seasonal variations. Examination of monthly average temperatures (Figure 2.7) indicate that January is the coldest month in stations 17126 and 3343 with average temperature values below zero while the hottest month is July with average temperature values of 22 ^oC. The monthly average temperatures at station No. 18088 operating since 2013 are lowest in December and January with values close to zero and highest in August and July with values of 23 ^oC.

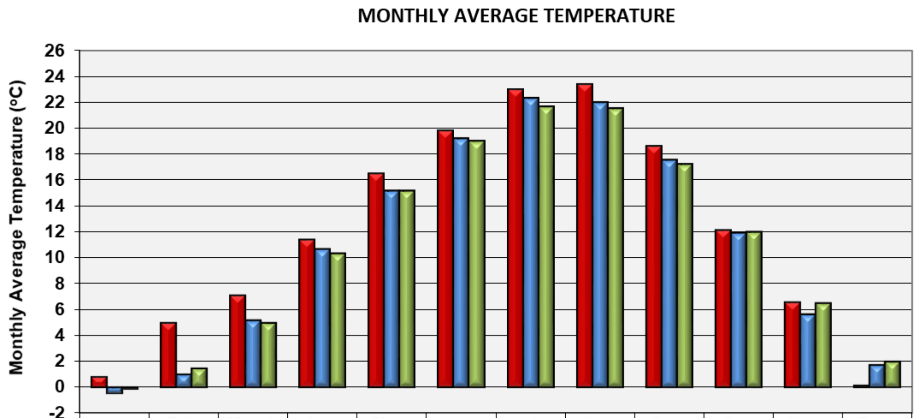

	Jan.	Feb.	March	Apr.	May.	June	July	Aug.	Sep.	Oct.	Nov.	Dec.
18088 (2013-2016)	0.7	4.9	7.1	11.4	16.4	19.8	23.0	23.4	18.6	12.1	6.5	0.1
3343 (1984-2002)	-0.5	1.0	5.2	10.7	15.1	19.2	22.3	22.0	17.5	11.9	5.6	1.7
17126 (1929-2016)	-0.1	1.4	4.9	10.3	15.1	19.0	21.7	21.5	17.2	12.0	6.5	2.0

Figure 2.7. Monthly average temperature data for Eskişehir city center (No:17126) and Alpu (No:3343 and No:18088) meteorological stations (Yazıcıgil et al., 2017).

Because the monthly average temperatures at Alpu and Eskişehir city center are very similar to each other, similar temperatures are also expected to be seen in the study area. However, the station 18088 operating since 2013 has higher monthly temperatures than station 17126 in Eskişehir city center and Alpu 3343 station which has operated in the past. This shows that the average monthly temperatures at Alpu increased in recent years.

Examination of the monthly average minimum temperature values (Figure 2.8) at Eskişehir meteorology station 17126 and Alpu meteorology station 3343 indicate that, the region is experiencing icing events in October-April period. Especially in December, January and February temperature values could lie below -10^oC. The monthly average minimum temperature data of Alpu metrological station 18088 which has been in operation between 2013 and 2016 period indicate that the average minimum temperatures increased 4-6 ^{o}C in the summer months and the icing period is shifted to November-March period.

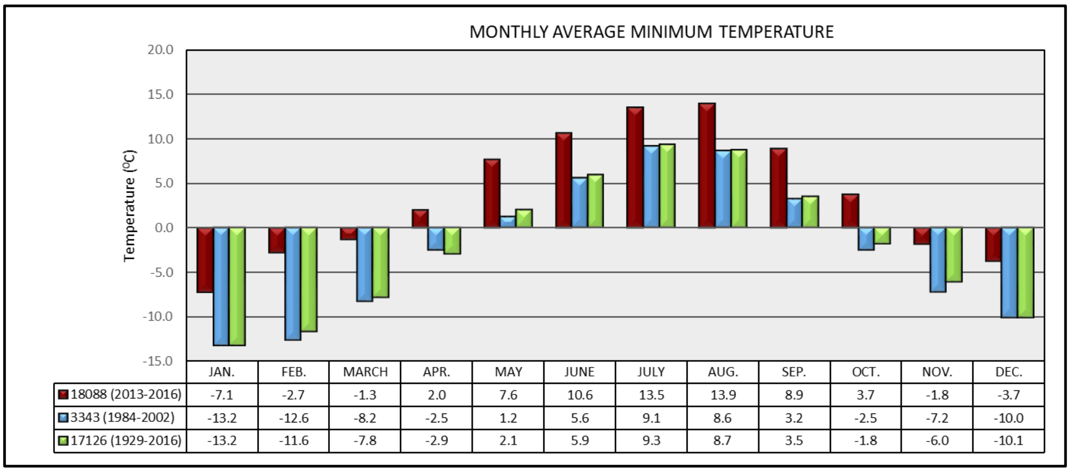

	JAN.	FEB.	MARCH	APR.	MAY	JUNE	JULY	AUG.	SEP.	OCT.	NOV.	DEC.
18088 (2013-2016)	-7.1	-2.7	-1.3	2.0	7.6	10.6	13.5	13.9	8.9	3.7	-1.8	-3.7
3343 (1984-2002)	-13.2	-12.6	-8.2	-2.5	1.2	5.6	9.1	8.6	3.2	-2.5	-7.2	-10.0
17126 (1929-2016)	-13.2	-11.6	-7.8	-2.9	2.1	5.9	9.3	8.7	3.5	-1.8	-6.0	-10.1

Figure 2.8. Monthly average minimum temperature data for Eskişehir city center (No:17126) and Alpu (No:3343 and No:18088) meteorological stations (Yazıcıgil et al., 2017).

When monthly average maximum temperature values are analyzed (Figure 2.9), July and August are the months during which average maximum temperatures are around 33^{o}C-36^{o}C. In December-January period, monthly average maximum temperature values could reach to the values of 7^{o}C-14^{o}C.

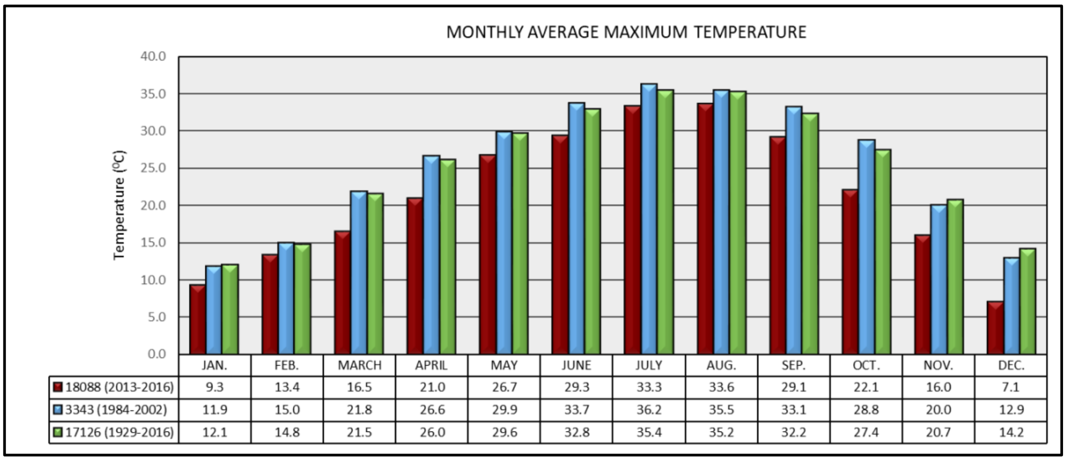

	JAN.	FEB.	MARCH	APRIL	MAY	JUNE	JULY	AUG.	SEP.	OCT.	NOV.	DEC.
18088 (2013-2016)	9.3	13.4	16.5	21.0	26.7	29.3	33.3	33.6	29.1	22.1	16.0	7.1
3343 (1984-2002)	11.9	15.0	21.8	26.6	29.9	33.7	36.2	35.5	33.1	28.8	20.0	12.9
17126 (1929-2016)	12.1	14.8	21.5	26.0	29.6	32.8	35.4	35.2	32.2	27.4	20.7	14.2

Figure 2.9. Monthly average maximum temperature data for Eskişehir city center (No:17126) and Alpu (No:3343 and No:18088) meteorological stations (Yazıcıgil et al., 2017).

Figure 2.9 also shows that the average maximum temperatures have been decreased in recent years based on data from 18088 Alpu meteorological station. While the average monthly temperatures have been increased, the observed decrease in the average maximum temperatures could be due to the short period of data (4 years) recorded at Station No. 18088. The temperatures above the seasonal normal values are to be expected in stations 17126 and 3343 having a longer period of data.

2.3.3. Relative Humidity

Monthly average relative humidity values measured in Alpu meteorological stations no. 3343 (years 1984-2002) and 18088 (years 2013-to date) and Eskişehir meteorology station no. 17126 (1929-2016) presented in Figure 2.10 show that they are generally similar. The highest monthly average relative humidity values are observed in December and January (77-90%) and the lowest monthly average relative humidity values are observed in July (49-55%).

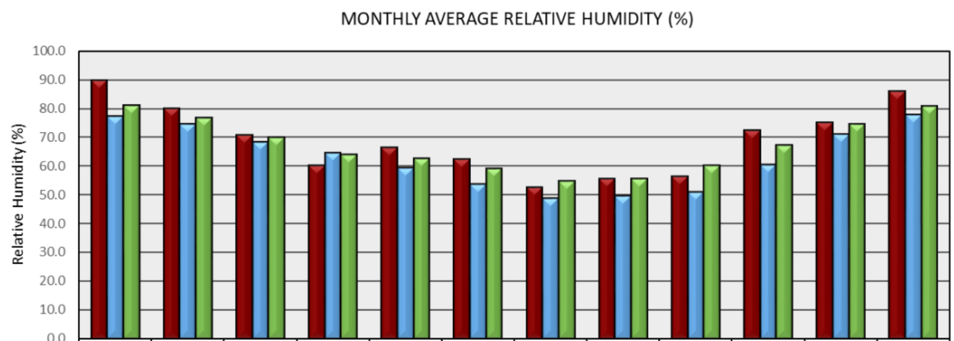

	JAN.	FEB.	MARCH	APRIL	MAY	JUNE	JULY	AUG.	SEP.	OCT.	NOV.	DEC.
18088 (2013-2016)	89.6	79.8	70.6	60.1	66.3	62.2	52.4	55.4	56.2	72.4	75.0	85.8
3343 (1984-2002)	77.2	74.3	68.2	64.4	59.4	53.7	48.7	49.6	50.9	60.4	70.8	77.6
17126 (1929-2016)	81.0	76.6	69.7	64.0	62.6	58.9	54.7	55.5	60.0	67.1	74.4	80.8

Figure 2.10. Monthly average relative humidity data for Eskişehir city center (No:17126) and Alpu (No:3343 and No:18088) meteorological stations (Yazıcıgil et al., 2017).

2.3.4. Evaporation

Monthly total open surface evaporation was measured during April-October period at meteorological stations located in the Eskisehir city center, namely Eskisehir Regional Directorate No. 17126 for years among 1962-1978 and Anadolu Civil Airport Regional Directorate of Meteorology station No. 17123 for years among 1990-2012. In addition to these stations, monthly total surface evaporation is also measured during 2015-2016 at Eskişehir military airport station No. 17124. The measured data for 2016 at this station is considered herein because the period of measurement overlaps with the study period.

As can be seen from Figure 2.11, Anadolu Civil Airport Regional Directorate of Meteorology station No. 17123, with more current data, measured the values of open surface evaporation about 30% higher than the values measured in Eskişehir Regional Directorate station No. 17126. This difference between meteorological stations may be related to the location of the station or urbanization. Taking into account the Anadolu Civil Airport Meteorology station No. 17123 with more recent data, July is the month with the maximum open surface evaporation (317.8 mm) and April is the month with minimum open surface evaporation (146.3 mm) among the months with measurements.

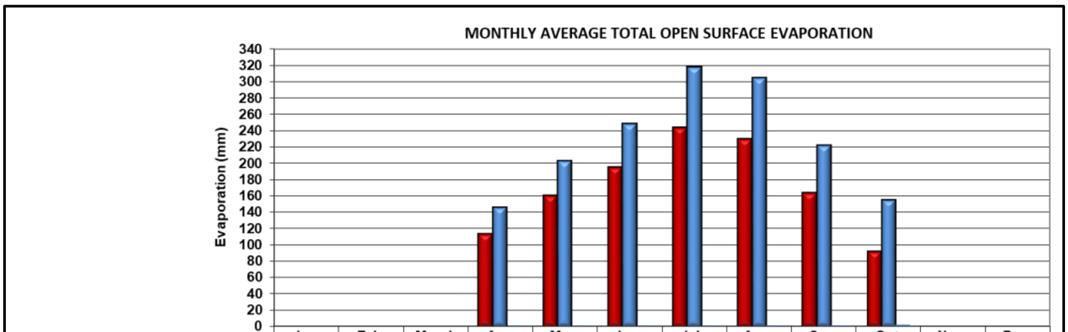

	Jan.	Feb.	March	Apr.	May.	June	July	Aug.	Sep.	Oct.	Nov.	Dec.
ESK. REG. DIR. (1962-1978)				113.8	161.1	196.1	244.0	230.0	164.7	92.9		
ESK. ANADOLU (1991-2012)				146.3	203.3	248.4	317.8	304.9	222.2	155.3		
ANADOLU / ESK. REG. DIR. Ratio				1.29	1.26	1.27	1.30	1.33	1.35	1.67		

Figure 2.11. Monthly average total open surface evaporation data for Anadolu Civil Airport Regional Directorate of Meteorology station (No:17123) and Eskisehir Regional Directorate No. 17126 station (Yazıcıgil et al., 2017)

2.4. Geology

2.4.1. Regional Geology

Regionally, the study area is located between the Sakarya Continent and Anatolide-Tauride block (Figure 2.12). The Intra-Pontide suture zone, which separates these two blocks, approximately passes through the Bozüyük-Eskişehir line. The NW-SE to WNW-ESE trending Eskişehir Fault zone extending from Uludağ in the northwest to Sultanhanı in the southeast shows a parallel trend to this line (Toprak et al., 2015). Eskişehir fault zone has been active since the Pleistocene and it is younger than the Upper Pliocene according to the neotectonic and sedimentary data. The fault zone has played a major role in the formation of Eskişehir and İnönü basins. Lower-Middle Miocene deposits in the Eskişehir graben, preserved in a restricted area at the northern end of Anatolide block, were cut by the İnönü segment of Eskişehir fault. Eskişehir-Alpu coalfield and surrounding units are composed of pre-Miocene basal and Miocene-Pliocene cover rock assemblages according to reports on the "Geology and Reservoir Drilling" studies conducted by MTA (Şengüler, 2011) (Figure 2.13). The coal bearing sediments were preserved beneath the Upper Miocene-Lower Pliocene deposits (Şengüler, 2013).

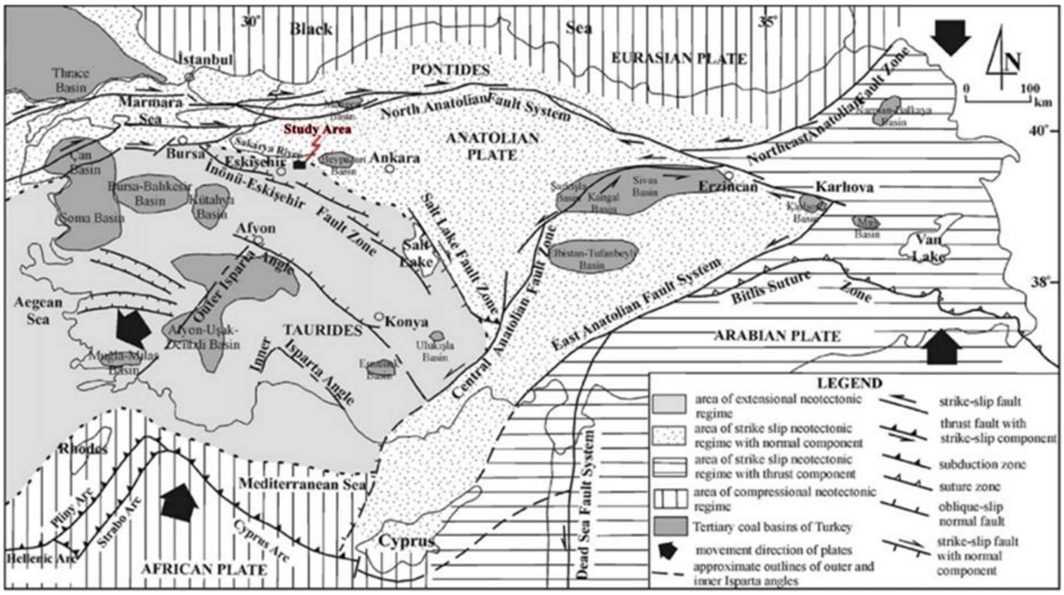

Figure 2.12 Tertiary coal basins and the simplified neotectonic sub basin of Turkey and its close vicinity (Toprak et al., 2015)

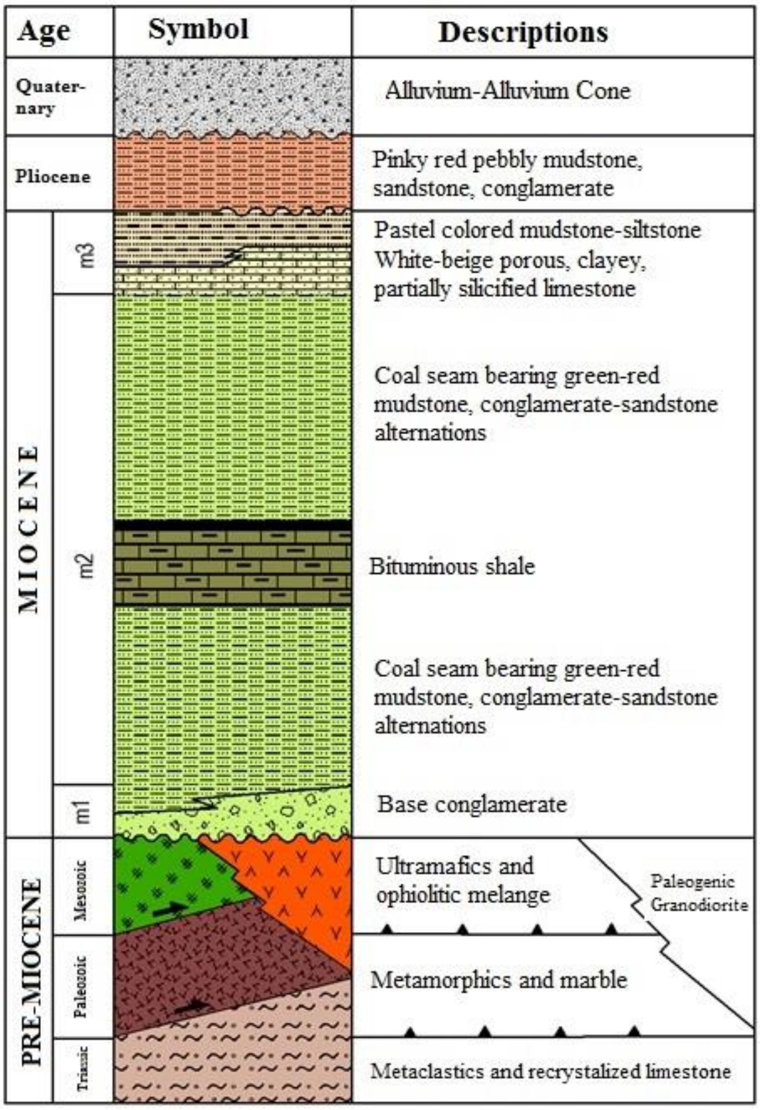

Figure 2.13 Generalized stratigraphic columnar section of study area and near vicinity (Yazıcıgil et al., 2018)

2.4.2. Geology and Stratigraphy of the Study Area

Generalized columnar section and 1/125.000 scaled geological map of the study area and its vicinity are presented in Figures 2.14 and 2.15, respectively. Within this area, Paleozoic metamorphics and Mesozoic units outcroping in the southeastern and northwestern parts of the study area and tectonically in contact with Paleozoic metamorphics form the basement rocks (Figures 2.14 and 2.15). This tectonic contact progressed from north to south as an imbricated structure (Gözler et al., 1997). Exact thicknesses of the metamorphics are not known due to their folded and jointed structure.

2.4.2.1. Pre-Miocene Rocks

Miocene and Pliocene sediments on the area form the cover rocks. These sediments are unconformably overlying the Palaeozoic and Mesozoic rock units that form the basement of the basin. On these Neogene units, younger, loosely packed gravel and sand grains and Quaternary units formed by organic muds (swamps) are observed.

It is composed of Pre-Miocene Paleozoic metamorphics, Triassic metaclastics and recrystallized limestones, Mesozoic ultramafics and ophiolitic melange, Paleogene deposits and Paleogene granodiorite in the Eskişehir Basin (Koçyiğit et al., 1991) (Figure 2.13). The tectonic relation developed from north to south as an imbricated structure (Figure 2.14, 2.15, 2.16 and 2.17). For metamorphic rocks, it is hard to measure their thickness due to its folded, highly fractured, deformed structure. However, it can be said that schists have a thickness of about 1000 meters and marbles have a thickness of 200 meters (Şengüler, 2013). Metamorphics are developed as blue schist facies.

Ophiolitic melange is observed as nappe on metamorphics and tectonic slices under ophiolites. The ophiolitic melange consists of radiolarites, crystallized limestones and marbles, mudstones, diabases, serpentinites, metamorphics, peridotites and gabbro blocks which are assembled in a tectonic way without matrix. The ophiolites associated with this unit are; peridotite, serpentinite, pyroxenite, metapyroxenite, hornblendite, metahornblendite, gabbro, metagabro, diabase, metadiabase, listvenite which is the determinant of tectonic zones and eclogite units considered as metamorphic equivalents of oceanic shell. It is also possible to observe these tectonic slices as nappe (Figure 2.14, 2.15, 2.16 and 2.17) (Gözler et al., 1997). The Triassic metadetritics, which are observed to be tectonically related to the ophiolites, consist of metamacitic, metaclastic, filtrate and recrystallized limestones. They crop out along the anticlinal axis extending in the direction of ENE-WSW (Figure 2.15). The Jurassic-Cretaceous limestone overlies this unit tectonically. Massive-looking, stratified limestones continue to micritic, finely dolomitic limestones upward and end up with thin to medium bedded and abundant fossiliferous micritic limestones containing chert bands of 1-5 cm thickness in pinkish, creamy and gray colors (Gözler et al., 1997). Mesozoic basement rocks are overlained by Paleogene sediments. It consists of Paleocene age conglomerates, Eocene aged conglomerates, sandstones and clayey limestones in the Eskisehir basin. All basic units are cut by Paleogene aged granodiorite. This granodiorite, which is predominantly porphyry, locally grained, with an approximate E-W extension, was predominantly altered (Figure 2.15).

2.4.2.2. Miocene-Pliocene-Quaternary Rocks

Miocene Deposits

Miocene and Pliocene sediments, unconformably overlying the Palaeozoic and Mesozoic rocks that form the basement of the basin, form the cover rocks. On these Neogene units, younger, loosely packed gravel and sand particles and Quaternary units consisting organic muds in places are observed.

Miocene sediments containing lignite seams in the region unconformably come over the basement rocks (Figure 2.13). At the bottom of these sediments, conglomerate, sandstone and claystone take place (m1 series). It is a distinctive unit with a massive and thick bedded, red, yellowish gray, gray and light gray in color, mostly red and brownish-red color. The conglamerates consist of boulders ranging in size from the gravel size to the block size, overlies older units (Siyako et al., 1991). Gravels are generally angular, semi-rounded and poorly sorted and have blocky levels and varying gravel tiles place to place. The gravels are mostly ultrabasic rocks. Radiolarite, marble and quartz pebbles are rarely seen as well.

Economic coal deposits in the Neogene Reservoir in Eskisehir are found in the Middle Miocene aged m2 series (Figure 2.15). Carbonization in the Eskişehir-Alpu area is in this unit. The series coming on top of the base conglomerate is composed of partially pebbley green colored claystone, coal seam (D), green claystone, coal seam (C), gray colored sandstone, bituminous shale, coal seam (B), bituminous shale, coal seam (A) and green colored claystone-sandstone-conglomerate sequence (m2 series) from bottom to top, respectively. It is mostly green and yellow and is multi-colored place to place. The thickness of these series ranges from 150 m to 600 m in the study area. Tuffite and mudstone interiors are widespread especially in the eastern part of the study area. There are lateral and vertical transitions with the units at the bottom and above and limestones are also seen between them. Generally, the coals are thin, locally thick layered seams. The thickness of coal seams reach up to 30 meters from 2 meters.

On the basis of the obtained drilling data, it is observed that the coal bearing sequence (from bottom to top) in Eskişehir-Alpu basin reach 200-250 m thickness.

The stratigraphically upper parts of the Miocene series are formed by silicified limestones (m3 series) that outcrop in the high peaks on the southwest and west sides of the Alpu basin (Figure 2.14 and Figure 2.15). These limestones are generally white, gray, yellowish beige colored, highly porous and locally (mostly deeper parts) silicified and are maximum 60 m thick. Miocene units uncormably overlain by Pliocene units.

Pliocene Deposits

The Pliocene begins with conglomerates and sandstone strata formed by small granular conglomerates on Miocene units. It is represented by cream, light brown colored, light reddish mudstone and loosely attached multi-type granular conglomerate-sandstone, floating gravelly sandstones (Figure 2.14). The size of the gravel varies between 1-10 cm, and the thickness of the unit reaches 370 m in the north-east of the basin. Highly porous, pinkish-brown clayey limestones are also defined by Siyako et al., 1991.

Quaternary (Pleistocene-Holocene) Units

There are pebble-sandy deposits on the Neogene units forming alluvial deposits and gravelly alluvial fans and marshlands (organic muds) on the sides of the basin (Figure 2.14 and Figure 2.15). The alluvial units are composed of gravel and sand grains, which are loosely packed in some places and composed of unpacked many types of gravel and sand grains that are dominant. The size of the gravel varies from 1 to 30 cm in diameter. The alluviums forming liquefied floors are exposed along the current and old bed of the Porsuk River. The thickness of the unit varies between 10-60 m. According to the vertebrate fossils found in sandy clayey levels, the age was given Villafransan (Pleistocene) (Şengüler, 2011).

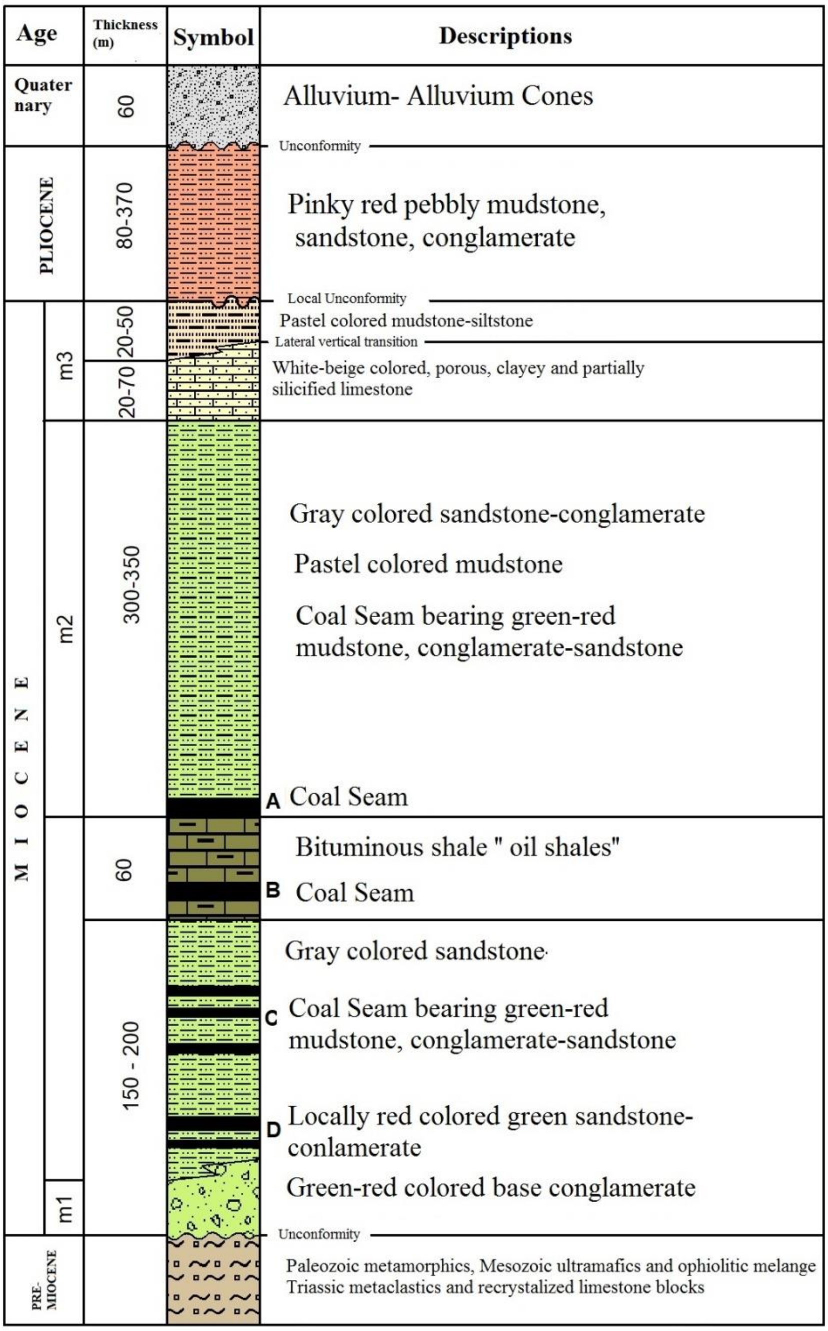

Figure 2.14. Columnar section of the study area derived from field studies and well logs and near vicinity (Yazıcıgil et al., 2018)

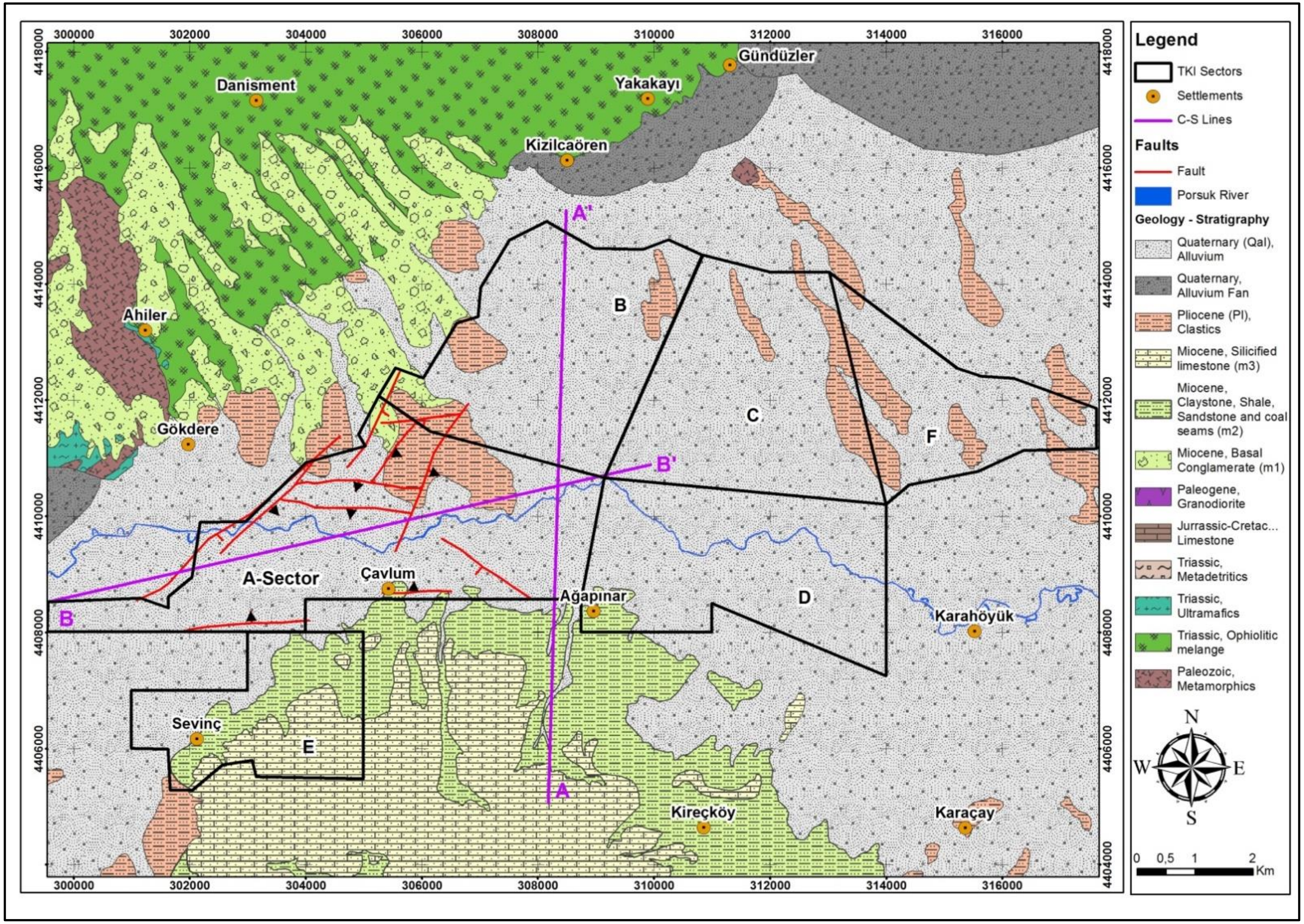

Figure 2.15 1/125.000 scaled geological map of the study area and its surroundings (Yazıcıgil et al., 2018)

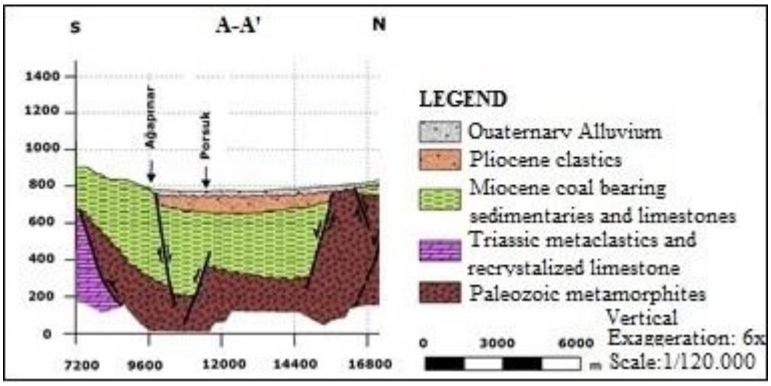

Figure 2.16 A-A' Geological Cross-Section (Modified from Yazıcıgil et al., 2018)

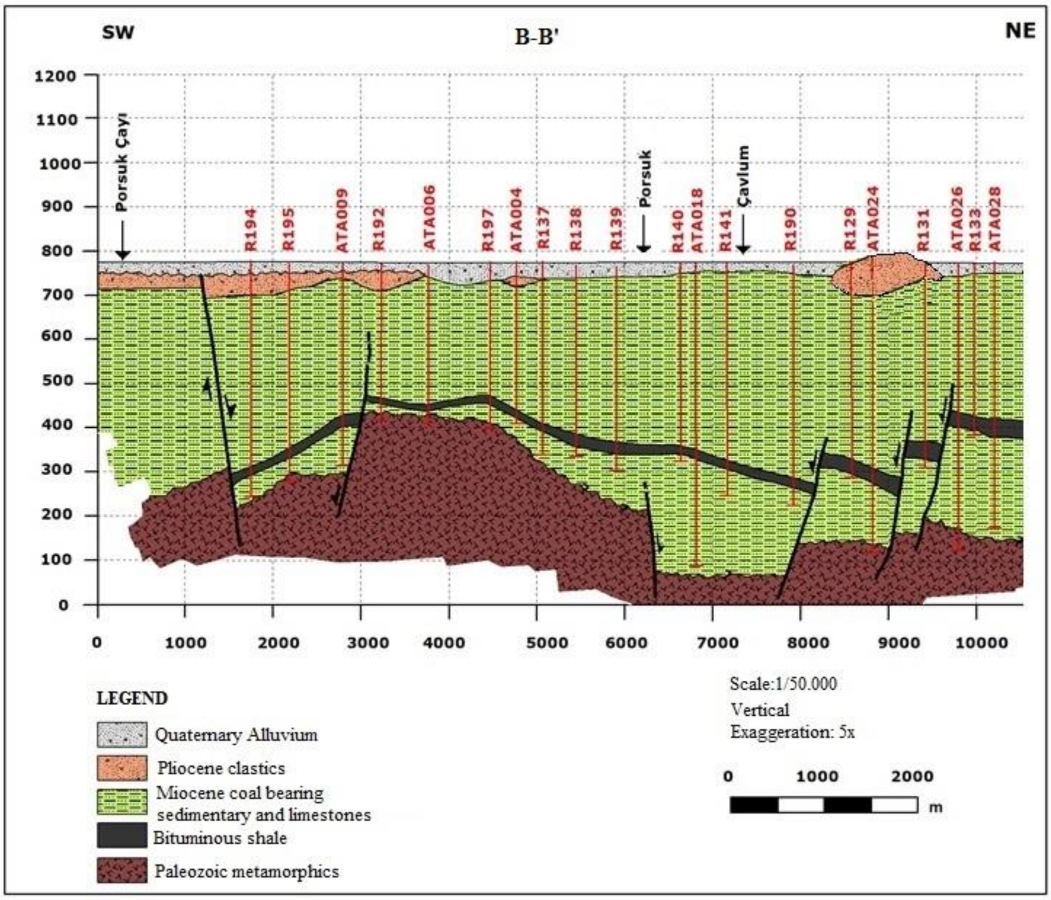

Figure 2.17 B-B' Geological Cross-Section (Modified from Yazıcıgil et al., 2018)

2.4.3. Structural Geology of the Study Area

Twelve faults have been determined within Sector-A in a study entitled 'Development of a Model for Bringing in Eskişehir Alpu Coal Basin's Resources into Country's Economics in an Optimal Manner' which had been conducted by the Hacettepe University Technology Transfer Center (HT-TTM, 2016) and these faults are shown on the map given in Figure 2.15. These faults extending mainly in NW, NE and EW directions have normal fault components. The lengths of the faults within the map prepared vary between 1.2 km and 4.6 km.

CHAPTER 3

HYDROLOGY

To understand the hydrologic structure and surface water potential of the watershed encompassing the study area, the surface water drainage network, the discharges of the rivers and creeks with significant drainage area and the water structures located upstream, downstream and around the study area have been investigated. In the paragraphs below, regional scale surface water hydrology will be evaluated first, followed by information on hydrological observations and analysis at the study area scale will be provided. Finally existing and planned water structures in the region, including their use will be discussed.

3.1. Regional Drainage Network

The most important surface water in Sector-A and its vicinity, located in the western part of Sakarya River Basin, is the Porsuk Stream which flows from west to east through Sector-A (Figure 3.1).

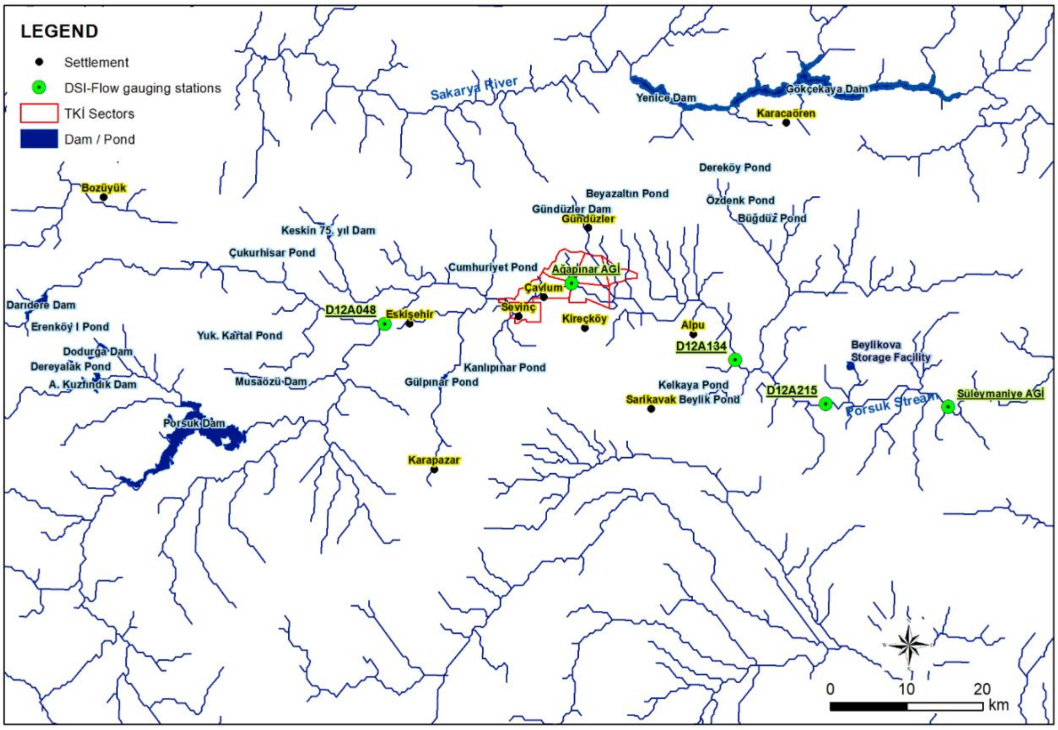

Figure 3.1. The map showing the regional drainage network of the study area and its surroundings, flow gauging stations and surface water structures (Yazıcıgil et al., 2018)

Porsuk Stream starts drainage from the Murat Mountain and combines with Kocaçay, Avşar Creek, Kokarçay and Kureyşler Creek near Eymir village in Altıntaş District at 1010 m elevation. It then runs through Kütahya Plain and after being collected behind the Porsuk Dam located in southwest of City of Eskişehir, passes through Eskişehir Plain and the Eskişehir city center. After the city center, Porsuk Stream enters the study area at the western part of Sector-A and flows 8.4 km through Sector-A and continue flowing east. Porsuk Stream finally joins Sakarya River around Sazılar-Yassıhöyük located 100 km east of Sector-A at an elevation of 676 m. Porsuk Stream is the longest tributary of the Sakarya River.

3.1.1. Flow Gauging Stations

To understand the hydrologic structure and surface water potential of the Sector-A and its vicinity, the discharge values of the surface water units should be monitored. For this purpose, the discharge values of the previously installed flow gauging stations

(AGI) located in the vicinity of the study area and operated by the State Hydraulic Works (DSI) were analyzed.

Existing five flow gauging stations operated by DSI within the watershed of the Porsuk Stream that flows across Sector-A (Figure 3.1) record the discharge rates of different locations of Porsuk Stream in different time periods or simultaneously. Table 3.1 lists the data inventory belonging to these gauging stations. The gauging stations located in Ağapınar and Süleymaniye villages were operated by DSI for a short period for a specific study (DSI 2010), and instantaneous discharge measurements are available once-a-month. The station No. D12A215 was operated only between 2012-2014 years. Other stations have more long-term data.

Table 3.1. Data inventory belonging to the current flow gauging stations operated by DSI (Yazıcıgil et al., 2017)

No	Station No.	Station Name	Stream/lake Name	Operation period	Coordinates		Elevation	Watershed
					Longitude	Latitude	(m)	(km^2)
1	E12A048	Eskişehir	Porsuk Stream	1973-2003	284619	4405262	793	6340
2	D12A134	Yeşildon	Porsuk Stream	1977-1984; 1988-1993; 1995-1998	330032	4400112	750	7580
3	D12A215	Parsibey	Porsuk Stream	2012-2014	342300	4395025	750	8671
4	D12A999	Ağapınar	Porsuk Stream	2007-2009	309147	4410574	771	--
5	-	Süleymaniye	Porsuk Stream	2007-2009	358531	4394335	755	--

Monthly based average discharge rates of flow gauges operated by DSI on Porsuk Stream are presented in Figure 3.2. For station No. E12A048, located in the upstream of the study area, the monthly average discharge values range between 2.90 m^3/s and 5.19 m^3/s; with a long-term average discharge rate of 3.99 m^3/s. For station No. D12A134, located to the east of Alpu, monthly average discharge rate ranges between 6.76 m^3/s and 12.29 m^3/s; with a long-term average discharge rate of 9.56 m^3/s. Since station No. D12A134 has a larger catchment area high discharge rate compared to station No. E12A048 is expected. In addition, the differences in the operation periods of the stations (Table 3.1) further complicate the comparisons. For example, the station No. D12A215 that was operated only for water years 2012-2014, has a larger watershed area compared to station No. D12A134, but generally lower discharge rates were measured.

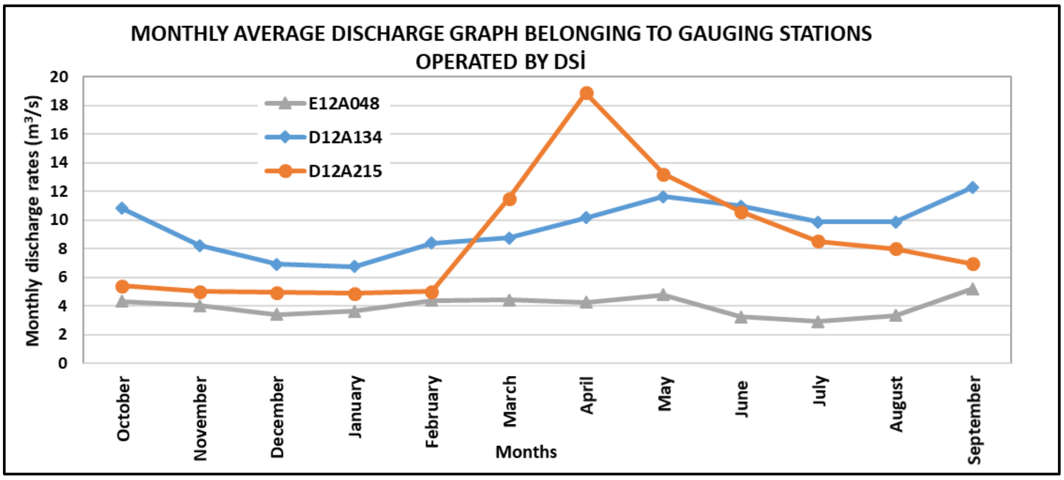

Figure 3.2. Monthly average discharge rates of the DSİ gauging stations (see Table 3.1 for the operation periods of gauging stations) (Yazıcıgil et al., 2018)

Within the scope of the study carried out by DSI (2010), instantenous disharge measurements were made on monthly basis at Ağapınar station and another station located nearly 60 km downstream, close to Süleymaniye (Table 3.1). The monthly instantaneous discharge measurements at these stations are shown in Figure 3.3.

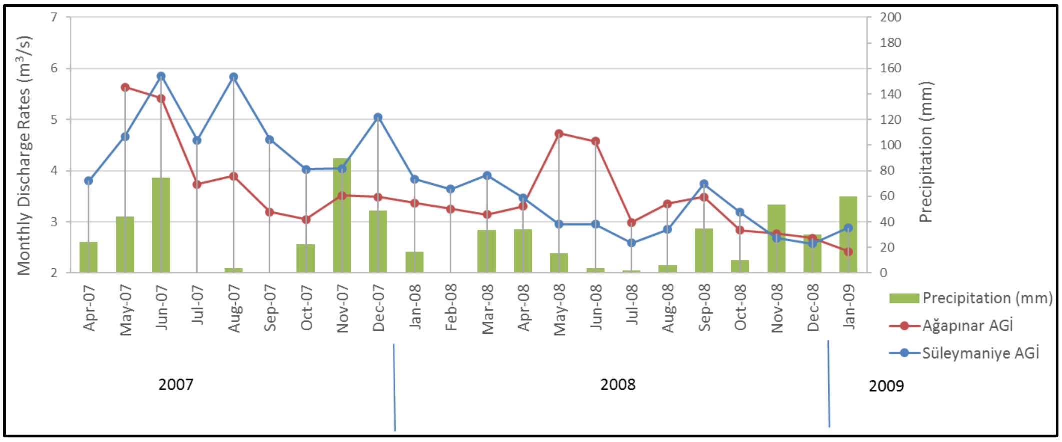

Figure 3.3. Monthly discharge rates at Ağapınar and Süleymaniye gauging stations between 2007-2009 (DSI, 2010) (Yazıcıgil et al., 2017)

At the measurement period, for Ağapınar station, located in the upstream of the study area, the instantaneous discharge values range between 2.42 m^3/s (January 2009) and 5.64 m^3/s (May 2007); with an average discharge rate of 3.56 m^3/s. In the same period, for Süleymaniye station, located in the downstream of the study area, the instantaneous discharge values range between 2.57 m^3/s (December 2009) and 5.86 m^3/s (June 2007); with an average discharge rate of 3.81 m^3/s.

3.2. Drainage Network of The Study Area

The drainage network of the study area is given in Figure 3.4. As it can be seen from Figure 3.4, the most important surface water in Sector-A and its vicinity is the Porsuk Stream that flows from west to east through Sector-A as mentioned in Section 3.1 in detail. Other than Porsuk stream, generally dry stream beds exist in the vicinity of Sector-A. These drainages show short-term flow after sudden rainfall and snow melt.

The surface water flow in the region encompassing Sector-A is also controlled by irrigation and dewatering channels located around the Porsuk Stream. Starting from the Porsuk Dam and the Karacaşehir regulator, located 7 km and 17.5 km southwest of Eskişehir and Sector-A, respectively, the right wing irrigation channel passes through south of Sector-A and left wing irrigation channel passes through the northern part of Sector-A and extend to Yeşildon. The connections between these irrigation channels are provided by ditches and dewatering channels (Figure 3.4). The irrigated agriculture in the region encompassing the study area is generally met by water from these channels.

The Porsuk Stream is investigated with the start of the study and two surface water flow stations in the upstream of Sector-A at Hasanbey locality (SW-5) and Yassıhöyük bridge (SW-5 alternative) and two stations in the downstream at Ağapınar bridge (SW-6) and Karahöyük bridge (SW-7) were established (Figure 3.4). The pictures of these monitoring points are shown in Figure 3.5. Starting from June 2016 till April 2017, the average and maximum water velocity, average and maximum depth, instantaneous flow rate and temperature are measured once a month by Ekoton Environmental and Agricultural Engineering Ltd. using Acoustic Doppler Flowmeter. With the Acoustic Doppler Flowmeter shown in Figure 3.6 it was possible to determine the wetted area in natural stream bed accurately and the flow area was divided into several blocks and the flow velocity was measured concurrently in each block. Thus, the flow measurements were conducted pretty accurately. As an example for the measurements taken, the flow profile at SW-5 monitoring point on June 2016 is shown in Figure 3.7 and measured results are shown in Figure 3.8. The measured flow rates between June 2016 and April 2017 encompassing the study period are given in Table 3.2 and displayed graphically on Figure 3.9. With the progress of the study, the flow measurements at SW-5 alternative point are discontinued due to the presence of channels mixing the Porsuk Stream at downstream and flow measurements are continued at SW-5 point at the upstream.

The flow values measured at stations (SW-5 and SW-alternative) upstream of Sector-A varied between 2.52 m^3/s and 7.24 m^3/s. The flow values at downstream station at Ağapınar Bridge (SW-6) varied between 3.40 m^3/s and 11.40 m^3/s and at Karahöyük Bridge (SW-7) they varied between 4.03 m^3/s and 11.1 m^3/s (Table 3.2). As it can be seen from Figure 3.9, the flow rates reached maximum values in August and September months and decreased to minimum values in October, November and December months. To be able to store water in winter months in the Porsuk Dam, significant amounts of water is released in the summer months.

While the flow rates measured at the downstream points (SW-6 and SW-7) are close to each other, the flow rates measured at the upstream points (SW-5 and SW-5 alternative) are 1.0 m^3/s to 5 m^3/s lower than the downstream points. This difference in flow rates are caused by the mixing of discharges from Organized Industrial District and Eskişehir city center between SW-5 and SW-6 points into the Porsuk Stream.

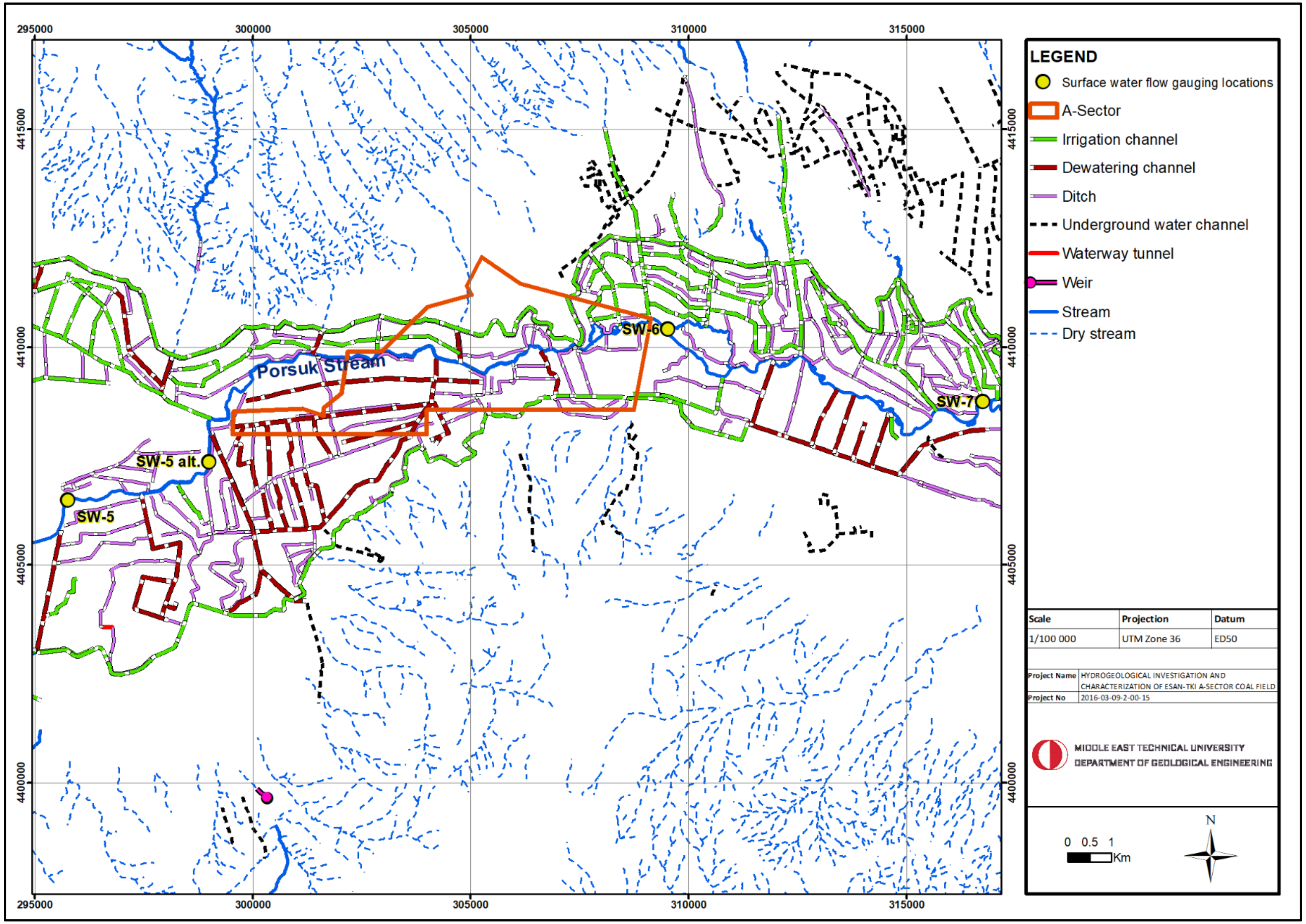

Figure 3.4. The drainage network of the study area (Yazıcıgil et al., 2017)

Figure 3.5. The field photograph of the surface water flow gauging points

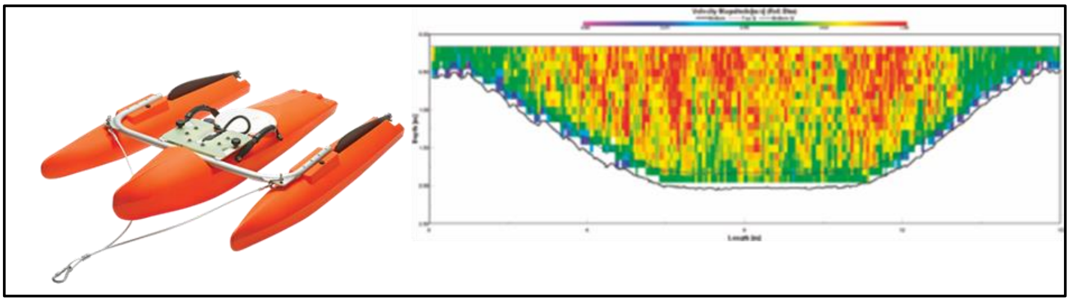

Figure 3.6. The Acoustic Doppler Flowmeter and wetted area section (Yazıcıgil et al., 2017)

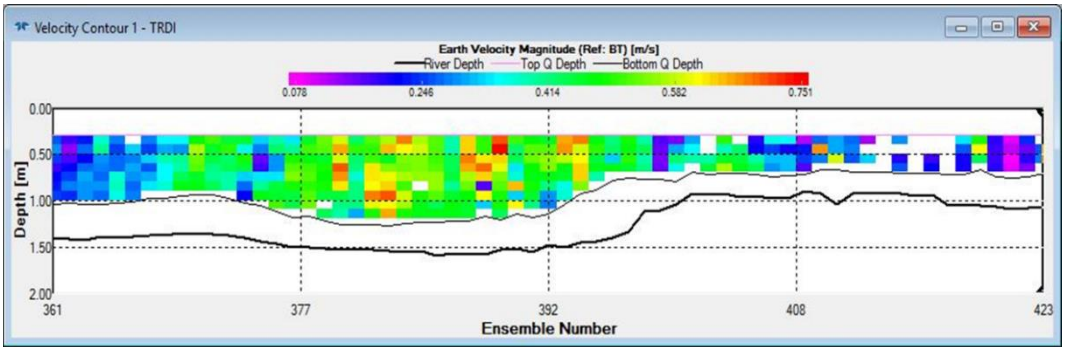

Figure 3.7. The flow profile prepared by using Acoustic Doppler Flowmeter (Yazıcıgil et al., 2017)

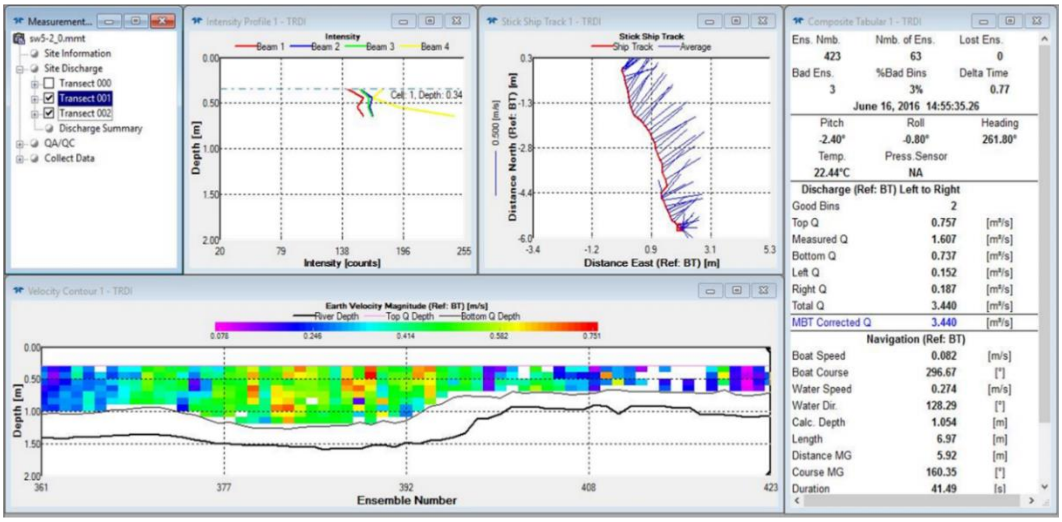

Figure 3.8. Acoustic Doppler Flowmeter measurement results (Yazıcıgil et al., 2017)

Table 3.2. The measurement results for surface water flow gauging points (Yazıcıgil et al., 2017)

Station Name	Coordinates		Date	Average water velocity (m/s)	Maximum water velocity (m/s)	Average depth (m)	Maximum depth (m)	Temp. (°C)	Discharge (m^3/s)
	East (m)	North (m)							
SW-5 (Hasanbey locality)	295770.308	4406495.275	16.06.2016	0.340	0.766	1.01	1.59	22.4	3.40
			21.09.2016	0.352	3.390	2.01	2.48	17.8	5.98
			15.10.2016	0.222	0.937	1.78	2.11	17.0	3.08
			19.11.2016	0.349	0.913	1.24	1.57	12.0	3.17
			21.12.2016	0.334	1.040	0.99	1.41	8.0	2.98
			19.01.2017	0.383	1.150	1.04	1.47	9.6	3.51
			20.02.2017	0.405	1.370	0.95	1.34	11.1	3.31
			16.03.2017	0.426	1.230	0.94	1.40	12.7	3.52
			14.04.2017	0.350	1.300	0.87	1.25	19.7	2.52
SW-5 Alternative	299002.000	4407374.000	16.06.2016	0.109	1.350	1.84	2.37	22.9	3.48
			19.07.2016	0.174	2.900	1.77	2.32	21.3	4.51
			16.08.2016	0.217	0.490	2.24	2.51	18.6	7.24
SW-6 (Ağapınar Bridge)	309535.595	4410410.959	16.06.2016	0.354	0.717	1.25	1.60	20.4	5.93
			19.07.2016	0.460	1.080	1.42	1.67	21.1	7.16
			16.08.2016	0.503	0.935	1.53	1.83	18.6	9.69
			21.09.2016	0.570	1.340	1.81	2.07	18.2	11.40
			15.10.2016	0.279	0.565	1.35	1.55	16.1	3.86
			19.11.2016	0.254	0.584	1.13	1.44	10.8	3.96
			21.12.2016	0.362	0.891	0.84	1.02	7.2	4.13
			19.01.2017	0.277	0.936	1.24	1.59	9.5	4.73
			20.02.2017	0.289	0.746	1.26	1.56	9.0	4.85
			16.03.2017	0.326	0.918	1.13	1.48	8.5	5.37
			14.04.2017	0.247	0.779	1.04	1.34	16.7	3.40
SW-7 (Karahöyük Bridge)	316754.729	4408751.134	16.06.2016	0.442	1.490	1.34	1.88	20.2	7.11
			19.07.2016	0.462	1.160	1.02	1.44	21.7	7.39
			16.08.2016	0.441	1.250	1.56	2.11	19.2	9.40
			21.09.2016	0.452	9.000	1.84	2.26	18.3	11.10
			15.10.2016	0.300	2.150	1.18	1.57	15.4	4.03
			19.11.2016	0.349	0.956	0.98	1.50	9.7	4.46
			21.12.2016	0.346	1.100	1.00	1.50	11.6	4.33
			19.01.2017	0.398	1.050	0.96	1.46	9.1	5.33
			20.02.2017	0.393	1.100	0.89	1.33	8.4	4.79
			16.03.2017	0.417	1.140	0.97	1.58	9.0	5.96
			14.04.2017	0.417	1.050	1.01	1.41	17.7	4.49

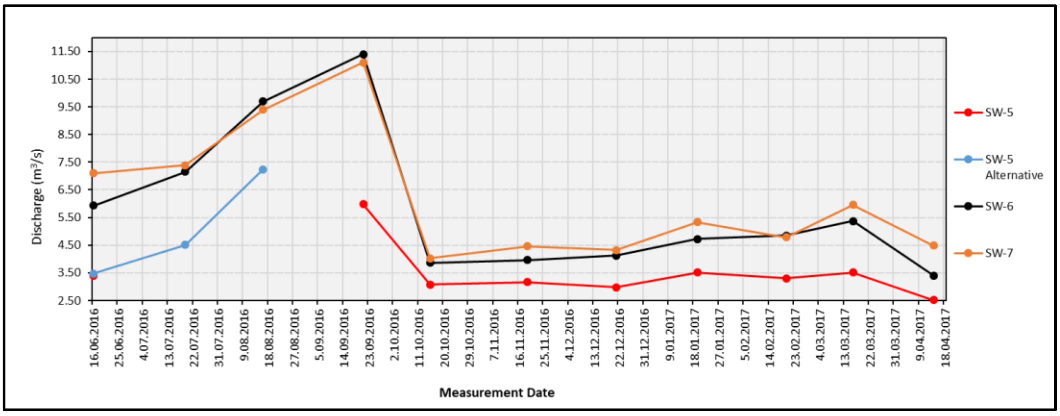

Figure 3.9. The measured flow rates between June 2016 and April 2017 (Yazıcıgil et al., 2017)

3.3. Existing and Planned Surface Water Structures and Their Use

Porsuk Stream is controlled by important water structures prior to reaching the study area (Figure 3.1, Table 3.3, Table 3.4). The most important one among these is the Porsuk Dam. Porsuk Dam started operation in 1948 and further expanded in 1972 for the purpose of supplying water to Eskişehir city center and flood control, in addition to irrigation water supply. Porsuk Dam is located 38 km to the southwest of the Sector-A. The information about other dams located in the vicinity of the study area is shown on Figure 3.1 and detailed information is provided in Table 3.3. The nearest dam to the Sector-A is the Gündüzler Dam which is situated 8 km northeast of the Sector-A and is under construction. There exist 9 ponds located around the Sector-A (Figure 3.1, Table 3.4). These ponds are primarily used for irrigation. The pond nearest to the Sector-A is the planned Cumhuriyet pond which is located 5 km towards northwest.

Table 3.3. Data inventory belonging to the existing and planned dams located around Sector-A (Yazıcıgil et al., 2017)

No.	Name	Location	River/stream /creek	Operation year	Purpose	Lake volume (hm^3)	Irrigation area (ha)	Drinking / Domestic (hm^3/year) Energy (MW)	Distance to Sector-A (km)
1	Aşağı Kuzfındık Dam	Eskişehir	Kocadere	2006	Irrigation	21.1	3241	--	53
2	Keskin 75. Yıl Dam	Eskişehir	Karagöz Creek	1998	Irrigation	8.4	1112	--	23
3	Musaözü Dam	Eskişehir	Mollaoğlu	1969	Irrigation	1.55	400	--	30
4	Porsuk Dam	Eskişehir	Porsuk	1972	Irrigation+Drinking /Domestic+flood	431	41020	--	38
5	Yenice Dam	Eskişehir	Sakarya	1999	Energy	57.6	--	38 MW	28
6	Gökçekaya Dam	Eskişehir	Sakarya	1972	Energy	910	--	278 MW	32
7	Gündüzler Dam	Eskişehir	Değirmen C.	Under construction	Irrigation	7.8	--	--	8

Table 3.4. Data inventory belonging to the existing and planned ponds located around Sector-A (Yazıcıgil et al., 2017)

No.	Name	Location	River/stream /creek	Operation year	Purpose	Lake volume (hm^3)	Irrigation area (ha)	Distance to Sector-A (km)
1	Beylik Pond	Eskişehir	Beylik	1985	Irrigation	0.40	150	23
2	Kanlıpınar Pond	Eskişehir	Tıngır Creek	1978	Irrigation	0.70	120	9
3	Kelkaya Pond	Eskişehir	Kelkaya Creek	1986	Irrigation	0.40	84	20
4	Büğdüz Pond	Eskişehir	--	Project phase	Irrigation	0.76	--	27
5	Beyazaltın Pond	Eskişehir	Gücük Creek	Under construction	Irrigation	1.02	--	14
6	Dereköy Pond	Eskişehir	Kapız Creek	Under construction	Irrigation	0.39	--	27
7	Cumhuriyet Pond	Eskişehir	--	Master plan and preliminary survey phase	--	--	--	5
8	Özdenk Pond	Eskişehir	--	In operation	--	--	--	25
9	Beylikova Storage Facility	Eskişehir	--	2016	Irrigation	71.36	1916	37

CHAPTER 4

HYDROGEOLOGY

4.1. Water Points

4.1.1. Surface Waters

The most important surface waters in Sector-A and its vicinity are the Porsuk Stream, which flows from west to east through Sector-A, and Eskişehir-Alpu left and right wing irrigation channels that start from Karacaşehir regulator and de-watering channels (Figure 3.1). Porsuk Stream starts drainage from the Murat Mountain, runs through Kütahya Plain and after being collected behind the Porsuk Dam located in southwest of City of Eskişehir, passes through Eskişehir Plain and the Eskişehir city center. After the city center, Porsuk Stream flows toward east and enters into Sector-A at the nortwest end, flows through the center of Sector-A toward east and leaves Sector-A around 2 km North of Ağapınar village. Porsuk Stream finally joins Sakarya River around Yassıhöyük located 100 km east of the study area. Porsuk Stream is the longest tributary of the Sakarya River.

In a scope of the study carried out by DSI (2010) in 2007-2009, monthly instantaneous flow measurements were conducted on the Porsuk Stream at Ağapınar Station and Süleymaniye Station which is approximately 60 km downstream (Figure 3.1). The measured instantaneous flow rates at these stations can be seen in Figure 3.3. At the measurement period instantaneous flow rates at the Ağapınar station which is upstream were observed in the range between 2.42 m^3/s (January 2009) and 5.64 m^3/s (May 2007), and the average value of the flow rate is 3.56 m^3/s. In the same period, flow rates at the Süleymaniye station, which is downstream, range between 2.57 m^3/s (December 2009) and 5.86 m^3/s (June 2007), and the average value of the flow rate is 3.81 m^3/s.

The interaction between surface water and groundwater as well as the recharge/discharge values should be known for the calculation of the groundwater budget for the study area. The Porsuk Stream which flows through the central part of Sector-A is recharged from groundwater. In other words, the Porsuk stream is a gaining stream. As explained in Section 4.3 it is decided that basin wide groundwater budget estimation is more appropriate. To calculate groundwater discharge to the Porsuk stream, the measured flow rates at Ağapınar and Süleymaniye stations were used. The difference between the dry seasons's (September) average flow rates at both stations give information about the groundwater discharge to the Porsuk Stream (base flow) from the area in between them. Accordingly, the base flow from an area of 2152.5 km^2 is calculated as $26.36x10^6$ m^3/year (0.836 m^3/s). When using the size of the Alpu basin (909.33 km^2), the base flow is estimated as $11.1x10^6$ m^3/year (0.353 m^3/s).

The baseflow value which was calculated for the whole plain area by DSI (2010) using discharge coefficient method is (0.879 m^3/s) $27.71x10^6$ m^3/year. This value is similar with the proceeding value which was calculated simply.

Apart from the Porsuk Stream, there is no other perennial streams in Sector-A. However, Eskişehir-Alpu left and right wing irrigation channels that start at Karacaşehir regulator and de-watering channels are situated in Sector-A. While the amount of water released to these channels through May and October period varies from year to year, the minimum value was $65x10^6$ m^3/year (2015) and the maximum was $147x10^6$ m^3/year (2006) between 2006 and 2016 period. The average rate of flow was $117x10^6$ m^3/year. Approximately 35% of this water is used for irrigation.

4.1.2. Wells

The wells in Sector-A and its vicinity can be grouped into four: (i) DSI wells, (ii) private wells, (iii) pumping and observation wells drilled within the context of the study and (iv) vibrating-wire piezometer wells. Locations of these wells are shown in Figure 4.1.

4.1.2.1. DSI Wells

There is no well drilled by DSI in Sector-A. However, 12 water wells have been drilled in the close vicinity of Sector-A by DSI and its sub-contractors between 1988 and 2012 for exploration, operation and observation purposes (Figure 4.1). All information (coordinates, elevation, depth, screened levels, water bearing formations, static and dynamic water levels) related with those wells are provided in Table 4.1. There are eight DSI wells which are located on the outside of the northeastern border of Sector-A. Five of these wells (54244, 54246, 54713, 60626, and 61566) are used by Kızılcaören Irrigation Cooperative and two (54247 ve 54248) are used by Danişment Irrigation Cooperative. Most of these wells generally penetrated a thin (10-25 m) Quaternary alluvium and ended in the Pliocene unit. However, they are fed by both lithologic units. Another well in this part of the area (54250) has been drilled for monitoring purposes. Two DSI wells in the outside of the southeast border of Sector-A were drilled for exploration (39005) and monitoring (61357) purposes. Apart from these wells, two wells (57820 and 57821) in the outside of the northwestern border of Sector-A have been used by Cumhuriyet Irrigation Cooperative for irrigational purposes. These wells penetrated 50 and 72 m thick alluvium and ended in Pliocene unit. They receive water from both lithological units. The greater thickness of the alluvium (50-72 m) and higher specific capacity of the wells (2.41 L/s/m – 1.53 L/s/m) are provided by the presence of the alluvial fan in this location.

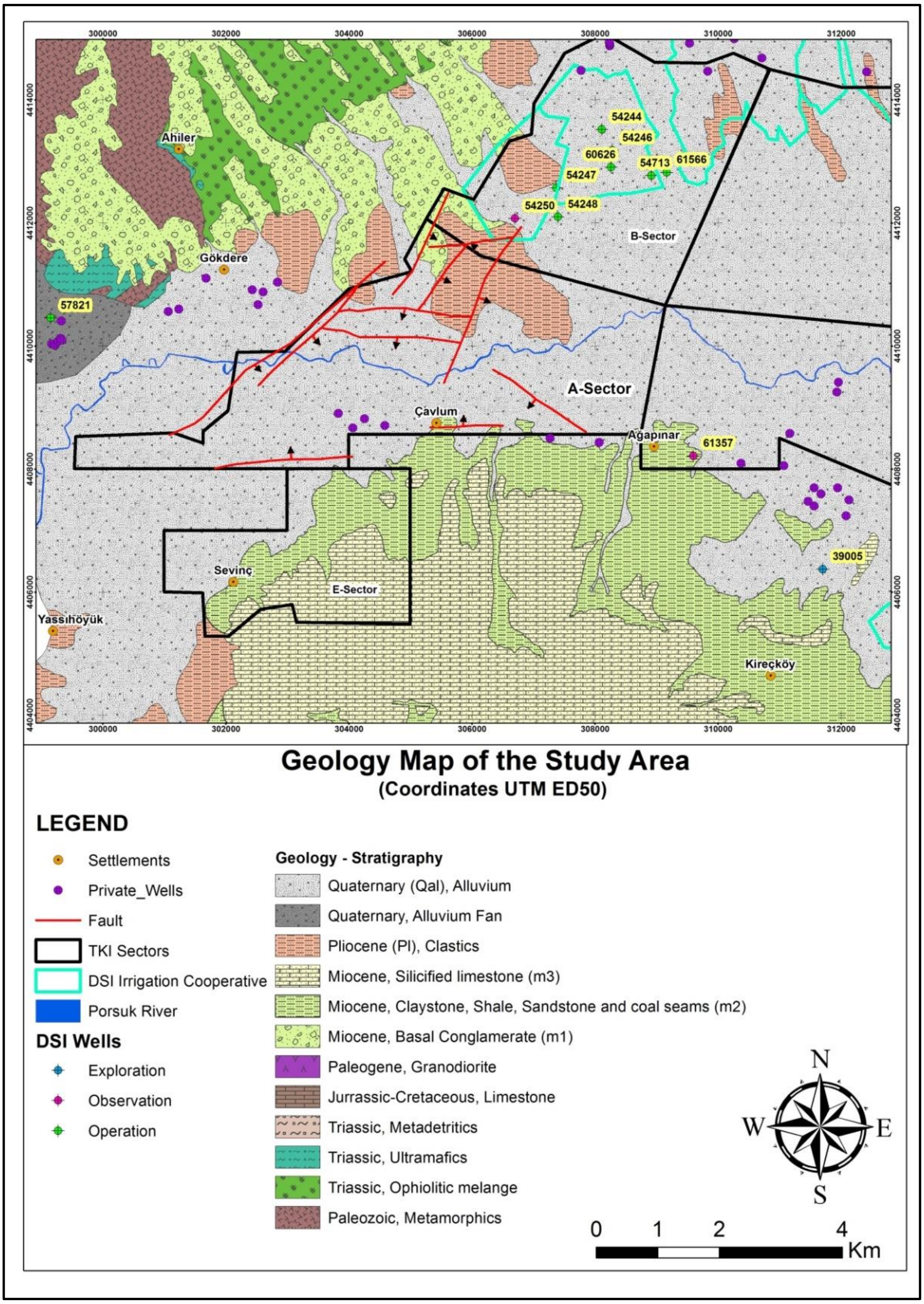

Figure 4.1. Location of the wells within Sector-A and its vicinity on geological map (Yazıcıgil et al., 2017).

Table 4.1. Information regarding the DSI wells in Sector-A and its vicinity (Yazıcıgil et al., 2017)

Well No	Drilling Contractor	Purpose	District	Well Location	Map Section No	Operation Year	Coordinates (ED50)		Elevation (m)	Well Depth	Screen (m)		Total Screen Length (m)	Aquifer Lithology	Static L. (m)	Dynaic L. (m)	Well Yield (L/s)	Specific Capacity (L/s/m)
							East	North			Top	Bottom						
39005	DSİ	Exploration	City Center	Ağapınar	i25b4	1988	311975	4406375	778	150	24	128	68	Conglamerate, Tuff, Marl, Schist	Artesian	54.05	4.00	0.07
54244	G&M Müh.	Operation	City Center	Kızılcaören	i25b4	1999	308175	4413175	789	102	16	96	40	Alluvium, Tuffite,Flysch	7.90	62.00	19.55	0.36
54246	G&M Müh.	Operation	City Center	Kızılcaören	i25b4	1999	308200	4412925	787	120	24	116	52	Alluvium, Tuffite,Flysch	8.60	61.06	17.66	0.34
54247	G&M Müh.	Operation	City Center	Danışment	i25b4	1999	307325	4412575	787	105	16	94	36	Alluvium, Flysch, Claystone, Mudstone, Marl	7.95	41.38	40.26	1.20
54248	G&M Müh.	Operation	City Center	Danışment	i25a3	1999	307400	4412100	780	150	22	90	32	Alluvium, Tuffite, Flysch, Claystone	5.60	39.42	53.42	1.58
54250	G&M Müh.	Observation	City Center	Danışment	i25a3	1999	306700	4412075	793	83	16	80	40	Alluvium, Tuffite, Flysch, Marl	14.80	63.07	5.17	0.11
54713	G&M Müh.	Operation	City Center	Kızılcaören	i25b4	1999	308850	4412750	781	117	16	112	40	Alluvium, Tuffite, Marl	2.00	52.34	42.13	0.84
57820	DENKA Jeo.	Operation	City Center	Cumhuriyet	i25a3	2002	298502	4410268	795	150	32	144	56	Alluvial Fan, Sandstone, Siltstone	13.10	29.96	40.62	2.41
57821	DENKA Jeo.	Operation	City Center	Cumhuriyet	i25a3	2002	299102	4410526	790	120	20	112	52	Alluvial Fan, Flysch	14.00	46.98	50.46	1.53
60626	DSİ	Operation	City Center	Kızılcaören	i25b4	2009	308427	4412692	780	136	20	130	54	Alluvium, Sandstone, Conglamerate, Sandstone	7.20	52.79	36.08	0.79
61357	DSİ	Observation	City Center	Ağapınar	i25b4	2012	309601	4408213	786	120	20	112	40	Marl, Sandstone	18.22	91.24	4.00	0.05
61566	DSİ	Operation	City Center	Kızılcaören	i25a2	2010	309177	4412857	783	120	24	112	56	Alluvium, Tuffite, Flysch	4.10	49.90	25.08	0.56

4.1.2.2. Private Wells

Field studies are conducted in Sector-A and its vicinity to determine the distribution of the private wells. The locations of these wells are presented in Figure 4.1. As a result of field surveys 32 private wells have been determined. Twenty-eight of these wells are outside of Sector-A, located mostly in the northwestern and southeastern part of Sector-A. Four wells that were determined in Sector-A are located in the west of Çavlum village and are used for irrigational purposes.

4.1.2.3. Pumping and Observation Wells

Five pumping and observation well clusters have been established to determine the water bearing properties of hydrogeological units in Sector-A, to estimate their hydraulic parameters and to investigate the hydraulic relations between each other and coal seams (Figure 4.2). A total of 1985.5 m of drilling is conducted between June and December 2016 for a total of 13 wells with depths ranging between 58.5 m and 460 m. The drilling and completion of these wells were done largely in accordance with the technical specifications prepared by METU (Yazıcıgil et al., 2017) but small variations were made due to the local ground and hydrogeological conditions. All well information such as type, depth, drilling and completion diameters, and screened intervals are provided in Table 4.2. The well logs showing the completion details of all wells are given in Appendix A.

After the completion and washing with clean water, each well is developed with air lifting using a compressor and pumping with submerged pumps. Pumping and recovery tests were conducted at some pumping wells. In those wells that were not possible to conduct pump tests due to low yields, slug tests were conducted to determine the hydraulic conductivity of the units.

The well clusters were established at 5 different locations in Sector-A as it can be seen from Figure 4.2. These locations were defined after analyzing the general hydrogeology of the study area and coal exploration well logs of MTA (R-wells).

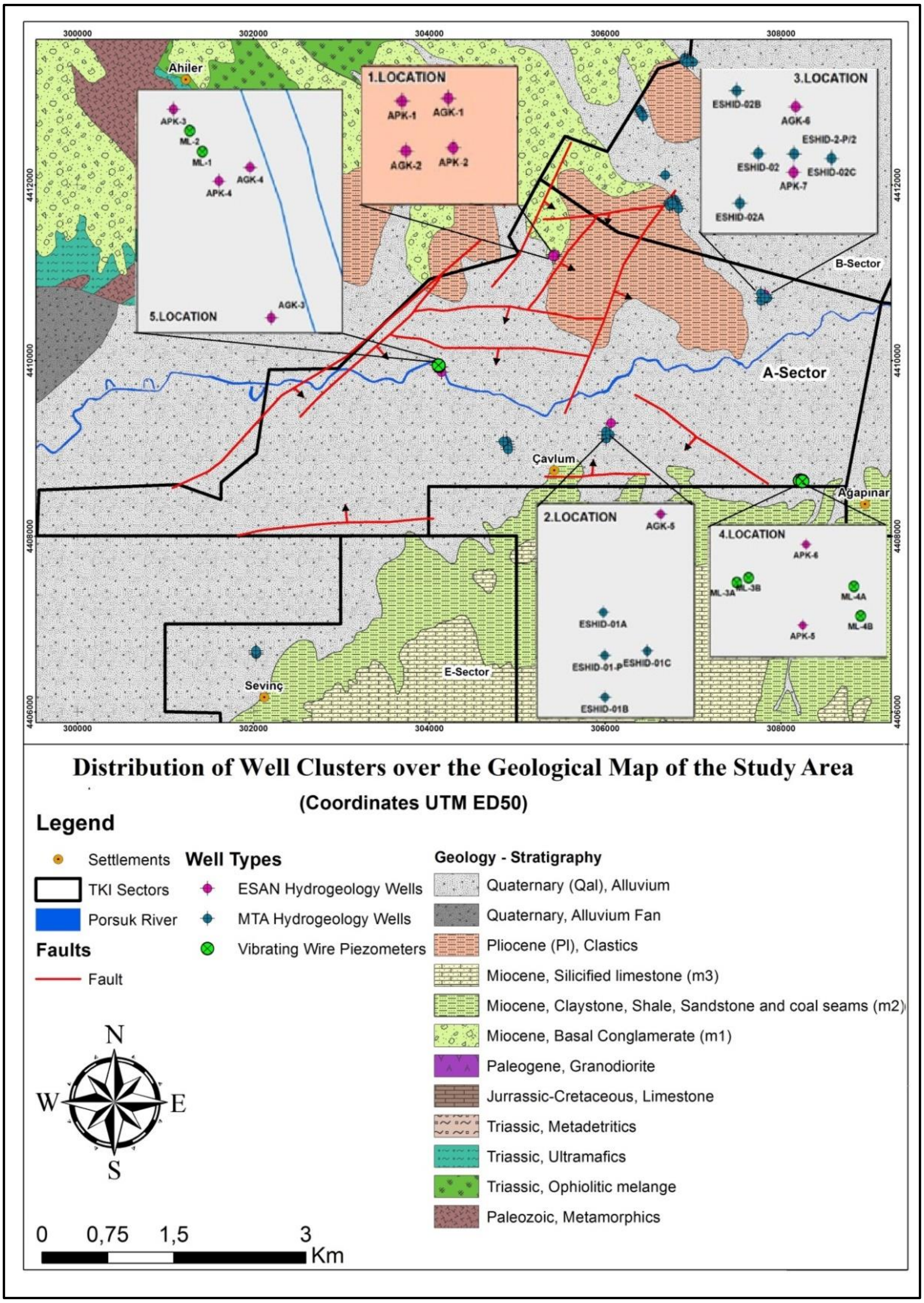

Figure 4.2. Pumping/observation wells and vibrating wire piezometer locations in Sector-A (Yazıcıgil et al., 2017).

Table 4.2. Information regarding the pumping/observation wells drilled within Sector-A (Yazıcıgil et al., 2017).

Well Location	Well ID	Well Type	East (m)	North (m)	Elev. (m)	Depth (m)	Screen Interval (m)	Well Diameter (inch)	Casing Diameter (mm)	Casing Interval	Target Geological Unit
1. Location	APK-1	Pumping Well	305407.68	4411207.21	803.027	280	200-272	17.5	219	Steel	Coal (A, B and C seam) and under coal Miocene (Claystone, Siltstone, Sandstone)
	AGK-1	Observation Well	305427.50	4411208.42	804.291	280	196-272	17.5	219	Steel	Coal (A, B and C seam) and under coal Miocene (Claystone, Siltstone, Sandstone)
	APK-2	Pumping Well	305429.75	4411188.39	803.972	58.5	14.5-54.5	17.5	280	PVC	Miocene (Claystone, sandstone and siltstone alternation)
	AGK-2	Observation Well	305409.33	4411187.18	802.450	60	12-56	12.5	175	PVC	Miocene (Claystone, sandstone and siltstone alternation)
2. Location	AGK-5	Observation Well	306069.65	4409289.19	773.918	60	12-56	12.5	175	PVC	Quaternary Alluvium (Clay, sand, gravel) and Miocene (Claystone, sandstone and siltstone alternation)
3. Location	AGK-6	Observation Well	307820.54	4410752.28	772.256	75	15-67	12.5	175	PVC	Pliocene (Claystone, sandstone, siltstone, conglomerate and limestone alternation)
	APK-7	Pumping Well	307818.88	4410704.19	772.264	72	16-68	17.5	280	PVC	Pliocene (Claystone, sandstone, siltstone, conglomerate and limestone alternation)
4. Location	APK-5	Pumping Well	308232.60	4408619.22	773.158	400	44-392	17.5	219	Steel	Miocene (Claystone, sandstone and siltstone alternation) and Coal (A, B and C seam)
	APK-6	Pumping Well	308233.44	4408638.93	773.104	60	16-56	17.5	280	PVC	Quaternary Alluvium (Clay, sand, gravel) and Miocene (Claystone, sandstone and siltstone alternation)
5. Location	APK-3	Pumping Well	304099.96	4409953.99	776.191	460	56-452	17.5	219	Steel	Quaternary Alluvium (Clay, sand, gravel) and Miocene (Claystone, sandstone and siltstone alternation) and Coal (A, B, C and D seam)
	AGK-3	Observation Well	304141.19	4409870.11	777.202	60	12-56	12.5	175	PVC	Quaternary Alluvium (Clay, sand, gravel)
	APK-4	Pumping Well	304119.13	4409925.05	777.504	60	16-56	17.5	280	PVC	Quaternary Alluvium (Clay, sand, gravel)
	AGK-4	Observation Well	304132.30	4409930.55	777.369	60	12-56	12.5	175	PVC	Quaternary Alluvium (Clay, sand, gravel)

The location of the first clusters of the wells is at the northern part of Sector-A, in the vicinity of exploration borehole ATA020 (Figure 4.2). At this location, claystone, sandstone and siltstone alternations, coal seams (A, B, C) and sub-coal claystone, siltstone and sandstone units belonging to Miocene units have been penetrated. To determine the water bearing properties among Miocene units and hydraulic relations between them, two wells, consisting of one pumping and one observation well, were drilled. The pumping well APK-1 and observation well AGK-1, having depths of 280 m each, were screened in lignite zones and Miocene units to determine their hydraulic parameters. In the near vicinity of these wells (~ 20 m), APK-2 pumping well was drilled at a depth of 58.5 meters and the AGK-2 observation well was drilled at a depth of 60 m in the claystone, sandstone and siltstone alternations belonging to Miocene units. The information regarding the aquifer tests conducted and water levels measured will be presented in the following sections.

The location for the second cluster of wells was selected in ESHID-01 cluster of wells drilled by MTA (Bayram, 2015) within the scope of the pre-hydrogeological survey conducted in 2015 in the Alpu Coal basin. This well cluster is located in the northeast of Çavlum village and there are four wells drilled by MTA, consisting of a ESHID-01P pumping well with a depth of 67 m and three observation wells, namely, ESHID-01A, ESHID-01B and ESHID-01C with depths of 76 m, 62 m and 62 m, respectively. Because the observation wells drilled by MTA were about the same distance (40-43 m) away from the pumping well and the pump test conducted was of short duration (22 hours), an observation well (AGK-5) with a depth of 60 m was drilled 148 m away from the ESHID-01P pump well. According to the information obtained from the report entitled Eskişehir-Alpu Coal Basin Detailed Hydrogeological Pre-Survey Report prepared by MTA (Bayram, 2015), the ESHID-01P pump well was drilled with a diameter of 15 inches and penetrated Quaternary alluvium deposits consisting of loosely bounded sand and gravel alternations with local clay lenses and entered into a gray clay at 52 m depth and terminated at a depth of 67 m. However, the examination of logs of diamond drill core hole R-190 drilled at 66 m north of ESHID-01P pump well by MTA in 2012 revealed that ESHID-01P well entered into Miocene unit after cutting 33 m thick alluvium consisting of clay, sand and gravel alternations. Consequently, all the wells drilled in this location recieve water from both the alluvium and Upper Miocene units. After completion of AGK-5 observation well, a pumping test with a duration of 80 hours (3 days 8 hours) was conducted at ESHID-01P pump well and joint hydraulic parameters of both units were determined.

The location for the third cluster of wells was selected in the northeast part of Sector-A where ESHID-02P and ESHID-02/P2 pump wells, drilled also by MTA (Bayram, 2015) within the scope of the pre-hydrogeological survey conducted in 2015, are located. There are four wells that consist of ESHID-02P pumping well and three observation wells (ESHID-02A, ESHID-02B and ESHID-02C), each having a depth of 350 m. Apart from these wells, there exist another pump well (ESHID-02/P2) having a depth of 75 m in this location. According to the information obtained from the report prepared by MTA (Bayram, 2015), the ESHID-02P pump well was drilled with a diameter of 17.5 inches and penetrated Quaternary alluvium deposits consisting of loosely bounded sand and gravel alternations with local clay lenses and entered into a gray clay at 52 m depth. Afterwards it penetrated Miocene claystone, locally sandstone and conglomerate banded, and limestone alternations and terminated at a depth of 350 m. However, the examination of logs of diamond drill core holes, R-82 drilled at 190 m southeast of ESHID-02P by MTA in 2011 and ATA001 drilled by ESAN at 350 m southwest of ESHID-02P, revealed that ESHID-02P well after cutting 4 m of Quaternary age alluvium consisting of clay, sand and gravel alternations entered into Pliocene unit that consists of alternations of claystone, sandstone, siltstone, conglomerate and limestone. The well continued within the Pliocene unit up to a depth of 153 m and entered into Miocene claystone, sandstone and siltstone alternations and finally terminated within this unit at a depth of 350 m. It is decided to conduct a long-term pumping test at ESHID-02P well because the test conducted by MTA was of short duration (15 hours). Furthermore, it has been also decided to drill an observation well in the vicinity of ESHID-02/P2 well, completed only within the Pliocene unit, and repeat the pumping test at ESHID-02/P2 pump well. Consequently, an observation well (AGK-6) having a depth of 75 m was drilled at 21 m north of ESHID-02/P2 pump well. However, when the pump was lowered to ESHID-02/P2 well to conduct the pump test, it could not be lowered because the well was plugged at about 20 m depth. Hence, a new pump well (APK-7), having a depth of 72 m, had to be drilled at 14 m south of ESHID-02/P2 well. Finally, pumping tests were conducted separately at both ESHID-02P and APK-7 wells and hydraulic parameters of the units screened by each well were calculated.

The location for the fourth cluster of wells was selected at the southeastern part of Sector-A. The criteria for selecting this location was the inadequate existing hydrogeological information at the southeastern part of Sector-A. The pumping wells APK-5 and APK-6, having depths of 400 m and 60 m, respectively, were drilled in this location. The APK-5 pump well has been screened lignite bearing (A, B, and C seams) Miocene units. The APK-6 pump well, however, was screened in the alluvium and Upper Miocene units. As it will be explained in Section 4.1.2.4, four (ML-3A, ML3-B, ML-4A ve ML-4B) diamond drill core holes were also drilled in this location and a total of 8 vibrating wire piezometers were installed to different depths. Following the installation of the vibrating wire piezometers, pumping tests were conducted separately at both APK-5 and APK-6 wells and joint hydraulic parameters of Miocene and Alluvium-Miocene units were calculated.

The location for the fifth cluster of wells was selected at the west of Sector-A in the near vicinity of the Porsuk Stream. The aim for selecting this location was to test the hydraulic connection with Porsuk Stream and the Alluvium aquifer and to establish a system which will test the whole units and only the alluvium unit. In this cluster, located about 20 m away from the Porsuk Stream, a pump well (APK-3) with a depth of 460 m was drilled and screened in all units (Alluvium, Pliocene and lignite bearing (A, B, C, and D seams) Miocene units). In addition, APK-4 pump well and AGK-3 and AGK-4 observation wells, each having 60 m depth, were drilled and all screened only in the alluvium. As it will be explained in Section 4.1.2.4, two (ML-1 and ML-2) diamond drill core holes were also drilled in this location and a total of 5 vibrating wire piezometers were installed to different depths. Following the installation of the vibrating wire piezometers, pumping tests were conducted separately at both APK-3 and APK-4 wells and joint hydraulic parameters of all units and the alluvium only and its relation with the Porsuk Stream were determined.

4.1.2.4. Vibrating Wire Piezometer Wells

Among 5 well cluster locations established in Sector-A for hydraulic testing, six diamond drill core holes were drilled at 4th and 5th well cluster locations, with a total drilling depth of 1558 m, to install vibrating wire piezometers. The coordinates, well depth and vibrating wire installation depths are given in Table 4.3 and locations are shown in Figure 4.2. Four (ML-3A, ML3-B, ML-4A ve ML-4B) diamond drill core holes were drilled in the 4th well cluster location near the southeastern border of Sector-A and 8 vibrating wire piezometers with depths ranging between 16 m and 390.2 m were installed in these core holes and each core hole was subsequently grouted with slurry consisting of 1 unit (by weight) cement, 2 units water and 0.36 unit bentonite mixture (Figure 4.3). After completion of grouting works data loggers were installed and kept within metal protective boxes as shown in Figure 4.4. The well logs showing the lithology and installation depth of vibrating wire piezometers for ML-3A & ML-3B and ML-4A & ML-4B core holes in the 4th well cluster location are given in Appendix B.

Table 4.3. Information regarding the vibrating wire piezometers (Yazıcıgil et al., 2017).

Well ID	Coordinates (UTM ED50)		Well Depth (m)	Vibrating Wire Piezometer Levels (m)
	X	Y		
ML-1	304112.034	4409936.69	144	32
				53
				70
ML-2	304106.726	4409945.124	458.5	375.4
				439.9
ML-3A	308215.926	4408629.582	180	108
				163
ML-3B	308218.929	4408630.736	39	16
				30
ML-4A	308245.585	4408628.639	328	224.95
				307.95
ML-4B	308247.275	4408621.42	408.5	332.2
				390.2

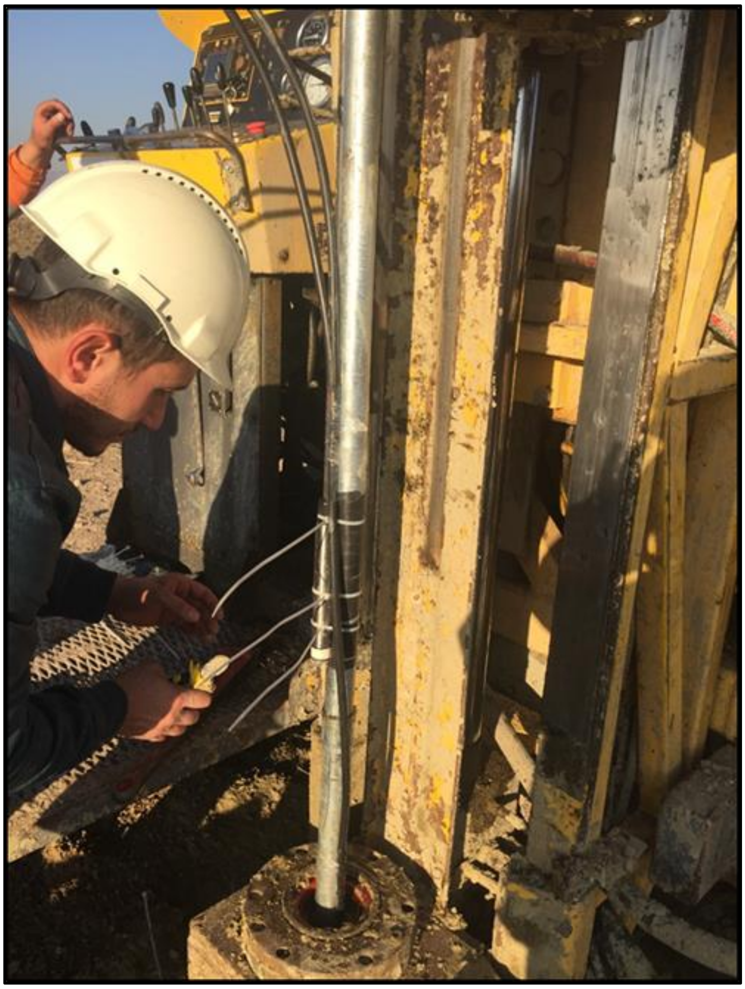

Figure 4.3. Installation process of vibrating wire piezometers in ML-3A well

Figure 4.4. Location of vibrating wire piezometers ML-3 and ML-4

Two (ML-1 and ML-2) diamond drill core holes were drilled in the 5th well cluster location in the west of Sector-A in the vicinity of the Porsuk Stream. Five vibrating wire piezometers with depths ranging between 32 m and 439.9 m were installed in these core holes and each core hole was subsequently grouted with slurry consisting of 1 unit (by weight) cement, 2 units water and 0.36 unit bentonite mixture. After completion of grouting works data loggers were installed and kept within metal protective boxes as shown in Figure 4.5. The well logs showing the lithology and installation depth of vibrating wire piezometers for ML-1 and ML-2 core holes in the 5th well cluster location are given in Appendix B.

Figure 4.5. Location of vibrating wire piezometers ML-1 and ML-2

The vibrating wire piezometers continually record groundwater pressures and temperatures at the installation depths. The pressure and temperature data monitored over the short period of duration (1-2 months) at the time of report writing will be presented in detail in Section 4.2.4. With the help of these piezometers the variations in the hydrogeological system and responses there to during mining activities will be continually monitored and will enable necessary precautions to be taken on time. In addition, knowing the groundwater pressures and temperatures in the coal seams and beneath them will provide important information for the design of panels and necessary support structures. However, the number of vibrating wire piezometers installed in this study are not sufficient and hence, more vibrating wire piezometers need to be installed at critical locations during the operation stage.

4.2. Hydrogeology of Sector-A

The hydrostratigraphic units in Sector-A are grouped into four: (i) Quaternary alluvium, (ii) Pliocene limestones, sandstones and conglomerates, (iii) lignite bearing Miocene units and (iv) basement rocks. The water bearing properties of these units are explained in the following sections.

The Paleozoic age metamorphic schists, Mesozoic age Ophiolites and the Jurassic-Cretaceous limestones form the basement in Sector-A and its close vicinity (Figure 4.1). These rocks are generally impervious and semi-pervious and may carry groundwater along fractures that result from faulting. The logs of coal exploration holes drilled in Sector-A and its vicinity are examined and are separated based upon the bedrock unit penetrated and are shown in the bedrock surface map prepared (Figure 4.6). The bedrock surface contours shown in this map are drawn without faults being considered. The examination of the bedrock surface contours shows that the bedrock attains its deepest elevation (less than 100 m) at the north of the Çavlum village. In ATA018 core hole the bedrock was not encountered even at a depth of 700 m. The drop in the northern blocks of the basement faults extending in East-West direction in the south of Sector-A probably caused a deepening of the Miocene coal basin in the vicinity of the Çavlum village. Starting from the Çavlum village and continuing in northeast direction this deep basin extends to the border between Sector-A and Sector-B. The basement rocks become elevated to the west, northwest and east of Sector-A. When the cores cutting the basement are examined it is seen that they are schists in the deepest part of the bedrock in the middle of Sector-A and are impervious. The basement rocks to the northwest of Sector-A consist of ophiolites and schists. These rocks are impervious units. No marble is encountered in the core holes penetrating the bedrock in Sector-A. The bedrock in the ESAN's license area in the south of Sector-A and in the south of Sector-E consists of Jurassic-Cretaceous limestones. The pumping test conducted in a well penetrating these limestones in the ESAN's license area by Yazıcıgil et al., 2016 revealed that they are higly impervious (K= 2.35x10^{-8} m/s). In summary, the bedrock in Sector-A consists of schists and ophiolites and they are hydrogeologically considered as impervious and semi-pervious in nature and can carry some water along fractures that result from faulting.

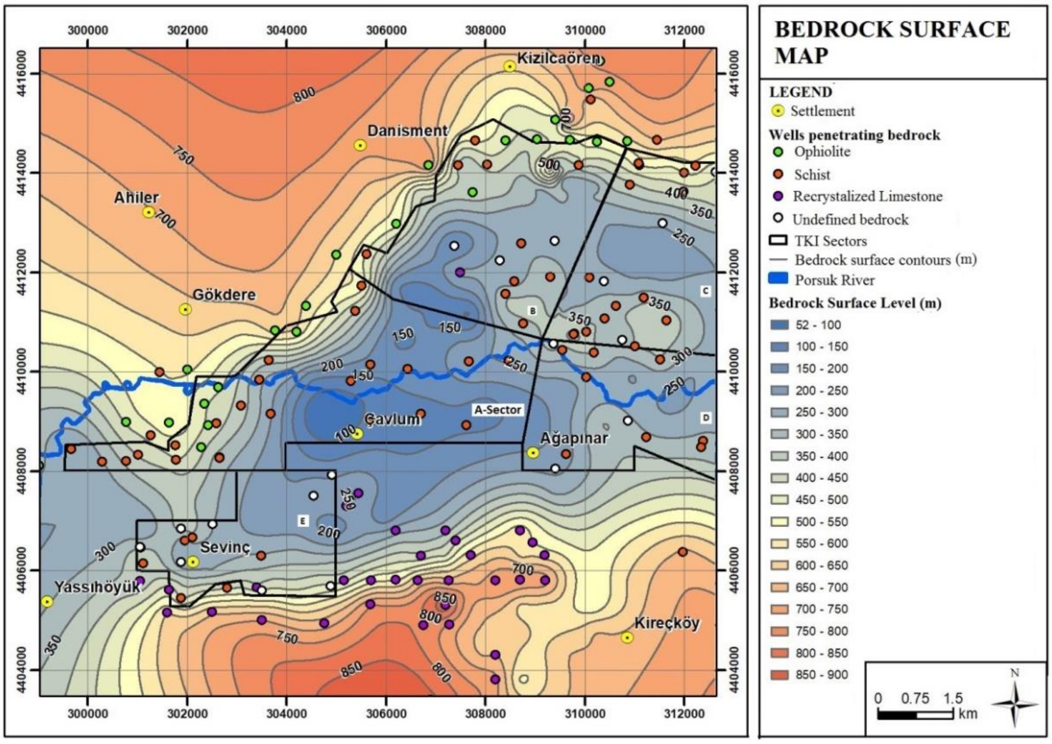

Figure 4.6. Bedrock surface contour map (Yazıcıgil et al., 2017).

The lignite bearing Middle-Upper Miocene Porsuk Formation is generally composed of claystones, sandstones, conglomerates and bituminous shales (Figure 4.1). The bottom of these deposits consists of basal conglomerates that are composed of conglomerates, sandstones and claystones (m1 series). This unit is overlain from the bottom to the top a sequence of conglomerate, green claystone, coal seam (D), green claystone, coal seam (C), gray sandstone, bituminous shale, coal seam (B), bituminous shale, coal seam (A) and green claystone-sandstone-conglomerate alternation (m2 series). The silicified limestones (m3 series) that form the upper part of the Miocene deposits outcrop in the south and are not encountered in Sector-A. The isopack map showing the thickness of the Miocene unit in Sector-A prepared from the core-hole data is given in Figure 4.7.

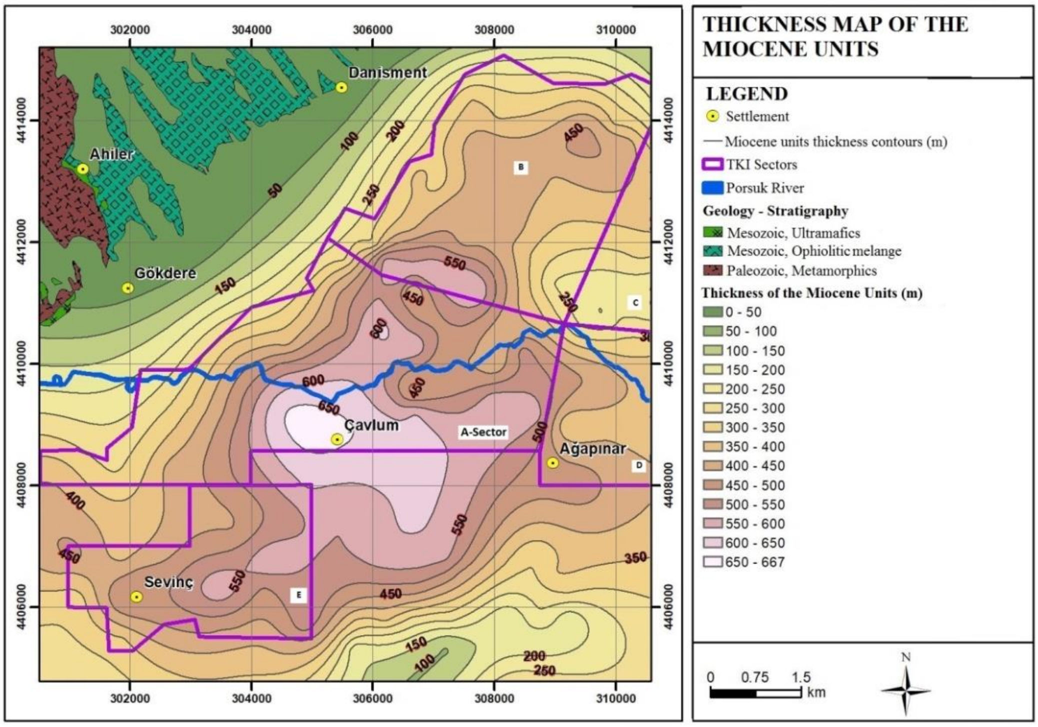

Figure 4.7. Miocene units thickness contour map (Yazıcıgil et al., 2017)

The thickness of the Miocene units increases to 650-670 m in the area around the Çavlum village. The thickest region overlaps with the deepest region in the bedrock surface map. The thickness of the Miocene units decreases to 200-250 m toward the west and northwest of Sector-A. The thickness increases upto 550 m in Sector-E. The pumping tests conducted to determine the hydraulic parameters of the lignite bearing Miocene unit in Sector-A show that the hydraulic conductivity of the unit varies between $5.64x10^{-9}$ m/s and $8.92x10^{-7}$ m/s, the geometric mean being equal to $1.41x10^{-7}$ m/s. The pumping tests conducted in ESAN’s license area gave similar ($2.4x10^{-7}$ m/s) values of hydraulic conductivity for this unit (Yazıcıgil et al., 2016). The storativity of the Miocene units in sector-A as obtained from the pumping tests varies between $8.60x10^{-3}$ and $2.50x10^{-2}$. Thus, lignite bearing Miocene series (m2) has a low hydraulic conductivity and display confined to semi-confined behavior.

The Pliocene units cropping out in the northern parts of Sector-A are one of the important water bearing units in the area. The Pliocene deposits in Sector-A consist of alternation of claystone, sandstone, siltstone, conglomerate and limestone (Figure 4.1). The isopack map showing the thickness of the Pliocene unit in Sector-A and its vicinity is given in Figure 4.8. While the thickness of the Pliocene unit is around 20 m in the vicinity of the Çavlum village, it increases to 180 m through northeast toward the margins of the basin. The conglomerates, sandstones and limestones within Pliocene deposits carry groundwater and many wells have been drilled in these deposits in Sector-B, located in the north of Sector-A, by DSI for operation and exploration purposes (Figure 4.1). The DSI wells drilled around Sector-A are shown in Figure 4.1. The depths, screen levels, tapped units, static and dynamic groundwater levels, yields and specific capacities of DSI wells are summarized in Table 4.1. As it can be seen from this table most of the DSI wells are screened both in the Quaternary alluvium and the Pliocene deposits. The pumping tests conducted to determine the hydraulic parameters of the Pliocene units in Sector-A show that the hydraulic conductivity of the unit varies over a narrow range between 3.00×10^{-5} m/s and 4.23×10^{-5}, the geometric mean of the hydraulic conductivity is equal to 3.44×10^{-5} m/s. The Pliocene unit is about 100 times more permeable than the Miocene unit. The mean hydraulic conductivity value calculated for the Pliocene unit is also conformable with the hydraulic conductivity values (1.86×10^{-6} m/s and 4.10×10^{-6} m/s) obtained from the pumping tests conducted by DSI (1977) in two wells completed in Pliocene deposits. These results show that, after the Quaternary alluvium, the Pliocene deposits are the most permeable unit within Sector-A. The storativity of the Pliocene unit in sector-A as obtained from the pumping tests varies between 2.00×10^{-2} and 4.92×10^{-2}.

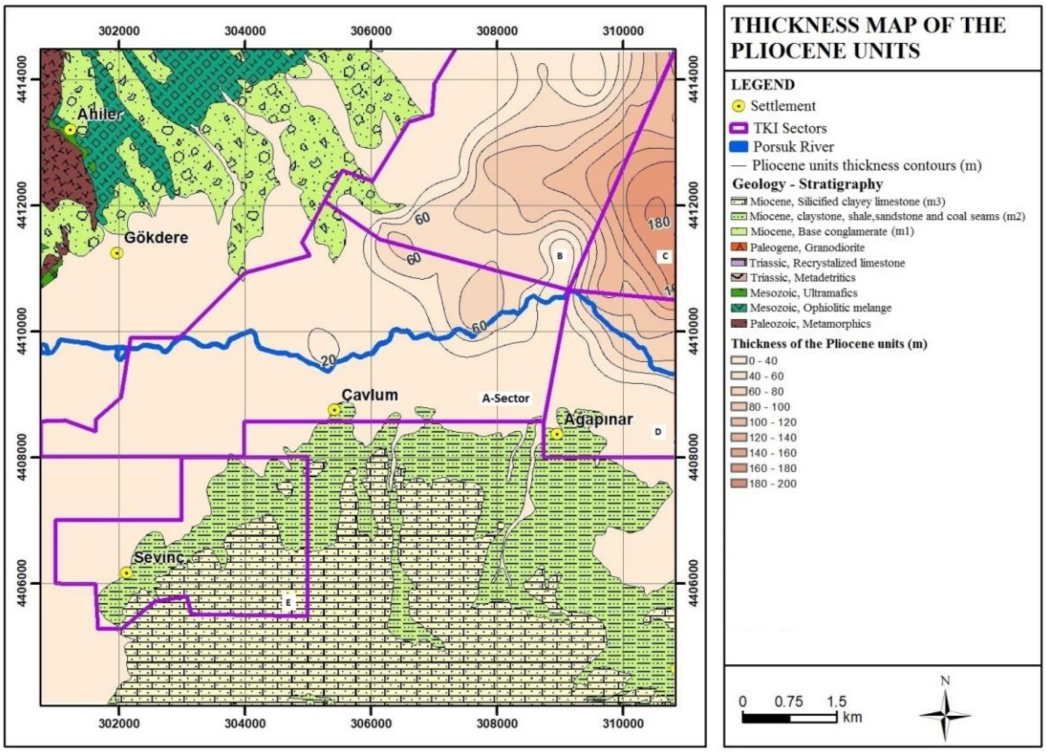

Figure 4.8. Pliocene units thickness contour map (Yazıcıgil et al., 2017).

The Quaternary alluvium consists of silt and clay intercalated sands and gravels. To determine the thickness of the alluvium, forming the main aquifer system in the Alpu plain, the well logs were examined and the isopack map showing the distribution of the thickness is given Figure 4.9. As it can be seen from this figure the thickness of the alluvium increases toward the Porsuk Stream, reaching values of 50-60 m. The thickness increases toward the west of Sector-A and in the northwest of the Çavlum village. The drinking, domestic and agricultural water needs in the basin are basically met from this unit and there are several wells drilled privately and State Hydraulic Works outside the Sector-A. The pumping tests conducted in the alluvium wells drilled within the scope of the study to determine the hydraulic parameters of the Quaternary alluvium show that the hydraulic conductivity of the unit varies from a minimum of 5.24×10^{-4} m/s to a maximum of 1.13×10^{-3} m/s, the geometric mean being equal to 7.76×10^{-4} m/s. In a hydrogeological investigation study in Alpu Plain conducted by DSI in 1977, 22 pumping tests were conducted in drainage wells to determine the hydraulic parameters of the alluvium. The test results show that the transmissivity of the alluvium ranges between 2.31×10^{-3} m^2/s and 4.21×10^{-2} m^2/s, the geometric mean being equal to 9.11x10^{-3} m^2/s. The hydraulic conductivity of the alluvium, on the other hand, varied between 1.29x10^{-4} m/s and 2.63x10^{-3} m/s, the geometric mean is 5.00x10^{-4} m/s. These values are conformable with the hydraulic conductivity values obtained within the scope of the study and show that the alluvium has high hydraulic conductivity (33 times more than the Pliocene unit). The results of the pumping tests conducted within the scope of the study show that the storativity (specific yield) of the alluvium ranges between 1.92x10^{-2} and 1.95x10^{-1}, indicating that the alluvium behaves as unconfined to semi-unconfined aquifer. These results are also conformable with the storativity values (between 3.00x10^{-3} and 2.00x10^{-1}) obtained for the alluvium in DSI (1977) study. The specific yield of the alluvium decreases as the proportion of the fine grained silt and clay lenses increase and it increases as the coarse grained sand and gravel materials become dominant. Most of the wells drilled by DSI in the plain are screened in both the alluvium and Pliocene deposits. Thus, the Quaternary alluvium deposits distributed over large areas in Sector-A, having a thickness of 50-60 m locally toward the Porsuk Stream, are the most prolific aquifer with high hydraulic conductivity and storativity values.

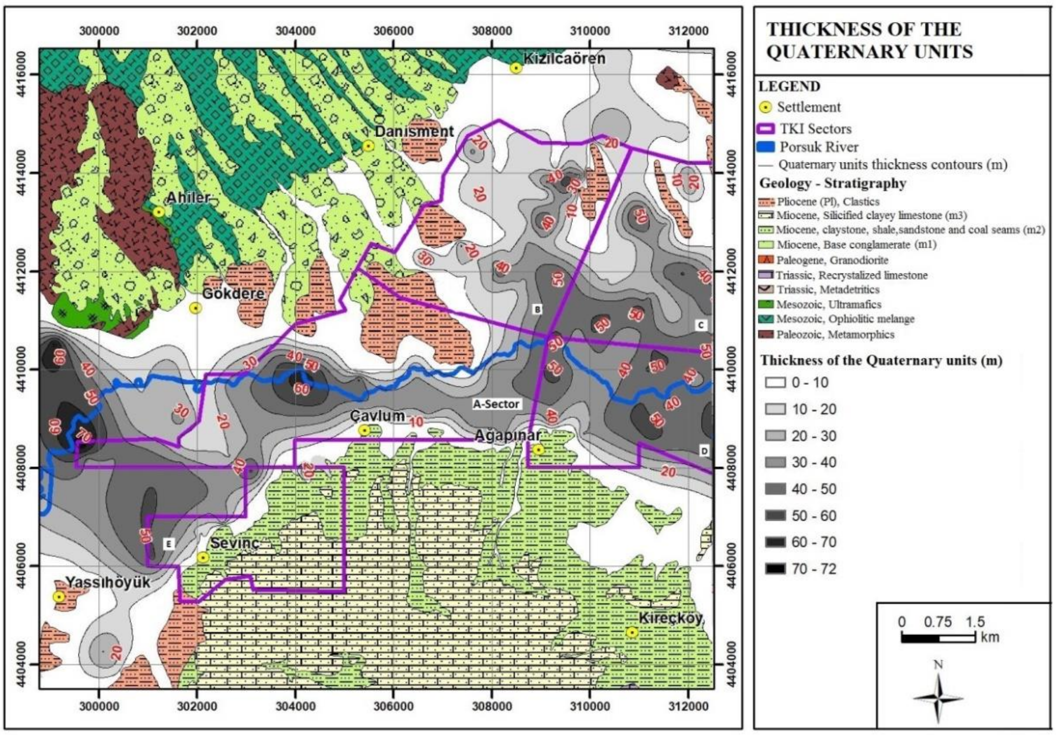

Figure 4.9. Alluvium aquifer thickness contour map (Yazıcıgil et al., 2017).

4.2.1. Hydraulic Parameters

The main hydraulic parameters that affect the groundwater flow are hydraulic conductivity and storage coefficient (storativity). These parameters are generally obtained from the results of pumping tests. Thus, after developing each well, constant rate pumping tests and recovery tests were conducted when required pumping yield was procured. In other cases, slug tests are carried out to determine the hydraulic conductivities.

In order to determine the hydraulic properties of the units outcropping in Sector-A and to reveal the hydraulic relations/interactions between each other and the coal seams, the intersected units were differentiated by screening each well in the target units.

The locations of the wells on which pumping tests are conducted are shown in Figure 4.2. The pump well APK-1, located in the northern part of Sector-A and screened in the lignite bearing Miocene units, did not have sufficient well yield to conduct a pump test; therefore, a slug test was carried out. Furthermore, the pumping test conducted at APK-2 well in this location which is screened in Miocene units lasted 33 minutes at a pumping rate of 2.3 L/s. Therefore, the results of the recovery test were evaluated using slug test methods. The pumping and recovery tests were conducted in all the other pumping wells. The detailed reports for the pumping tests conducted at each well are given by Yazıcıgil et al., (2017). The pumping and recovery test data were analyzed via using Aqtesolv (Aquifer Test Solver) Pro v4.5 software package. The calculated hydraulic parameters from the pumping and recovery tests are summarized in Table 4.4.

The tests conducted were analyzed and obtained hydraulic conductivity values were grouped considering the screened and gravel packed units. The groups were Quaternary alluvium; Pliocene claystone, sandstone, siltstone, conglomerate and limestone alternations; Miocene claystone, sandstone and siltstone alternations; and composite group consisting of two or more groups. The hydraulic conductivity values obtained from the tests enabled the comparison of geological units penetrated by each well and different groups with each other.

Table 4.4. The calculated hydraulic parameters from the results of pumping and recovery tests (Yazıcıgil et al., 2017).

Well ID	Elevation (m)	Filter (m)		Average GW Level (m)	Screened Level	Target Geological Unit	Test Type		Solution Method	Calculated T Values (m^2/s)	Calculated K Values (m/s)	Calculated Storage Coefficient	Average K Value (m/s)	
		Top	Bottom										Aritmetic Ave.	Geometric Ave.
APK-1	803.027	200.0	272.0	6.74	Coal and Under Coal	The alternation of claystone, sandstone, siltstone and lignite seams (Miocene)	Slug Test	Falling Phase	Hvorslev	-	1.70E-08	-	8.79E-09	5.65E-09
									Bouwer&Rice	-	1.37E-08	-		
									Cooper-Bredehoeft-Papadopulos	4.05E-07	4.18E-09	-		
									Dougherty-Babu	1.43E-06	1.48E-08	1.01E-02		
								Rising Phase	Hvorslev	-	1.57E-09	-		
									Bouwer&Rice	-	1.43E-09	-		
APK-2	803.972	14.5	54.5	15.07	Above Coal	The alternation of claystone, sandstone, siltstone and lignite seams (Miocene)	Pumping Test (APK-2)		Bouwer-Rice	-	4.56E-08	-	6.77E-08	6.44E-08
									Hvorslev	-	6.03E-08	-		
									KGS Model	-	9.72E-08	-		
APK-3	776.191	56	452	4.38	Above Coal and Coal	Clay, sand, gravel (Alluvium), The alternation of claystone, sandstone, siltstone and lignite seams (Miocene)	Pumping Test (APK-3)		Cooper&Jacob	1.55E-03	3.79E-06	-	1.61E-05	6.82E-06
									Theis (Jacob corrected)	1.53E-03	3.73E-06	-		
									Theis Recovery	2.21E-02	5.41E-05	-		
									Tartakovsky-Neuman	1.16E-03	2.83E-06	-		
APK-4	777.504	16	56	5.94	Above Coal	Clay, sand, gravel (Alluvium)	Pumping Test (APK-4)		Cooper&Jacob	3.23E-02	5.98E-04	-	8.18E-04	7.09E-04
									Theis (Jacob corrected)	3.23E-02	5.98E-04	-		
									Theis Recovery	8.89E-02	1.65E-03	-		
									Tartakovsky-Neuman	2.32E-02	4.30E-04	-		
APK-5	773.158	44	392	0.46	Above Coal and Coal	The alternation of claystone, sandstone, siltstone and lignite seams (Miocene)	Pumping Test (APK-5)		Cooper&Jacob	4.96E-05	1.39E-07	-	1.53E-07	1.52E-07
									Theis (Jacob corrected)	5.04E-05	1.42E-07	-		
									Theis Recovery	6.48E-05	1.82E-07	-		
									Daugherty-Babu	5.27E-05	1.48E-07	-		
APK-6	773.104	16	56	4.21	Above Coal	Clay, sand, gravel (Alluvium), The alternation of claystone, sandstone, siltstone and lignite seams (Miocene))	Pumping Test (APK-6)		Cooper&Jacob	5.10E-02	9.28E-04	-	1.30E-03	1.21E-03
									Theis (Jacob corrected)	5.05E-02	9.17E-04	-		
									Theis Recovery	1.14E-01	2.06E-03	-		
APK-7	772.264	16	68	2.29	Above Coal	The alternation of claystone, sandstone, siltstone, conglomerate and limestone (Pliocene)	Pumping Test (APK-7)		Cooper&Jacob	3.01E-03	4.12E-05	-	3.26E-05	3.00E-05
									Theis (Jacob corrected)	2.40E-03	3.33E-05	-		
									Theis Recovery	3.00E-03	4.17E-05	-		
									Tartakovsky-Neuman	1.01E-03	1.41E-05	-		
AGK-2	802.450	12	56	13.25	Above Coal	The alternation of claystone, sandstone, siltstone and lignite seams (Miocene)	Pumping Test (APK-2)		Bouwer-Rice	-	4.63E-08	-	6.50E-08	6.28E-08
									Hvorslev	-	6.17E-08	-		
									KGS Model	-	8.70E-08	-		
AGK-3	777.202	12	56	5.14	Above Coal	Clay, sand, gravel (Alluvium)	Pumping Test (APK-4)		Cooper&Jacob	1.10E-01	2.04E-03	1.50E-03	1.97E-03	1.96E-03
									Theis (Jacob corrected)	1.14E-01	2.10E-03	1.54E-03		
									Theis Recovery	9.86E-02	1.83E-03	-		
									Tartakovsky-Neuman	1.03E-01	1.90E-03	1.62E-03		
AGK-4	777.369	12	56	5.5	Above Coal	Clay, sand, gravel (Alluvium)	Pumping Test (APK-4)		Cooper&Jacob	1.13E-01	2.08E-03	4.71E-03	2.04E-03	2.03E-03
									Theis (Jacob corrected)	1.27E-01	2.34E-03	3.03E-03		
									Theis Recovery	9.83E-02	1.82E-03	-		
									Tartakovsky-Neuman	1.02E-01	1.90E-03	7.10E-03		
AGK-5	773.918	12	56	2.67	Above Coal	Clay, sand, gravel (Alluvium), The alternation of claystone, sandstone, siltstone and lignite seams (Miocene)	Pumping Test (ESHID-01P)		Cooper&Jacob	5.40E-02	8.55E-04	2.51E-02	7.85E-04	7.81E-04
									Theis (Jacob corrected)	5.40E-02	8.55E-04	2.45E-02		
									Neuman	4.80E-02	7.60E-04	2.14E-02		
									Tartakovsky-Neuman	4.24E-02	6.71E-04	2.01E-02		
AGK-6	772.256	15	67	1.32	Above Coal	The alternation of claystone, sandstone, siltstone, conglomerate and limestone (Pliocene)	Pumping Test (APK-7)		Cooper&Jacob	4.38E-03	6.01E-05	-	4.74E-05	4.23E-05
									Theis (Jacob corrected)	4.51E-03	6.26E-05	-		
									Theis Recovery	3.58E-03	4.97E-05	-		
									Tartakovsky-Neuman	1.24E-03	1.72E-05	4.92E-02		

Table 4.4. continued

Well ID	Elevation (m)	Filter (m) Top	Filter (m) Bottom	Average GW Level (m)	Screened Level	Target Geological Unit	Test Type	Solution Method	Calculated T Values (m^2/s)	Calculated K Values (m/s)	Calculated Storage Coefficient	Average K Value (m/s) Aritmetic Ave.	Average K Value (m/s) Geometric Ave.
ESHID-01P	774.069	6	54	3.72	Above Coal	Clay, sand, gravel (Alluvium), The alternation of claystone, sandstone, siltstone and lignite seams (Miocene)	Pumping Test (ESHID-01P)	Cooper&Jacob	6.62E-02	1.05E-03	-	9.97E-04	9.96E-04
								Theis (Jacob corrected)	5.87E-02	9.30E-04	-		
								Neuman	6.52E-02	1.03E-03	-		
								Tartakovsky-Neuman	6.17E-02	9.77E-04	-		
ESHID-01A	773.563	6	54	3.19	Above Coal	Clay, sand, gravel (Alluvium), The alternation of claystone, sandstone, siltstone and lignite seams (Miocene)	Pumping Test (ESHID-01P)	Cooper&Jacob	5.86E-02	9.28E-04	6.83E-02	8.45E-04	8.41E-04
								Theis (Jacob corrected)	5.81E-02	9.20E-04	6.17E-02		
								Neuman	4.78E-02	7.56E-04	7.06E-02		
								Tartakovsky-Neuman	4.90E-02	7.76E-04	7.06E-02		
ESHID-01B	774.035	6	54	3.68	Above Coal	Clay, sand, gravel (Alluvium), The alternation of claystone, sandstone, siltstone and lignite seams (Miocene)	Pumping Test (ESHID-01P)	Cooper&Jacob	5.24E-02	8.30E-04	4.37E-02	8.82E-04	8.78E-04
								Theis (Jacob corrected)	6.29E-02	9.96E-04	2.23E-02		
								Neuman	5.83E-02	9.22E-04	2.11E-02		
								Tartakovsky-Neuman	4.91E-02	7.78E-04	1.67E-02		
ESHID-01C	773.777	6	54	3.45	Above Coal	Clay, sand, gravel (Alluvium), The alternation of claystone, sandstone, siltstone and lignite seams (Miocene)	Pumping Test (ESHID-01P)	Cooper&Jacob	5.15E-02	8.15E-04	8.12E-02	9.15E-04	9.11E-04
								Theis (Jacob corrected)	6.42E-02	1.02E-03	3.13E-02		
								Neuman	6.26E-02	9.91E-04	3.30E-02		
								Tartakovsky-Neuman	5.28E-02	8.35E-04	3.03E-02		
ESHID-02P	772.592	62	342	Artezyen	Above Coal	The alternation of claystone, sandstone, siltstone, conglomerate and limestone (Pliocene), The alternation of claystone, sandstone, siltstone and lignite seams (Miocene)	Pumping Test (ESHID-02P)	Cooper&Jacob	1.40E-05	4.00E-08	-	4.44E-08	4.43E-08
								Theis (Jacob corrected)	1.72E-05	4.91E-08	-		
								Dougherty-Babu	1.55E-05	4.43E-08	-		
ESHID-02A	772.544	72	344	0.06	Above Coal	The alternation of claystone, sandstone, siltstone, conglomerate and limestone (Pliocene), The alternation of claystone, sandstone, siltstone and lignite seams (Miocene)	Pumping Test (ESHID-02P)	Cooper&Jacob	1.58E-05	4.50E-08	2.29E-04	4.69E-08	4.69E-08
								Theis (Jacob corrected)	1.63E-05	4.66E-08	2.19E-04		
								Dougherty-Babu	1.72E-05	4.91E-08	1.68E-04		
ESHID-02C	772.221	72	344	Artezyen	Above Coal	The alternation of claystone, sandstone, siltstone, conglomerate and limestone (Pliocene), The alternation of claystone, sandstone, siltstone and lignite seams (Miocene)	Pumping Test (ESHID-02P)	Cooper&Jacob	1.54E-05	4.39E-08	1.33E-04	4.63E-08	4.63E-08
								Theis (Jacob corrected)	1.66E-05	4.75E-08	1.53E-04		
								Dougherty-Babu	1.66E-05	4.75E-08	1.21E-04		
ESHID-02P2	772.321	3	71	2.78	Above Coal	Clay, sand, gravel (Alluvium), The alternation of claystone, sandstone, siltstone, conglomerate and limestone (Pliocene)	Pumping Test (APK-7)	Cooper&Jacob	3.32E-03	4.54E-05	-	3.59E-05	3.20E-05
								Theis (Jacob corrected)	3.25E-03	4.52E-05	-		
								Theis Recovery	2.91E-03	4.04E-05	-		
								Tartakovsky-Neuman	9.06E-04	1.26E-05	2.93E-02		
ML-3B (16 m)	772.890	-	-	4.41	Above Coal	Clay, sand, gravel (Alluvium)	Pumping Test (APK-6)	Cooper&Jacob	2.09E-02	3.80E-04	1.95E-01	5.43E-04	5.24E-04
								Theis (Jacob corrected)	2.84E-02	5.16E-04	5.05E-02		
								Theis Recovery	4.03E-02	7.33E-04	-		
ML-3B (30 m)	772.890	-	-	5.06	Above Coal	Clay, sand, gravel (Alluvium)	Pumping Test (APK-6)	Cooper&Jacob	2.17E-02	3.94E-04	2.93E-02	7.30E-04	6.25E-04
								Theis (Jacob corrected)	2.56E-02	4.65E-04	-		
								Theis Recovery	7.34E-02	1.33E-03	1.26E-02		
ML-3A(108 m)	772.966	-	-	-9.10	Above Coal	The alternation of claystone, sandstone, siltstone and lignite seams (Miocene)	Pumping Test (APK-5)	Cooper&Jacob	1.03E-04	9.78E-07	2.00E-02	1.07E-06	8.92E-07
								Theis (Jacob corrected)	5.73E-05	5.46E-07	4.00E-02		
								Theis Recovery	2.32E-04	2.21E-06	-		
								Daugherty-Babu	5.63E-05	5.36E-07	4.20E-02		
ML-4A (307.95 m)	772.840	-	-	-12.29	Above Coal	The alternation of claystone, sandstone, siltstone and lignite seams (Miocene)	Pumping Test (APK-5)	Cooper&Jacop	6.82E-05	2.72E-07	1.20E-02	3.56E-07	3.50E-07
								Theis (Jacob corrected)	9.36E-05	3.73E-07	1.00E-02		
								Daugherty-Babu	1.06E-04	4.24E-07	1.60E-02		
ML-4B (332.2 m)	772.656	-	-	-26.60	Coal	Coal Seamı (A) (Miocene)	Pumping Test (APK-5)	Cooper&Jacob	2.44E-04	9.72E-07	1.40E-02	8.07E-07	7.96E-07
								Theis (Jacob corrected)	1.70E-04	6.76E-07	2.40E-02		
								Theis Recovery	2.23E-04	8.90E-07	-		
								Daugherty-Babu	1.73E-04	6.88E-07	2.50E-02		
ML-4B (390.2 m)	772.656	-	-	-29.80	Coal	Claystone underCoal Seamı(C) (Miocene)	Pumping Test (APK-5)	Cooper&Jacob	4.81E-05	1.91E-07	8.60E-03	1.85E-07	1.84E-07
								Theis (Jacob corrected)	3.97E-05	1.58E-07	1.11E-02		
								Theis Recovery	5.30E-05	2.11E-07	-		
								Daugherty-Babu	4.49E-05	1.79E-07	1.00E-02		

4.2.1.1. Hydraulic Parameters of the Quaternary Alluvium

The data from wells APK-4, AGK-3 and AGK-4 as well as those obtained from vibrating wire piezometers located at depths of 16 m and 30 m in ML-3 well in the alluvium have been used to estimate the hydraulic parameters of the Quaternary alluvium. The results are summarized in Table 4.5.

Table 4.5. Hydraulic parameters of the Quaternary alluvium (Yazıcıgil et al., 2017).

Tested Unit	Well ID	Hydraulic Conductivity (m/s)	Hydraulic Conductivity-Geomean (m/s)	Min. Storage Coefficient	Max. Storage Coefficient
Alluvium (Quaternary)	APK-4	7.09E-04	9.84E-04	-	-
	AGK-3	1.96E-03		1.50E-03	1.62E-03
	AGK-4	2.03E-03		3.03E-03	7.10E-03
	ML-3B (16 m)	5.24E-04		5.05E-02	1.95E-01
	ML-3B (30 m)	6.25E-04		1.26E-02	2.93E-02

The results of the analyses have shown that the hydraulic conductivity of the alluvium varied little regionally, ranging from a minimum of 5.24×10^{-4} m/s to a maximum of 2.03×10^{-3} m/s. The geometric mean of the hydraulic conductivity obtained from the wells and vibrating wire piezometers representing the alluvium is 9.84×10^{-4} m/s. The calculated storativity values (specific yield for unconfined aquifers) varied between 1.50×10^{-3} and 1.95×10^{-1}, depending upon the proportion of clay within the penetrated sections. The tests conducted have shown that the Quaternary alluvium is the most prolific aquifer in Sector-A with storativity values ranging over a wide limit between 0.15% and 20%. The well yield from APK-4 well screened only in the alluvium was 51.3 L/s and the maximum drawdown was 2.80 m. The specific capacity of the well, which is also fed from the Porsuk Stream, was 18.3 L/s/m.

4.2.1.2. Hydraulic Parameters of Pliocene Claystone, Sandstone, Siltstone, Conglomerate and Limestone Alternations

The wells APK-7, AGK-6, ESHID-02/P2 have been completed to represent the Pliocene claystone, sandstone, siltstone, conglomerate and limestone alternations and isolated from the other units. The hydraulic parameters of the Pliocene unit are summarized in Table 4.6.

Table 4.6. Hydraulic parameters of Pliocene claystone, sandstone, siltstone, conglomerate and limestone alternations (Yazıcıgil et al., 2017).

Tested Unit	Well ID	Hydraulic Conductivity (m/s)	Hydraulic Conductivity-Geomean (m/s)	Min. Storage Coefficient	Max. Storage Coefficient
The alternation of claystone, sandstone, siltstone, conglomerate and limestone (Pliocene)	APK-7	3.00E-05	3.44E-05	-	-
	AGK-6	4.23E-05		4.92E-02	4.92E-02
	ESHİD-02P2	3.20E-05		2.93E-02	2.93E-02

The hydraulic conductivity of the Pliocene unit, having a thickness locally reaching up to 300 m, is higher in the shallow levels with values 3.00×10^{-5} m/s, 4.23×10^{-5} m/s and 3.20×10^{-5} m/s (respectively for APK-7, AGK-6 and ESHID-02/P2). The hydraulic conductivity values over this range are conformable within itself and the geometric mean of the hydraulic conductivity is calculated as 3.44×10^{-5} m/s. The storativity values obtained from the tests varied between 2.93×10^{-2} and 4.92×10^{-2}. A well yield of 19.2 L/s was obtained from APK-7 well screened only in this unit and the maximum drawdown was 18.78 m. The specific capacity of the well is calculated as 1.02 L/s/m. In summary, after the Quaternary alluvium, the Pliocene deposits, consisting of alternations of claystone, sandstone, siltstone, conglomerate and limestone, are the second important units within Sector-A as far as the yield is considered.

4.2.1.3. Hydraulic Parameters of Miocene Claystone, Sandstone, Siltstone and Lignite Seam Alternations

The data from APK-1, APK-2, AGK-2 and APK-5 pump and observation wells and those obtained from vibrating wire piezometers located at depths of 108 m in ML-3A well, 307.95 m in ML-4A well and 332.2 m and 390.2 m in ML-4B well have been used to estimate the hydraulic parameters of the lignite bearing Miocene claystone, sandstone and siltstone alternations. Due to insufficient well yield, only a slug test was conducted at APK-1 well. The hydraulic parameters of the Miocene unit are summarized in Table 4.7.

Table 4.7. Hydraulic parameters of Miocene claystone, sandstone, siltstone and lignite seam alternations (Yazıcıgil et al., 2017).

Tested Unit	Well ID	Hydraulic Conductivity (m/s)	Hydraulic Conductivity-Geomean (m/s)	Min. Storage Coefficient	Max. Storage Coefficient
The alternation of claystone, sandstone, siltstone and lignite seams (Miocene)	APK-1	5.64E-09	1.41E-07	-	-
	APK-2	6.44E-08		-	-
	AGK-2	6.28E-08		-	-
	APK-5	1.52E-07		-	-
	ML-3A (108m)	8.92E-07		2.00E-02	4.20E-02
	ML-4A (307.95 m)	3.50E-07		1.00E-02	1.60E-02
	ML-4B (332.2 m)	7.96E-07		1.40E-02	2.50E-02
	ML-4B (390.2 m)	1.84E-07		8.60E-03	1.11E-02

The pumping tests conducted show that the hydraulic conductivity of the lignite bearing Miocene claystone, sandstone and siltstone alternations varies between $5.64x10^{-9}$ m/s and $8.92x10^{-7}$ m/s, the geometric mean being equal to $1.41x10^{-7}$ m/s. The storativity of the Miocene claystone, sandstone and siltstone alternations varies between $8.6x10^{-3}$ and $2.5x10^{-2}$. Thus, lignite bearing Miocene series has a low hydraulic conductivity and show confined to semi-confined behavior.

4.2.1.4. Hydraulic Parameters of the Composite Units

Composite Hydraulic Parameters of Quaternary Alluvium and Miocene

Filter intervals and gravel packs of ESHID-01P, ESHID-01A, ESHID-01B, ESHID-01C, AGK-5, APK-6 and APK-3 wells drilled in Sector-A show that these wells are fed from both Quaternary Alluvium and Miocene units. In addition, during the test of APK-3 well has a total depth of 460 m and filtered in 56-456 m interval, the wells APK-4, AGK-3 and AGK-4, which are 60 m in depth and filtered only in Alluvium, were observed to have drawdowns as well. However, the hydraulic conductivity values calculated from these wells are not included in the grouping because they do not reflect the hydraulic conductivity value of the composite units. The hydraulic parameters obtained for this composite unit are summarized in Table 4.8.

Table 4.8. Composite hydraulic parameters of Quaternary Alluvium and Miocene units (Yazıcıgil et al., 2017).

Tested Unit	Well ID	Hydraulic Conductivity (m/s)	Hydraulic Conductivity-Geomean (m/s)	Min. Storage Coefficient	Max. Storage Coefficient
Quaternary & Miocene	ESHİD-01	9.96E-04	4.59E-04	-	-
	ESHİD-01A	8.41E-04		6.17E-02	7.06E-02
	ESHİD-01B	8.78E-04		1.67E-02	4.37E-02
	ESHİD-01C	9.11E-04		3.03E-02	8.12E-02
	AGK-5	7.81E-04		2.01E-02	2.51E-02
	APK-6	1.21E-03		-	-
	APK-3	6.82E-06		-	-

The mean hydraulic conductivity values of the Quaternary Alluvium and Miocene units were estimated from 6.82×10^{-6} m/s to 1.21×10^{-3} m/s and the geometric mean of the hydraulic conductivity coefficient was calculated to be 4.59×10^{-4} m/s. Considering the hydraulic conductivity and storage coefficients of the ESHİD-01P, ESHİD-01A, ESHİD-01B, AGK-5 and APK-6 wells, Quaternary Alluvium and young members of the Miocene units give high conductivity values. For this reason, it is predicted that the low conductivities of Miocene units are masked again by the high conductivity values of the Quaternary Alluvium. However, despite the fact that the APK-3 well is fed from the Quaternary Alluvium, the hydraulic conductivity value is lower than other wells because a large part of the well is filtered through the Miocene units. The storage coefficient calculated from the wells is between 1.67×10^{-2} and 8.12×10^{-2}.

Composite Hydraulic Parameters of Pliocene and Miocene

The ESHID-02P, ESHID-02A and ESHID-02C wells represent some of the Pliocene claystone, sandstone, siltstone, conglomerate and limestone alternations and are mainly filtered in Miocene claystone, sandstone and siltstone alternating units with coal bearing units. The hydraulic parameters of the Pliocene and Miocene composite units obtained from these wells are summarized in Table 4.9.

Table 4.9. Composite hydraulic parameters of Pliocene and Miocene units (Yazıcıgil et al., 2017).

Tested Unit	Well ID	Hydraulic Conductivity (m/s)	Hydraulic Conductivity-Geomean (m/s)	Min. Storage Coefficient	Max. Storage Coefficient
Pliocene & Miocene	ESHİD-02	4.43E-08	4.58E-08	-	-
	ESHİD-02A	4.69E-08		1.68E-04	2.29E-04
	ESHİD-02C	4.63E-08		1.21E-04	1.53E-04

While hydraulic conductivities calculated from ESHID-02P, ESHID-02A and ESHID-02C wells vary between 4.43x10^{-8} m/s and 4.69x10^{-8} m/s, geometric mean of the calculated hydraulic conductivity coefficients is estimated as 4.58x10^{-8} and storage coefficient values calculated from the wells vary between 1.21x10^{-4} and 2.29x10^{-4}. This range of storage coefficients is thought to be representative for Miocene units because of the the fact that the ESHID-02 well group is mainly in Miocene units.

4.2.2. Groundwater Levels

4.2.2.1. Areal Variations in Groundwater Levels

To determine the groundwater flow directions and hydraulic gradients in Sector-A and its vicinity, the static water levels measured in wells drilled within the scope of the study, in DSI and MTA wells are used to develop a groundwater level (groundwater table) map. Because there is not sufficient number of wells in Pliocene and Miocene units to establish the areal distribution of hydraulic heads in these units, the groundwater table map developed largely represents the Quaternary alluvium aquifer. However, the static water levels measured in wells drilled in Pliocene and Miocene units where they outcrop are also used in developing groundwater table map. The groundwater table contours developed using the average of the measured static water levels are shown on the geological map given in Figure 4.10.

Although the general direction of groundwater flow in Sector-A is from west to the east, there are also groundwater flow from the elevated lands in the north and south toward the Porsuk Stream (Figure 4.10). While the groundwater levels at the west of Sector-A is 775 m, they decrease to 768 m in the vicinity of the Porsuk stream in the east of the Sector-A. Moreover, the groundwater levels decrease with a steep gradient from 800 m in the northern part of Sector-A to 770 m in the vicinity of the Porsuk Stream in the south. Thus, the Porsuk stream forms the discharge area for the groundwater system.

While the hydraulic gradient of the groundwater table is 6.66×10^{-4} in the west-east direction in the vicinity of the Porsuk stream, it increases to 1.43×10^{-2} in the northern part of the Sector-A. The rapid decrease in hydraulic gradient in the vicinity of the Porsuk Stream is mainly due to the high transmissivity of the groundwater system (alluvium) in this part. The steep hydraulic gradient noted in the northern part of Sector-A is validated with the low transmissivity calculated from the pumping tests conducted in the Pliocene unit cropping out in the north.

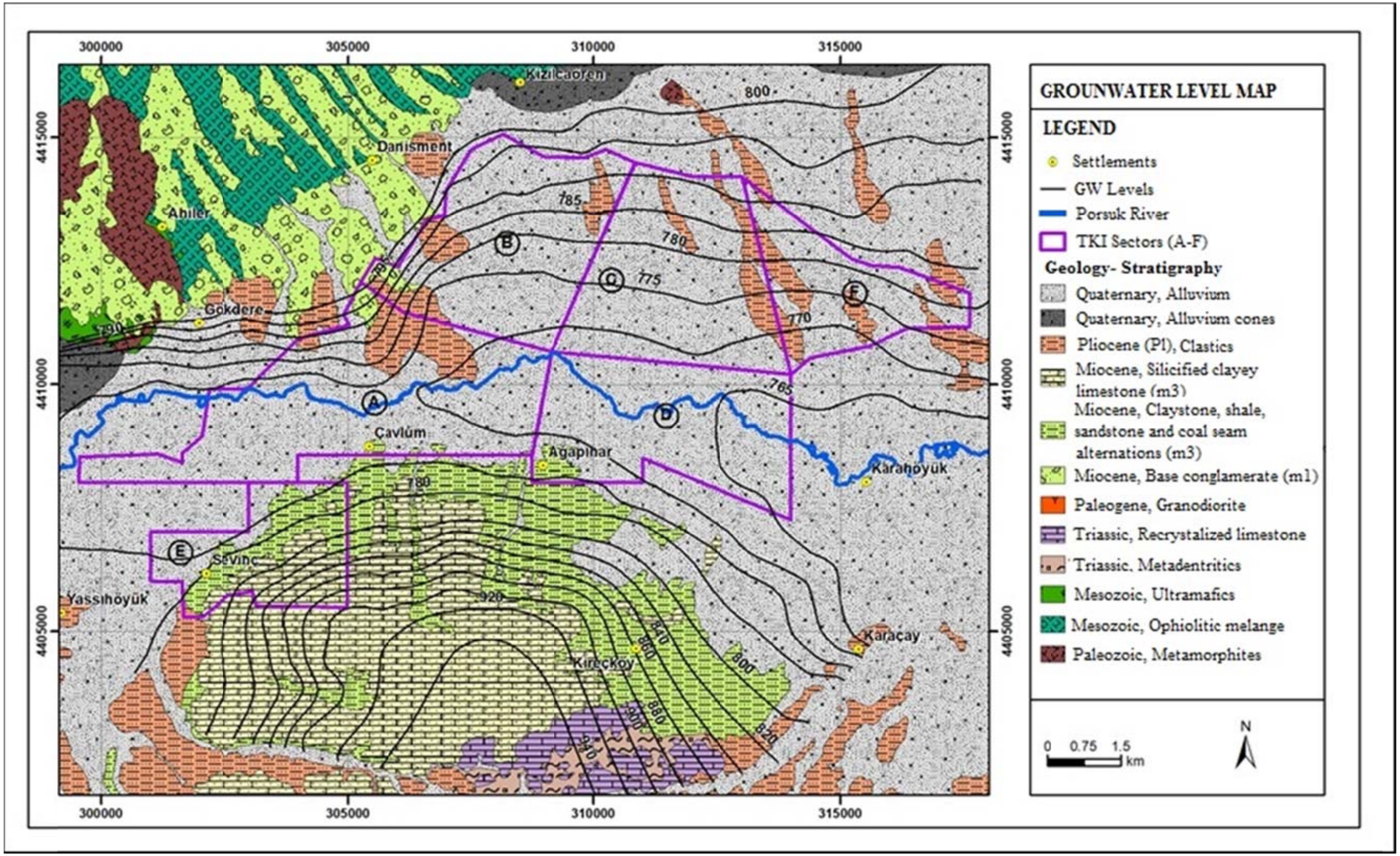

Figure 4.10. The distribution of groundwater levels shown on geological map (Yazıcıgil et al., 2017).

4.2.2.2. Temporal Variations in Groundwater Levels

Following the completion of pumping and observation wells, the elevations and coordinates of the water level measuring points in all wells are measured using DGPS (Differential Global Positioning System). Groundwater levels measured monthly in all wells drilled within the scope of the study and MTA (Bayram, 2015) are shown respectively in Tables 4.10 and 4.11, as elevation and depth data.

Table 4.10. Static groundwater level depths and elevations measured in pumping and observation wells drilled within the scope of the study (Yazıcıgil et al., 2017).

Static Water Level (m)													
Well name / Meas. Date	APK-1	AGK-1	APK-2	AGK-2	APK-3	APK-4	AGK-3	AGK-4	APK-5	APK-6	APK-7	AGK-6	AGK-5
24.08.2016	-	-	15.07	13.50	-	-	-	-	-	-	-	-	-
26.08.2016	-	-	-	13.67	-	-	-	-	-	-	-	-	-
30.08.2016	-	0.75	15.11	-	-	-	-	-	-	-	-	-	2.67
31.08.2016	-	0.61	-	-	-	-	-	-	-	-	-	-	-
01.09.2016	-	-	15.08	13.57	-	-	-	-	-	-	-	-	-
09.09.2016	12.77	0.50	-	-	-	-	-	-	-	-	-	-	-
21.09.2016	-	-	-	-	-	-	-	-	-	-	-	-	2.95
16.10.2016	7.69	0.31	14.81	-	-	-	-	-	-	-	-	1.97	3.53
20.10.2016	-	-	-	13.32	-	-	-	-	-	-	-	-	-
16.11.2016	6.74	-	14.73	13.25	-	-	-	-	-	-	2.31	2.26	3.65
19.11.2016	-	-	-	-	-	-	-	-	1.10	4.23	-	-	-
20.12.2016	-	-	-	-	-	-	-	-	-	-	2.51	2.46	-
21.12.2016	6.28	-	14.75	13.26	4.34	5.65	5.19	5.55	-	-	-	-	3.69
24.01.2017	5.77	-	14.82	13.26	-	-	-	-	0.02	-	-	-	3.62
26.01.2017	-	-	-	-	-	-	-	-	-	-	2.60	2.55	-
01.02.2017	-	-	-	-	4.38	5.69	5.23	5.59	-	-	-	-	-
20.02.2017	-	-	-	-	-	-	-	-	-	-	2.70	2.65	-
21.02.2017	5.91	-	14.90	13.41	-	-	-	-	0.81	4.30	-	-	3.70
15.03.2017	5.56	-	14.96	13.46	4.25	5.56	5.19	5.56	-	-	2.72	2.69	3.58
16.03.2017	-	-	-	-	-	-	-	-	0.46	4.21	-	-	-
13.04.2017	5.51	0.19	15.02	13.53	4.36	5.81	5.30	5.71	-	-	2.71	2.67	-
15.04.2017	-	-	-	-	-	-	-	-	0.45	4.45	-	-	-

Water Level Elevation (m)													
Well name / Meas. Date	APK-1	AGK-1	APK-2	AGK-2	APK-3	APK-4	AGK-3	AGK-4	APK-5	APK-6	APK-7	AGK-6	AGK-5
24.08.2016	-	-	788.90	788.95	-	-	-	-	-	-	-	-	-
26.08.2016	-	-	-	788.78	-	-	-	-	-	-	-	-	-
30.08.2016	-	803.54	788.86	-	-	-	-	-	-	-	-	-	771.25
31.08.2016	-	803.68	-	-	-	-	-	-	-	-	-	-	-
01.09.2016	-	-	788.89	788.89	-	-	-	-	-	-	-	-	-
09.09.2016	790.26	803.79	-	-	-	-	-	-	-	-	-	-	-
21.09.2016	-	-	-	-	-	-	-	-	-	-	-	-	770.97
16.10.2016	795.34	803.98	789.16	-	-	-	-	-	-	-	-	770.29	770.39
20.10.2016	-	-	-	789.13	-	-	-	-	-	-	-	-	-
16.11.2016	796.29	-	789.24	789.20	-	-	-	-	-	-	769.95	770.00	770.27
19.11.2016	-	-	-	-	-	-	-	-	772.06	768.87	-	-	-
20.12.2016	-	-	-	-	-	-	-	-	-	-	769.75	769.80	-
21.12.2016	796.75	-	789.22	789.19	771.85	771.85	772.01	771.82	-	-	-	-	770.23
24.01.2017	797.26	-	789.15	789.19	-	-	-	-	773.14	-	-	-	770.30
26.01.2017	-	-	-	-	-	-	-	-	-	-	769.66	769.71	-
01.02.2017	-	-	-	-	771.81	771.81	771.97	771.78	-	-	-	-	-
20.02.2017	-	-	-	-	-	-	-	-	-	-	769.56	769.61	-
21.02.2017	797.12	-	789.07	789.04	-	-	-	-	772.35	768.80	-	-	770.22
15.03.2017	797.47	-	789.01	788.99	771.94	771.94	772.01	771.81	-	-	769.54	769.57	770.34
16.03.2017	-	-	-	-	-	-	-	-	772.70	768.89	-	-	-
13.04.2017	797.52	804.10	788.95	788.92	771.83	771.69	771.90	771.66	-	-	769.55	769.59	-
15.04.2017	-	-	-	-	-	-	-	-	772.71	768.65	-	-	-

Table 4.11. Static groundwater level depths and elevations measured in pumping and observation wells drilled by MTA (Yazıcıgil et al., 2017).

	Static Water Level (m)								
Well name / Meas. Date	ESHİD-01P	ESHİD-01-A	ESHİD-01-B	ESHİD-01-C	ESHİD-02	ESHİD-02-A	ESHİD-02-B	ESHİD-02-C	ESHİD-02-P/2
19.07.2016	3.49	2.95	3.52	-	-	0.15	0.35	0	1.78
16.08.2016	3.09	2.60	3.06	2.80	0	0.15	0.35	0	1.80
21.09.2016	3.16	2.57	3.13	2.80	0	0.16	0.35	0	1.74
16.10.2016	3.66	3.14	3.61	3.39	0	0.10	0.41	0	2.09
16.11.2016	3.79	3.26	3.74	3.52	-	-	-	-	2.35
17.11.2016	-	-	-	-	0.36	0.10	0.49	0	-
20.12.2016	-	-	-	-	0	0.06	0.40	0	2.59
21.12.2016	3.83	3.29	3.78	3.55	-	-	-	-	-
24.01.2017	3.76	3.26	3.71	3.49	-	-	-	-	-
26.01.2017	-	-	-	-	0	0.05	0.43	0	2.65
20.02.2017	-	-	-	-	0	0.07	0.45	0	2.75
21.02.2017	3.84	3.31	3.79	3.57	-	-	-	-	-
15.03.2017	3.72	3.19	3.68	3.45	0	0.07	0.44	0	2.78
13.04.2017	3.93	3.40	3.89	3.67	0	0.06	0.44	0	2.76

	Water Level Elevation (m)								
Well name / Meas. Date	ESHİD-01P	ESHİD-01-A	ESHİD-01-B	ESHİD-01-C	ESHİD-02	ESHİD-02-A	ESHİD-02-B	ESHİD-02-C	ESHİD-02-P/2
19.07.2016	770.58	770.61	770.52	-	-	772.39	772.29	772.22	770.54
16.08.2016	770.98	770.96	770.98	770.98	772.59	772.39	772.29	772.22	770.52
21.09.2016	770.91	770.99	770.91	770.98	772.59	772.38	772.29	772.22	770.58
16.10.2016	770.41	770.42	770.43	770.39	772.59	772.44	772.23	772.22	770.23
16.11.2016	770.28	770.30	770.30	770.26	-	-	-	-	769.97
17.11.2016	-	-	-	-	772.23	772.44	772.15	772.22	-
20.12.2016	-	-	-	-	772.59	772.48	772.24	772.22	769.73
21.12.2016	770.24	770.27	770.26	770.23	-	-	-	-	-
24.01.2017	770.31	770.30	770.33	770.29	-	-	-	-	-
26.01.2017	-	-	-	-	772.59	772.49	772.21	772.22	769.67
20.02.2017	-	-	-	-	772.59	772.47	772.19	772.22	769.57
21.02.2017	770.23	770.25	770.25	770.21	-	-	-	-	-
15.03.2017	770.35	770.37	770.36	770.33	772.59	772.47	772.20	772.22	769.54
13.04.2017	770.14	770.16	770.15	770.11	772.59	772.48	772.20	772.22	769.56

To investigate the water level variations and relations in wells drilled into different lithological units in different locations, the groundwater level hydrographs are grouped in well clusters and are shown in Figure 4.11. Daily precipitation data measured at Alpu meteorological station is also added to these hydrographs in order to determine the relationship between the measured groundwater levels and precipitation.

The groundwater levels measured in APK-1 and AGK-1 wells, screened in the lignite bearing Miocene unit in the 1st well cluster location in the northern part of sector-A, are 8-22 m higher than the groundwater levels in APK-2 and AGK-2 wells screened in the Upper Miocene units. This shows the existence of an upward vertical gradient from the deep Miocene units to the shallow Miocene units. The groundwater levels in AGK-1 well, following the completion of well development works, have risen and reached into the water level measuring point, causing artesian flow conditions. Following the development works, the groundwater levels in APK-1 well drilled in the same unit, although slowly, also risen steadily but did not reach yet to the water level measuring point at the time of report writing. The slow rise in groundwater level observed in APK-1 well may be explained with the low hydraulic conductivity (5.64×10^{-9} m/s) of the Miocene unit in this well location. The artesian flow conditions are expected to occur with time in this well too. The variations in groundwater levels observed in shallow APK-2 and AGK-2 wells completed in the upper levels of Miocene unit are similar to each other and show small seasonal variations. Following well development works, the groundwater levels have risen and reached into 789.2 m elevation in November 2016 and decreased afterwards to 788.9 m elevation (Figure 4.11).

The variations in groundwater levels in 5 wells, four (ESHID-01P, ESHID-01A, ESHID-01B and ESHID-01C) drilled by MTA and one (AGK-5) drilled in this study, all penetrating the Quaternary alluvium and Miocene units located in the 2nd well cluster in the northeast of the Çavlum village are similar to each other and show seasonal fluctuations depending upon precipitation. The water levels in these wells have risen till September 2016 and declined 0.85 m-1.0 m afterwards (Figure 4.11).

There are 7 wells located in the 3rd well cluster in the northeastern part of Sector-A. Four of these wells (ESHID-02P, ESHID-02A, ESHID-02B ve ESHID-02C), each 350 m deep, were drilled by MTA (Bayram 2015) and screened into the Pliocene and Miocene units, one (ESHID-02/P2), again drilled by MTA with a depth of 71 m, penetrates the Pliocene units and two (APK-7 and AGK-6) with depths of 67-68 m, respectively were drilled within the scope of this study and were screened in the Pliocene units. The examination of temporal variations in measured water levels in these wells shows that the water levels representing the deep system (350 m deep ESHID-02P, ESHID-02A, ESHID-02B and ESHID-02C) are artesian and some show free flow conditions. However, flow is also observed taking place through the annular space between the casing and borehole-wall because the isolation of the annular space were not done properly. Apart from them, the water level variations in the shallow wells (ESHID-02/P2, APK-7 and AGK-6) screened in the Pliocene unit are similar to each other and measured water levels are 3 m lower compared to the deep system. In this location too, there is a vertical upward gradient from the deep system to the shallow system. While groundwater levels measured in wells in the deep system did not vary seasonally, the groundwater levels measured in wells in the shallow system showed seasonal variations. For example, the groundwater levels in ESHID-02/P2, APK-7 and AGK-6 wells screened in the Pliocene units decreased 0.3-0.4 m between November 2016 and April 2017.

APK-5 and APK-6 wells with depths of 400 m and 60 m, respectively, were drilled in the 4th well cluster location in the southeast border of Sector-A. The APK-5 pump well is screened in the lignite bearing (seams A, B, and C) Miocene units. The APK-6 pump well however is screened in Quaternary alluvium and Miocene units. In this location too, the water level for the deep system is about 3.8 m higher than the water level in the shallow system, indicating a vertical upward gradient from the deep system to the shallow system. The hydraulic head data obtained from the vibrating wire piezometers in this location also confirm this vertical gradient from the lignite bearing lower Miocene units to upper Miocene units, as will be explained in Section 4.2.4. No seasonal fluctuations were observed in both wells probably due to the short period (4-5 months) of monitoring.

The APK-3 pump well with a depth of 460 m was drilled in the 5th well cluster location in the west of sector-A in the near vicinity of the Porsuk Stream and is screened through alluvium, and lignite bearing Miocene units. The wells APK-4, AGK-3 and AGK-4, each with a depth of 60 m, were also drilled in this location and screened only in the alluvium. The water levels measured in APK-3 well screened in all the units are almost the same as the water levels measured in the wells screened only in the alluvium. No seasonal fluctuations were observed in measured levels due to the short period (4 months) of monitoring. As it will be explained in Section 4.2.4, the five vibrating wire piezometers installed in this location will provide point data and hence they will be more useful to identify the hydraulic relations between different units.

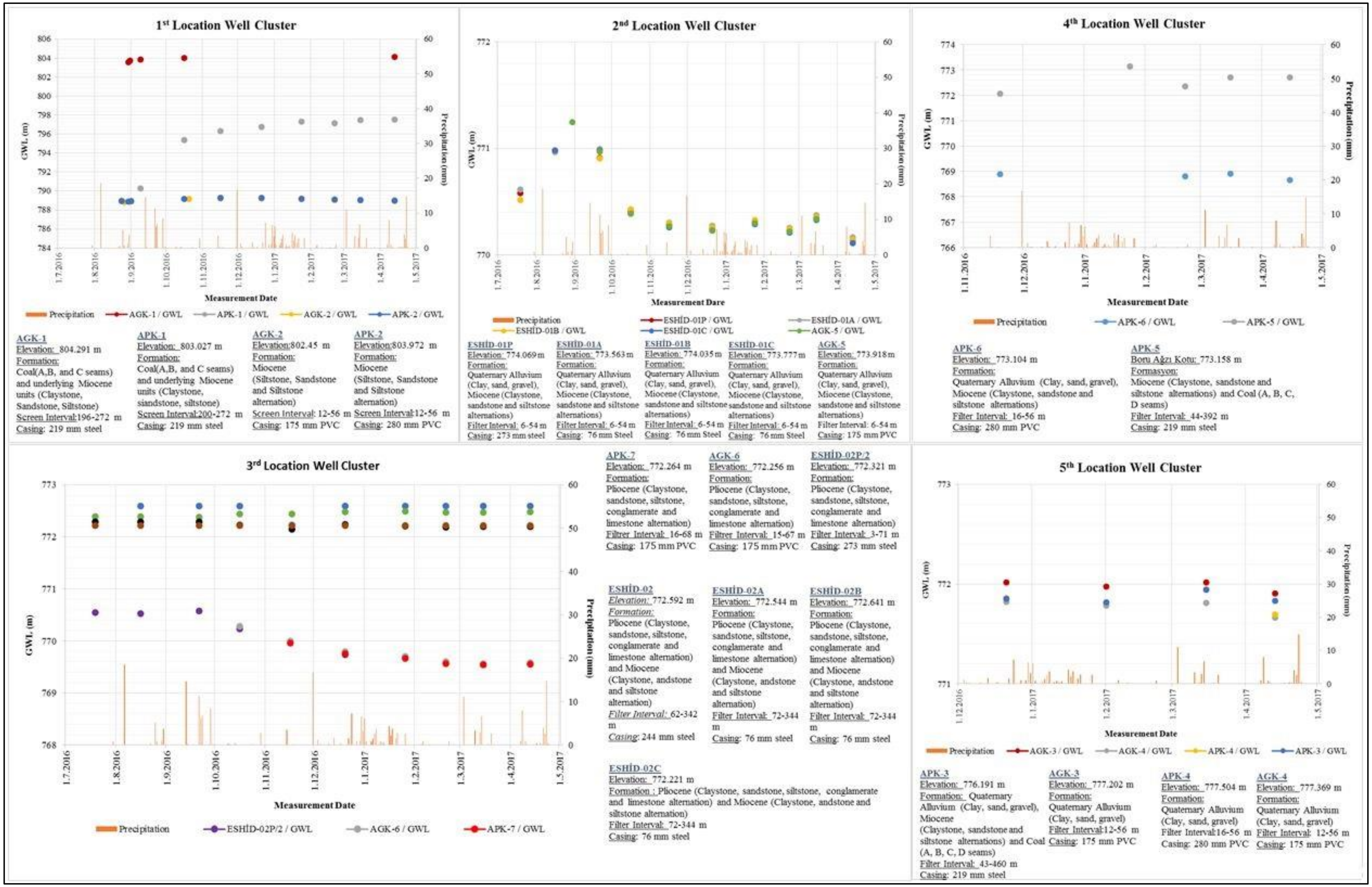

Figure 4.11. Temporal changes in groundwater levels measured at well clusters (Yazıcıgil et al., 2017).

4.2.3. Alluvium Aquifer and Porsuk Stream Interactions

The knowledge, about the interaction between the Alluvium aquifer and the Porsuk Stream running through the middle of Sector-A and the hydraulic relation between the alluvium aquifer and the underlying Pliocene and/or Miocene units, will provide very useful information in several topics including the environmental studies and displacement of the Porsuk Stream bed, in addition to the dewatering and depressurization studies that may be required during mining activities. The interaction between the Porsuk Stream and the alluvium aquifer is discussed herein while the relations between the alluvium and underlying Pliocene and/or Miocene units are explained in Section 4.2.4.

Although a constant discharge rate is applied to the pump wells during pumping tests conducted in APK-3, APK-4 and ESHID-01P wells, the drawdowns observed in all wells rhythmically fluctuated between day and night hours (Please see Figure 4.12). The studies for investigating the cause of these fluctuations in the water levels determined that they are produced by the day and night changes in the amount of water discharged from the Eskisehir Waste Water Treatment Plant to the Porsuk Stream. It has been determined that treated waters are regularly discharged into the Porsuk Stream from the Eskişehir waste water treatment plant located in Karacahöyük at the west of the basin boundaries. The amount of discharged water is about 0.9 m^3/sec in daytime hours and 1.5 m^3/sec at midnight. Therefore, fluctuations in drawdowns noted in the observation wells are produced by the difference in day and night flow rate of treated water discharged to the Porsuk Stream. In other words, when the amount of discharged water to the Porsuk Stream at 12:00 pm was about 1.5 m^3/sec, the drawdown in the wells slowed down and even about 3-4 cm rise in the water levels was noticed at 7-8 am. Therefore, the time required for the discharged excess treated waste water from the Waste Water Treatment plant at 12:00 pm to reach to the location of the wells is roughly calculated using the distance between the two points and the average flow velocity data obtained from the SW-4B and SW-5 Flow Monitoring Stations on the Porsuk Stream. The calculations confirmed that the water discharged from the treatment plant at around 12:00 pm at night reaches to the location of the pumping wells after about 7-8 hours. As a result, when discharged treated water from the treatment plant to the Porsuk stream reached to the location of wells, the drawdowns in the wells were directly influenced. This clearly shows that the alluvium aquifer is in direct interaction with the Porsuk Stream.

A second observation is conducted to determine the extent of the interaction between the Porsuk Stream and the alluvium aquifer. Pressure probes were installed to monitor the water level changes in APK-4 and AGK-4 wells screened in the alluvium near the Porsuk Stream and SW-6 Flow Monitoring Station on the Porsuk Stream. The data measured at 5 minute intervals between 24 April 2017 and 15 May 2017, after being corrected for barometric pressure variations, are displayed graphically as water level variations in Figure 4.12. As it can be seen from this figure the water level variations in the Porsuk Stream and the wells are similarly fluctuated between day and night times in a rhythmic manner. These graphics show that the water levels in both the Porsuk Stream and the wells are lowest between 19:30 and 21:00 pm at night and depending on the amount of discharged water, the water levels have risen 5-8 cm between 06:30 and 09:00 am at daytime. The cause of rise of about 30 cm in water levels observed on 6-7 May 2017 in both the Porsuk Stream and the wells has not been determined yet. Thus, the Porsuk Stream and the alluvium aquifer are interacting with each other and this point has to be taken into account in dewatering and similar studies.

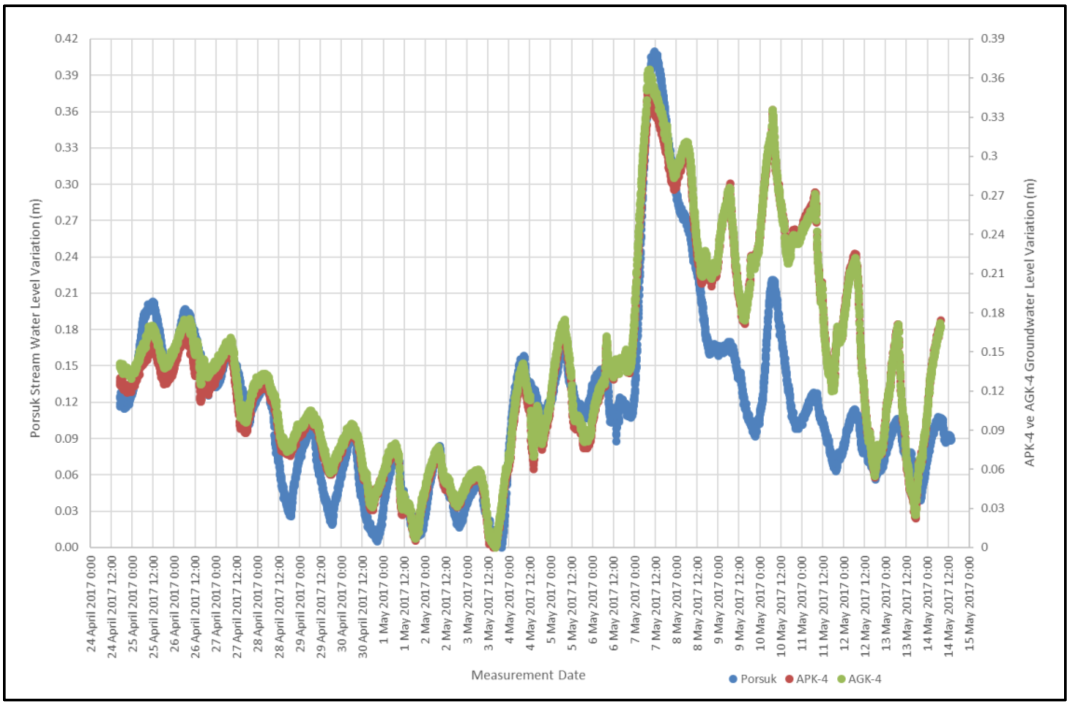

Figure 4.12. Porsuk Stream and well water level variations (Yazıcıgil et al., 2017).

4.2.4. Groundwater Pressures and Relations between Aquifers

As explained in Section 4.1.2.4, two (ML-1 and ML-2) diamond drill core holes were drilled in the 5th well cluster location in the west of Sector-A in the vicinity of the Porsuk Stream and five vibrating wire piezometers with depths of 32 m, 53 m, 70 m, 375.4 m and 439.9 m were installed in these core holes. The first two piezometers were installed in the alluvium, and the last three in the Miocene unit (the 4th is 4 m below Seam-A and 5th is 22 m below Seam-C). The groundwater pressures, hydraulic heads and temperature values monitored in these piezometers between 16 March 2017 and 22 April 2017 are displayed graphically as a function of time in Figures 4.13, 4.14 and 4.15, respectively. The groundwater pressures below Seam-C (at 439.9 m depth) varied between 5.22 and 5.28 MPa while below Seam-A (375.4 m depth) they varied between 4.33 and 4.36 MPa. The groundwater pressures decrease upward and vary between 612 and 622 kPa at 70 m depth in the Miocene unit. Within the Alluvium aquifer, groundwater pressures vary between 463 kPa and 469 kPa at 53 m depth and between 269 kPa and 272 kPa at 30 m depth. The observed groundwater pressures below the coal seams are excessive and may cause groundwater inrush into galleries or panels during mining activities. As it can be seen from Figure 4.14, the hydraulic heads varied between 868 m and 875 m below Seam-C at a depth of 439.9 m, between 843 m and 845 m below Seam-A at a depth of 375.4 m and between 768.2 m and 769.2 m at 70 m depth in the Miocene unit. These results show that there is an upward vertical hydraulic gradient and groundwater flow takes place from the bottom (Miocene unit) to the upward. The temperature values, on the other hand, decrease from 34.9˚C below Seam-C (439.9 m depth) to 30.6˚C below Seam-A (375.4 m depth) and to 16.4˚C in the Miocene unit (70 m depth). The temperatures in the Alluvium aquifer are 15.3˚C at 53 m depth and 14.6˚C at 32 m depth (Figure 4.15).

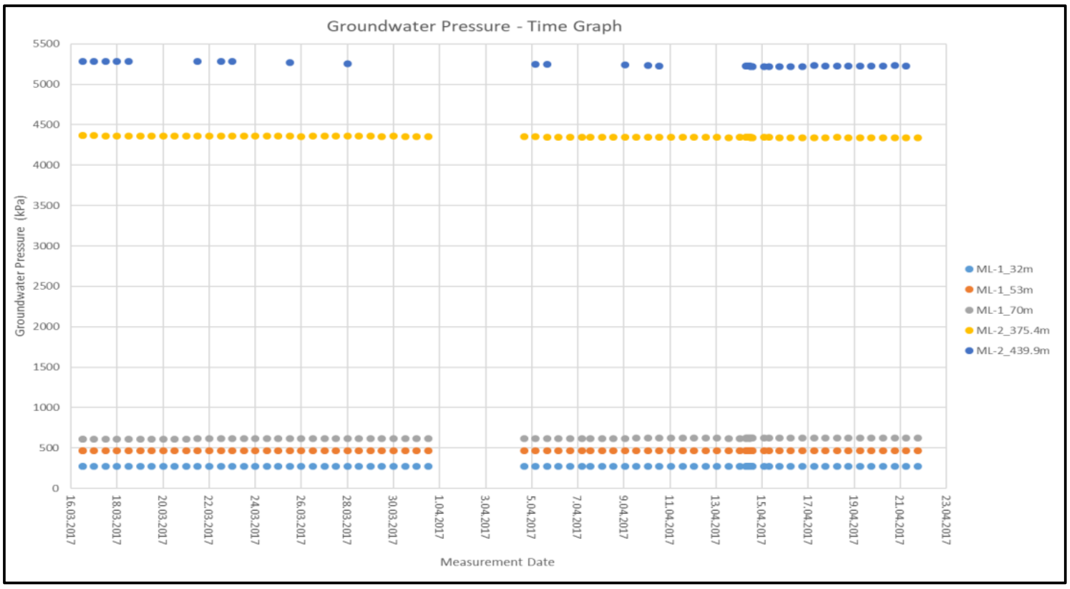

Figure 4.13. The temporal variations in groundwater pressures measured at piezometers installed in different levels in ML-1 and ML-2 wells (Yazıcıgil et al., 2017).

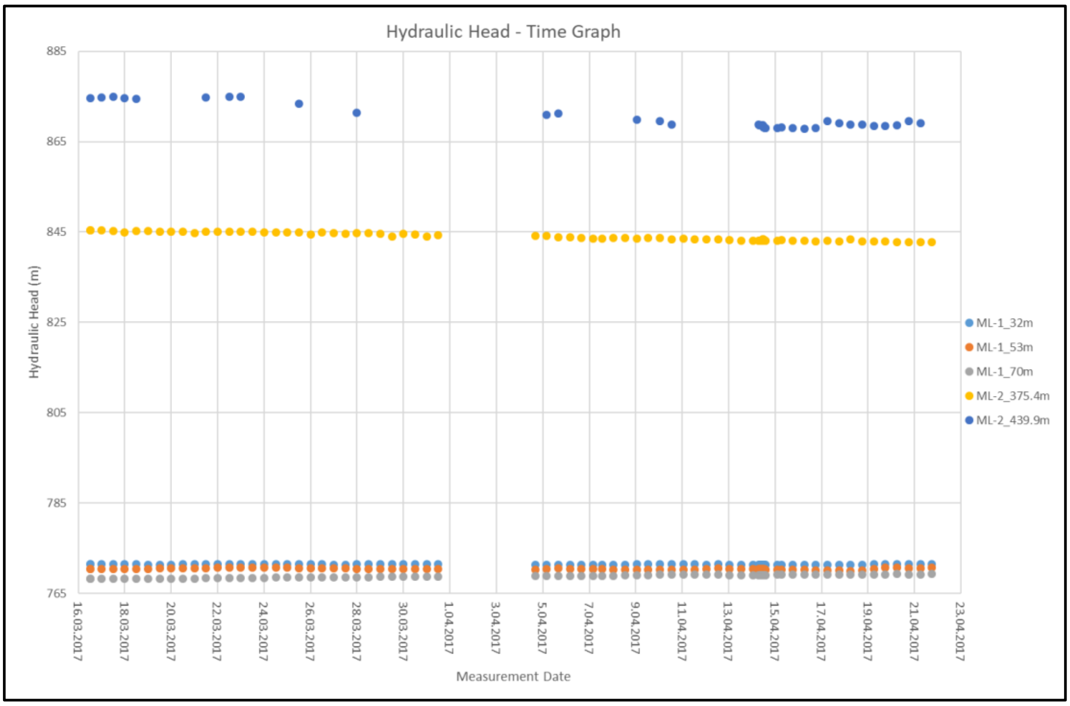

Figure 4.14. The temporal variations in hydraulic heads measured at piezometers installed in different levels in ML-1 and ML-2 wells (Yazıcıgil et al., 2017).

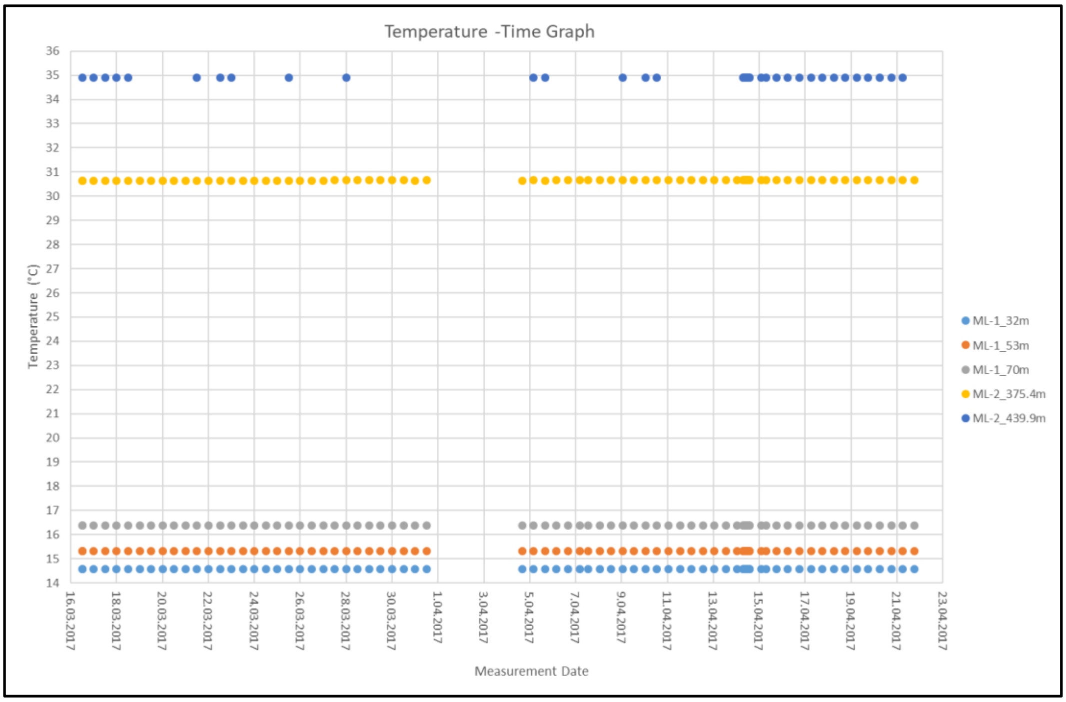

Figure 4.15. The temporal variations in temperatures measured at piezometers installed in different levels in ML-1 and ML-2 wells (Yazıcıgil et al., 2017).

The hydraulic heads observed in the Alluvium aquifer at 32 m depth varied between 771.3 m and 771.5 m while they varied between 770.0 m and 770.9 m at 53 m depth, thus indicating the existence of a downward vertical gradient (Figure 4.14). Although the hydraulic head observed in the shallow piezometer (32 m) is compatible with the observed groundwater levels (771.7 m -772 m) in APK-4, AGK-3 and AGK-4 wells screened in the Alluvium in this location, the relatively lower hydraulic head observed at 53 m depth indicates a downward groundwater flow. The reasons for this could be explained by the occurrence of recharge from the Porsuk Stream to the aquifer but also the installation of the piezometers within the gravel lenses that may have a lower hydraulic head compared to the water table. Consequently, the monitoring of the groundwater pressures at vibrating wire piezometers over a longer period which will include wet and dry seasons may provide information on the occurrence of one of the explanations given above.

Four (ML-3A, ML3-B, ML-4A and ML-4B) diamond drill core holes were drilled in the 4th well cluster location near the southeastern border of Sector-A and 8 vibrating wire piezometers with depths of 16 m, 30 m, 108 m, 163 m, 225 m, 308 m, 332.2 m and 390.2 m were installed in these core holes. The first two piezometers were installed in the alluvium and the last six in the Miocene unit. The groundwater pressures, hydraulic heads and temperature values monitored in these piezometers between 21 February 2017 and 24 April 2017 are displayed graphically as a function of time in Figures 4.16, 4.17 and 4.18, respectively. As it can be seen from Figure 4.16, the groundwater pressures in the Miocene unit are 4.1 MPa at 390.2 m depth (10 m below Seam-C), 3.5 MPa at 332.2 m depth (inside Seam-A), 3.1 MPa at 308 m depth (20 m above Seam-A), 2.3-2.44 MPa at 225 m depth and 1.79 MPa at 163 m depth. While the groundwater pressure is 1.15 MPa at 108 m depth in the relatively younger Miocene units, they decrease to 223-245 kPa and 114 kPa in the alluvium at depths of 30 m and 16 m, respectively. In summary, the groundwater pressures decrease in upward direction as can be seen in Figure 4.16. In this location too, the groundwater pressures below coal seams are excessive. As it can be seen from Figure 4.17, while the hydraulic heads below Seam-C (at 390.2 m depth) decreased from 803.5 m to 799.6 m over the monitoring period, they increased from 798.5 m to 801 m in Seam-A (at 332.2 m depth). Moreover, the hydraulic head recorded at 307 m depth is lower than the hydraulic head values recorded at 225 and 163 m depths. The hydraulic head at 225 m-depth piezometer stayed uniform at a value of 784 m between 21 February 2017 and 02 March 2017 but afterwards it increased continuously, reaching a value of 796.8 at 24 April 2017. The examination of the core logs revealed the existence of a 3.80 m thick soil-like disturbed material (between 225.80-228 m) which may be a fault zone and consequently, the groundwater pressures after the installation increased until they are stabilized. The hydraulic head in relatively younger Miocene units (108 m depth) is around 782 m and lower than all the recorded hydraulic heads in the underlying Miocene units, indicating an upward vertical gradient from the lower Miocene to upper Miocene units and hence a groundwater flow. Because the hydraulic head values (between 766 m – 768.5 m) in the alluvium (at 16 m and 30 m depths) are lower compared to the Pliocene unit, there is also a vertical gradient from relatively younger Miocene to the Alluvium and consequently, a vertical groundwater flow. In this location as well, the hydraulic head at shallow piezometer (16 m) being higher than the hydraulic head recorded piezometer at 30 m-depth may be explained by the installation of the piezometers within the gravel lenses in the alluvium.

The temperature values, as it can be seen from Figure 4.18, are 33.3˚C, 28.8˚C, 26.5˚C, 23.5˚C, 21.2˚C and 18.5˚C in the Miocene units at depths 390.2 m (10 m below Seam-C), 332.2 m (in Seam-A), 308 m (20 m above Seam-A), 225 m 163 m and 108 m respectively. They decrease in the Alluvium aquifer to 14.5˚C and 14.1˚C at depths of 30 m and 16 m, respectively (Figure 4.18).

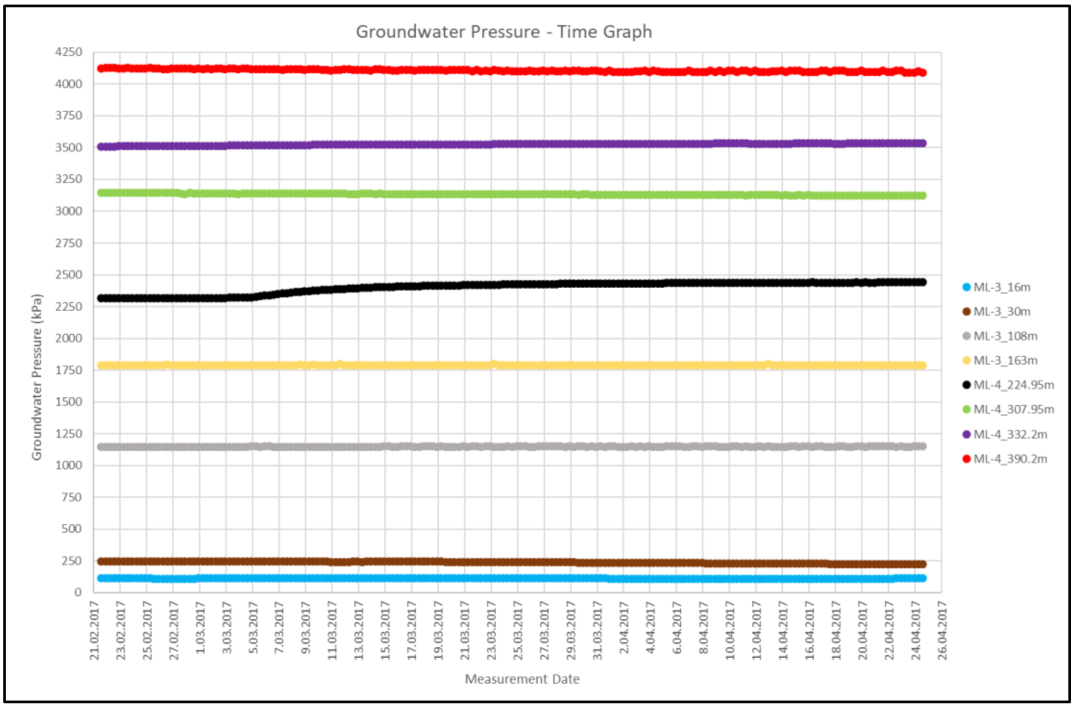

Figure 4.16. The temporal variations in groundwater pressures measured at piezometers installed in different levels in ML-3 and ML-4 wells (Yazıcıgil et al., 2017).

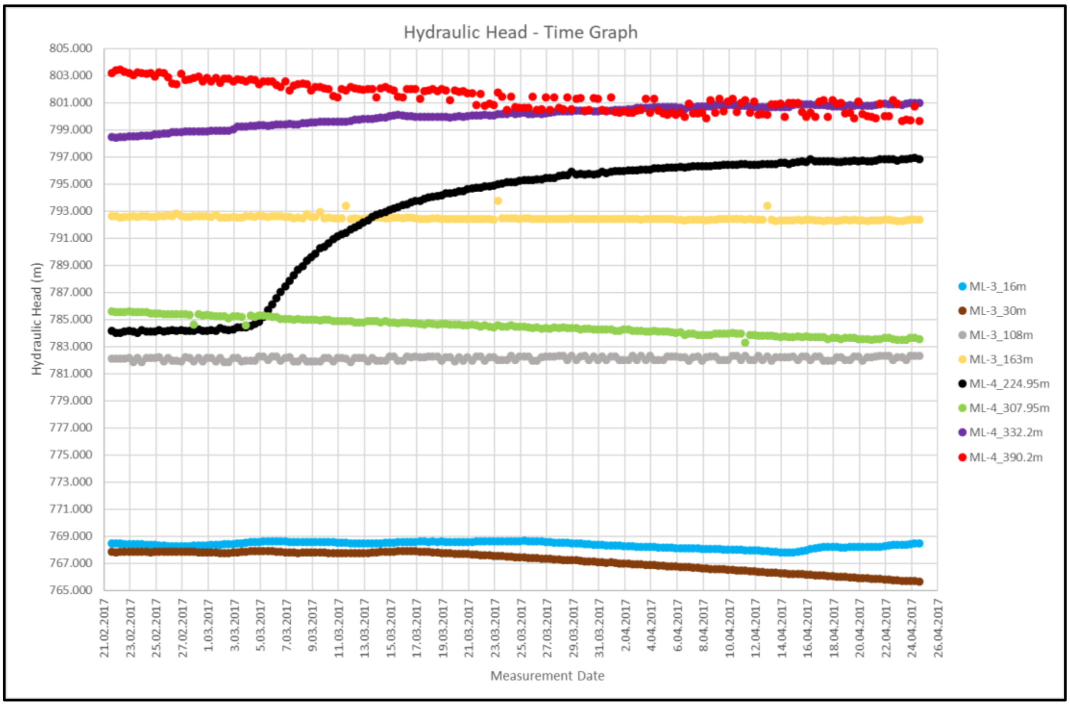

Figure 4.17. The temporal variations in hydraulic heads measured at piezometers installed in different levels in ML-3 and ML-4 wells (Yazıcıgil et al., 2017).

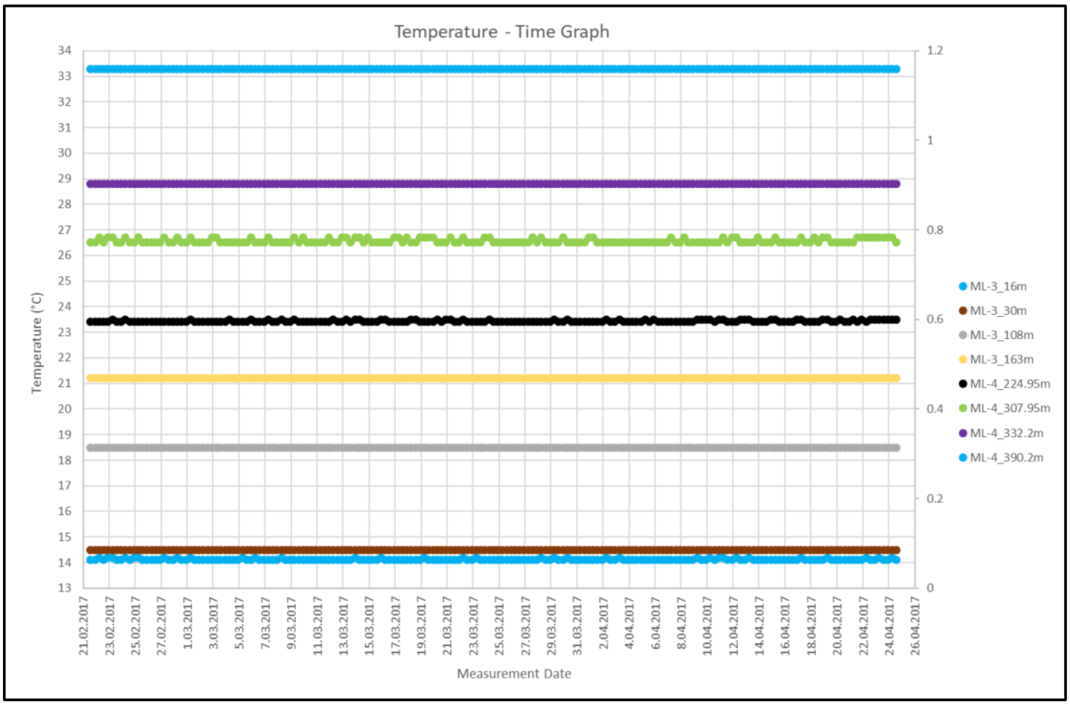

Figure 4.18. The temporal variations in temperatures measured at piezometers installed in different levels in ML-3 and ML-4 wells (Yazıcıgil et al., 2017).

4.3. Existing and Planned Groundwater Use

The only settlement in Sector-A is the Çavlum village and its drinking and domestic water need is met from a captage located in the license area of ESAN in the south of Sector-A. Therefore, no groundwater is used for drinking and domestic purposes in Sector-A. Moreover, the irrigation water needs are generally met from the irrigation and drainage channels located along the Porsuk Stream and hence no significant amount of groundwater is pumped for irrigation. No planned groundwater usage is available within Sector-A.

Detailed studies are required to determine the alternative sources of water supply for the mining activities. Additionally, the impacts of mining activities on irrigation water usage in the area should be assessed through groundwater modelling studies.

4.4. Thermal Water Sources

No area with thermal potential has been encountered in Sector-A. However, there are four geothermal areas nearby the study area which have water temperatures ranging between 26°C and 45°C. The most important of them is Alpu-Uyuzhamamı geothermal field which is located at 22 km southeast of the study area. This field has one source with 30°C and it is used for the spa. Kızılinler and Hasırca geothermal fields are located at 20 km west of Sector-A. Kızılinler geothermal field has 5 sources with temperatures ranging between 30°C and 45°C and are used for balneology and swimming pools. Hasırca geothermal field has 4 sources with temperatures ranging between 30°C and 33.5°C and are used for Kızılay Atatürk Youth Camp and in a small fish pool. The last one is Aşağılıc geothermal field which is located at 24 km southwest of Sector-A. This field is not used for anything due to the low temperature of the sources (26-27°C) (MTA, 2005).

Apart from the thermal water sources explained above, the presence of a geothermal well is mentioned in the hydrogeological studies conducted within the scope of the project entitled ‘Development of a Model for Bringing in Eskişehir Alpu Coal Basin’s Resources into Country’s Economics in an Optimal Manner’ which is being conducted at the Hacettepe University Technology Transfer Center

(HT-TTM, 2016). This geothermal well, named as EMA-2013/12 and drilled by MTA between the Ağapınar and Kızılcaören villages, 1 km north from the Porsuk Stream, has a depth of 1017 m. The lower half of the well penetrated marbles and schists of the bedrock and has a bottom hole temperature of around 53ºC. The presence of a geothermal fluid has been mentioned.

CHAPTER 5

HYDROCHEMISTRY AND WATER QUALITY

The hydrogeochemical characterization of Sector-A coal field is based upon the study conducted by Yazıcıgil et al., (2017). Pertinent information from this study is summarized herein.

5.1. Data Collection and Quality Control

5.1.1. Data Collection

Field works related to the hydrochemical monitoring program have been carried out between June 2016 and April 2017 on the monitoring locations (Table 5.1 and Figure 5.1). The APK coded well monitoring locations after drillings and ESHİD coded MTA wells (01P and 02P) after July 2016 have been taken into the monitoring program.

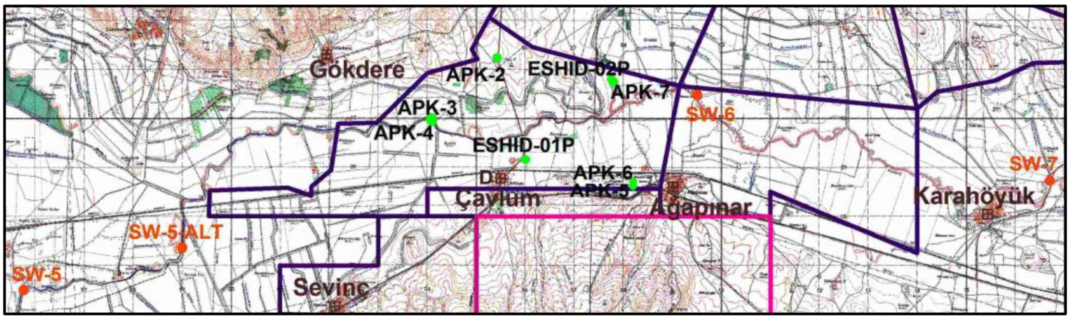

Figure 5.1. Distribution of hydrochemical monitoring locations

Temperature (T), electrical conductivity (EC), total dissolved solids (TDS), salinity (S), pH, oxidation-reduction potential (ORP) and dissolved oxygen (DO) measurements were carried out during the monthly monitoring program for waters.

Table 5.1. Hydrochemical monitoring locations

STATION NO	LATITUDE	LONGITUDE	EXPLANATION
SW-5	295770	4406495	Porsuk stream; upstream of study area (Bridge on the main road after the Logistics complex road turn)
SW-5-ALT	299002	4407374	Porsuk stream; upstream of study area (Bridge after the road turn across Yassıhöyük village)
SW-6	309536	4410411	Porsuk stream; middle of study area (Bridge at the North of Ağapınar village)
SW-7	316755	4408751	Porsuk stream; downstream of study area (Bridge on the main road after Karahöyük village).
APK-2	305430	4411188	Upper Miocene (shale-sandstone-siltstone sequences) aquifer
APK-3	304100	4409954	Alluvium+Pliocene+Miocene+In Coal aquifers
APK-4	304119	4409925	Alluvium aquifer (silt, sand, gravel)
APK-5	308233	4408619	Miocene+In coal aquifers
APK-6	308233	4408639	Alluvium + Miocene aquifers
APK-7	307819	4410704	Pliocene aquifer
ESHID-01P	306013	4409153	Alluvium+ Miocene aquifers
ESHID-02P	307791	4410718	Pliocene+Miocene (shale-sandstone-siltstone sequences) aquifers

Because special pumpage is required for wells to purge, the monthly monitoring of field parameters for non-flowing well waters was not carried out. In addition to the measurement of parameters listed above, waters from all monitoring locations and sediments from the upstream location (SW-5) of Porsuk stream were sampled between September 2016 and February 2016 (after pumping tests; wells APK-2 and ESHID-01P in September 2016, wells APK-7 and ESHID-02P in November 2016, well APK-6 in January 2017, wells APK-3, APK-4 and APK-5 in February 2017 and Porsuk Stream in September 2016) by staff of TÜRKAK accredited ALKA laboratory. These samples were chemically analyzed by the laboratory. Water samples were preserved for metal analysis by nitric acid after filtering (0.45 μ) in the field. Chemical parameters for the analyses were determined using water body (stream, groundwater, water depot etc.) related regulations of quality control and monitoring directives (ISYSKY 2012, ITAS 2005, SKKY 2008, YKBKK 2012, YSKYY 2012, YSYSIY 2014, YSKYYD 2015). The detailed information about the well water sampling is given in Table 5.2.

Table 5.2. Well water sampling information

	Depth of pump (m)	Static level (m)	Level at the time of sampling (m)	Level before ending pumpage (m)	Filter interval in well (m)	Aquifer
APK-2	43	15.07	35	42.3	14.5-54.5	Upper Miocene
APK-3	374	4.68	6.01	6	56-452	Alluvium + Pliocene + Miocene + In coal
APK-4	48	5.71	8.12	8.52	16-56	Alluvium
APK-5	380	1.01	15.64	15.67	44-392	Miocene + In coal
APK-6	48	4.97	8.05	8.06	16-56	Alluvium + Miocene
APK-7	60	2.285	19.99	20.02	16-68	Pliocene
ESHID-01P	24	2.84	3.81	3.81	6-54	Alluvium + Miocene
ESHID-02P	250	0.33	38.08	38.23	62-342	Pliocene + Miocene

5.1.2. Quality Control

The standard and replicate measurements related to the measurement quality (accuracy and precision) of field parameters indicate that the following error percentages are associated with these measurements: EC 0.8%, pH 0.4%, dissolved oxygen 1.2% and ORP 3.6%.

The average ionic charge balance error calculated using all measurements is about 15%. APK-3 and APK-5 samples with high TDS (1726-2920 mg/l) content screen all units and include relatively high charge balance error (30%). When these data were not included into the balance error calculation, the error reduces to about 9.5%.

Quality control evaluation results indicate that measurements performed in the field as well as in the laboratories are reliable and could be used for hydrochemical evaluations.

However, fore mentioned balance error percentages should be taken into consideration when evaluating APK-3 and APK-5 data.

5.2. Surface Water Hydrochemistry

5.2.1. Field Measurements

The results of hydrochemical field parameter measurements in the monitoring locations of Porsuk Stream are listed in Table 5.3 together with measurement dates, average values (AV) and average deviations (ADEV = sum of the absolute values of the differences between data and average divided by the number of data).

Average values of T, EC, pH, DO and ORP parameters are shown in Figure 5.2. Average electrical conductivity values change between 944 μS/cm and 987 μS/cm. Total dissolved solids and salinity average values estimated using EC measurements are in the range of 614-641 mg/l and 0.47-0.49 ppt, respectively in Porsuk Stream waters. The values slightly increase from upstream to the middle monitoring location, and then decrease toward downstream.

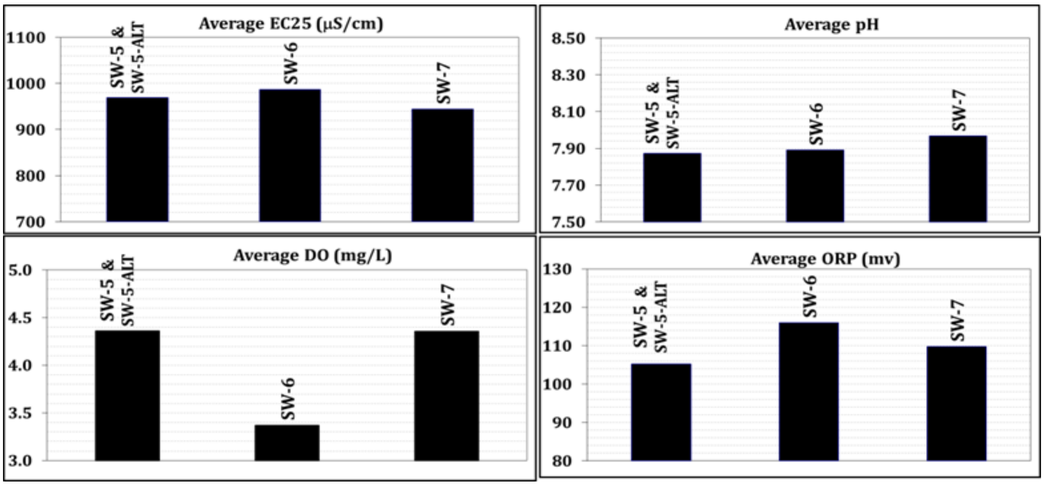

Figure 5.2. Average pH, EC, DO and ORP values measured in Porsuk Stream (Yazıcıgil et al., 2017).

Table 5.3. Values of hydrochemical field parameters measured in Porsuk Stream. AV: Average, (ADEV) average deviation (Yazıcıgil et al., 2017).

NO	DATE	T(oC)	pH	ORP (mv)	EC 25oC (µS/cm)	S (ppt)	TDS (mg/l)	DO (mg/l)	DO%
SW-5-ALT	16.06.16	23.8	7.86	118.4	1158	0.57	752	3.72	49
	19.07.16	22.3	-	84	882	0.43	573	3.38	44
	16.08.16	19.2	7.85	150	721	0.35	469	4.80	59
SW-5	21.09.16	18.6	7.63	121	664	0.33	432	4.61	56
	15.10.16	17.3	8.10	132	1031	0.51	670	1.84	29
	19.11.16	10.7	8.13	86	877	0.43	570	3.77	38
	21.12.16	7.1	8.16	103	1022	0.50	664	6.37	58
	19.01.17	7.7	7.16	95	1119	0.55	727	4.85	44
	20.02.17	8.0	7.85	66	1173	0.58	762	3.92	38
	16.03.17	8.6	8.11	97	1043	0.52	678	6.34	59
SW-5 & SW-5-ALT	AV(ADEV)	14.3(5.9)	7.87(0.23)	105(20)	969(146)	0.48(0.07)	630(95)	4.36(1.03)	47(8.7)
SW-6	16.06.16	22.1	7.93	87	1046	0.52	680	3.42	44
	19.07.16	22.1	-	140	866	0.43	563	2.98	34
	16.08.16	19.9	7.72	148	760	0.37	494	3.82	46
	21.09.16	19.1	7.45	125	701	0.34	455	1.78	22
	15.10.16	15.6	8.16	198	1007	0.50	654	2.87	40
	19.11.16	11.8	8.06	101	942	0.46	612	3.57	33
	21.12.16	6.4	8.14	108	1103	0.55	717	4.11	35
	19.01.17	7.9	7.71	83	1193	0.59	775	2.67	23
	20.02.17	8.8	7.83	95	1260	0.62	819	3.22	28
	16.03.17	8.5	8.02	75	988	0.49	642	5.26	49
	AV(ADEV)	14.2(5.5)	7.89(0.19)	116(29)	987(136)	0.49(0.07)	641(88)	3.37(0.67)	35(7.5)
SW-7	16.06.16	23.9	8.06	98	903	0.45	587	4.90	63
	19.07.16	22.9	-	87	863	0.43	561	3.91	50
	24.08.16	20.2	7.74	181	789	0.39	513	4.26	53
	21.09.16	19.0	7.60	156	862	0.42	560	3.56	42
	15.10.16	16.7	8.29	128	981	0.48	637	4.28	56
	19.11.16	10.2	7.97	107	809	0.40	526	4.73	48
	21.12.16	5.4	8.23	108	965	0.48	627	5.78	53
	19.01.17	7.8	7.86	71	1084	0.54	704	3.83	36
	20.02.17	7.8	7.95	73	1160	0.57	754	3.49	32
	16.03.17	8.5	8.00	89	1027	0.51	667	4.85	58
	AV(ADEV)	14.2(6.3)	7.97(0.16)	110(27)	944(99)	0.47(0.05)	614(64)	4.36(0.57)	49(7.8)

Porsuk Stream water is in basic character and monitoring period averages of pH values are in the range of 7.87-7.97. The values are slightly higher in the downstream location.

Average dissolved oxygen concentrations changing between 3.37 mg/l and 4.36 mg/l are similar in the downstream and upstream locations but lower in the middle monitoring location (SW-6). The differences among the monitoring locations probably indicate that DO consuming reactions are increasing between the locations of SW-5 and SW-6 and/or high DO including water feeding decreases between the locations and reverse processes are effective from SW-6 to SW-7 locations.

The stream water has oxidizing character with average ORP values in the range of 105-116 mV. The trend of ORP values is reverse that of dissolved oxygen; the value increases from upstream to the middle location, then slightly decreases toward downstream.

Monitoring period percent changes in the field parameter values are shown in Figure 5.3 as percent average deviation (PAD=ADEV*100/AV) which is determined after the measurement percent error subtraction. The averages of percent average deviations from higher to lower values were determined in temperature (41%), ORP (19%), dissolved oxygen (18%), EC (12%) and pH (2%) parameters. The averages of the parameter deviations in the stream are 127 µS/cm in electrical conductivity, 0.19 in pH, 25 mV in ORP and 0.75 mg/l in dissolved oxygen parameters.

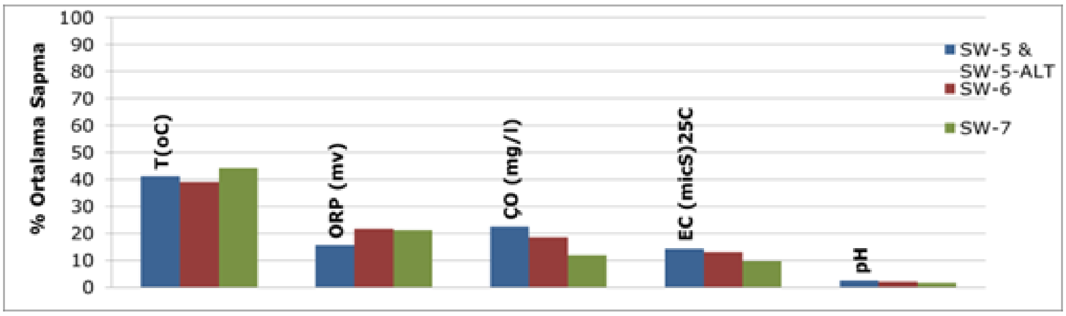

Figure 5.3. Percent average deviations of the field parameters measured in Porsuk Stream (Yazıcıgil et al., 2017).

Monthly changes of the field parameters in the stream water are shown in Figure 5.4. The chemical content of the stream water is affected not only by natural processes but also by many anthropogenic discharge sources as it flows through different basins. Therefore evaluations of monthly value changes due to natural processes should be based on the assumption that anthropogenic inputs are nearly constant. The evaluations in this section are based on this assumption.

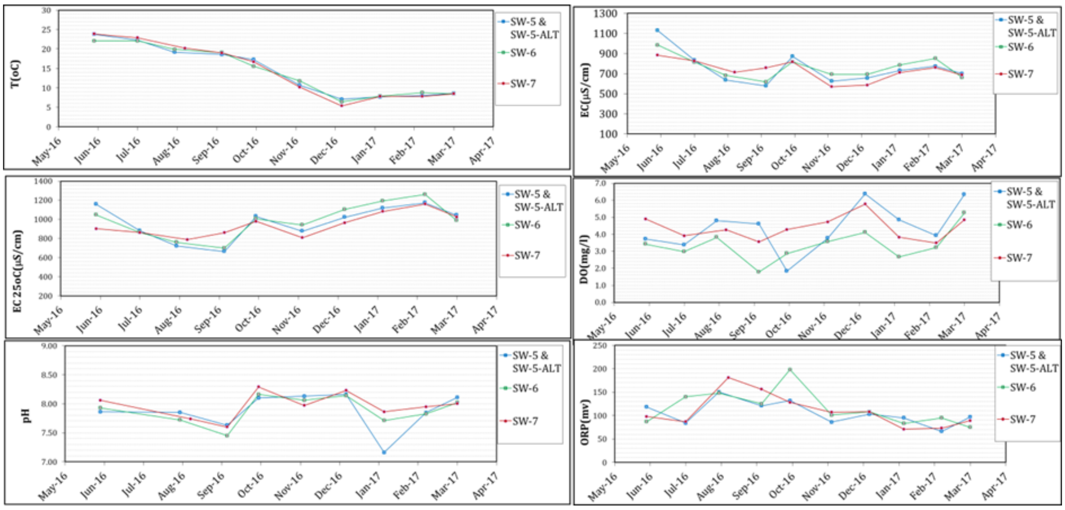

Figure 5.4. Monthly changes of temperature, pH, EC, DO, ORP values in Porsuk Stream (Yazıcıgil et al., 2017).

Temperature, precipitation and discharge relationships of stream water with the field parameter values are shown in Figure 5.5. Electrical conductivity values increase with increasing temperature, 25 degree normalized values, on the other hand, show decrease with increasing discharge and precipitation (if very high precipitation, 50 mm, observed January data excluded; black colored trend line in the figure).

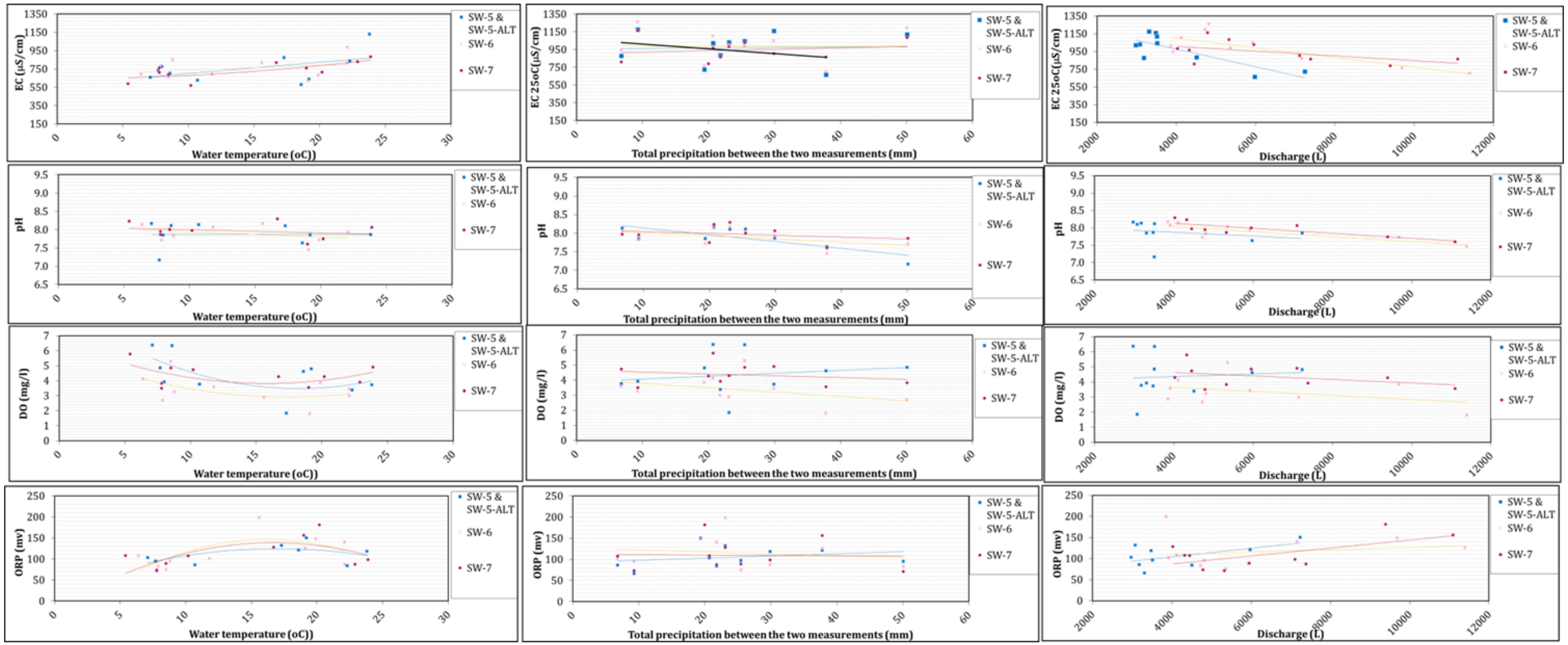

Figure 5.5. Changes of pH, EC, DO, ORP values with respect to temperature, total precipitation between the two measurements and discharge in Porsuk Stream (Yazıcıgil et al., 2017).

When compared with precipitation, the discharge dependent EC decrease, especially in the upstream area is higher. pH values decrease with increasing temperature, precipitation and discharge. Dissolved oxygen values decrease (slightly increase in upstream) upon increasing precipitation and discharge. Although dissolved oxygen values exhibit increasing trend between 15-24 ^{o}C, in other temperatures they decrease with increasing temperature which is the expected trend under normal conditions. The fore mentioned increasing trend indicates that factors other than temperature (e.g. precipitation, groundwater feeding and anthropogenic inputs) dominantly control dissolved oxygen content of surface waters in this temperature range. The ORP values increase upon increasing precipitation and discharge. The discharge dependent ORP increase is higher than that of precipitation. The temperature dependent trend of ORP values is reverse of the dissolved oxygen trend.

5.2.2. Laboratory Measurements

The results of detailed chemical analyses from Porsuk Stream monitoring locations are listed in Table 5.4. Water facies of Porsuk Stream as determined from relative major ion concentration distribution are shown in Figure 5.6. The stream includes Mg (mixed)-HCO_3 type of water in SW-5 and SW-7 monitoring locations. The facies is Mixed (Mg)-HCO_3 type in SW-6 location.

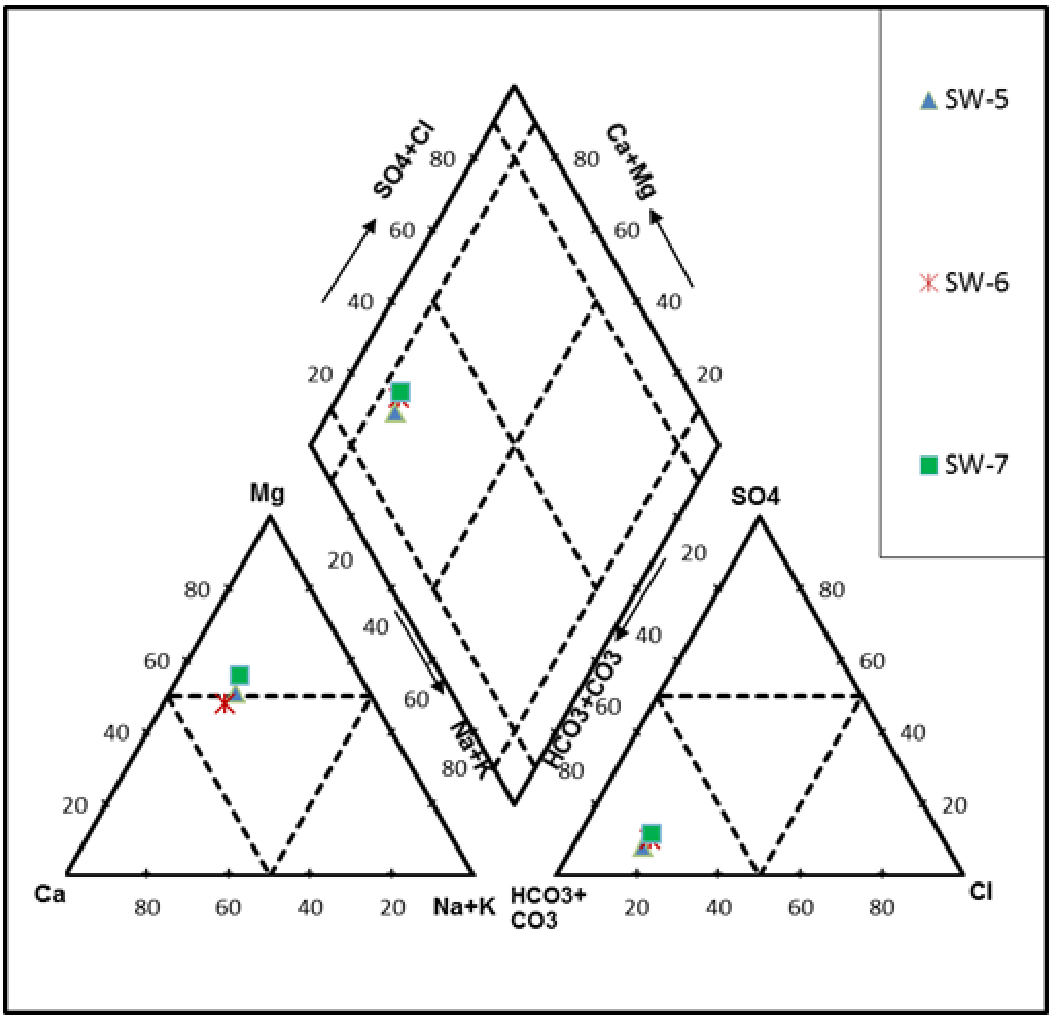

Figure 5.6. Relative major ion concentration distribution in Porsuk Stream waters on Piper graph (Yazıcıgil et al., 2017).

Table 5.4. Values of laboratory parameters measured in Porsuk Stream (Yazıcıgil et al., 2017).

Parameter	SW-5	SW-6	SW-7
DATE	Oct-16	Oct-16	Oct-16
Temperature	17.2	15.7	17
pH	8.18	8.23	8.13
EC	1040	1055	996
DO	3.28	4.57	6.33
DO%	37.1	50.6	70.7
Color	27.385	41.332	25.647
TDS	506	508	484
TSS	<10	<10	<10
Turbidity	0.99	0.29	3.49
Cl	60.97	67.58	64.62
SO4	38.68	51.26	57.15
F	0.327	0.327	0.306
Alkalinity-Total	370	375	360
Alkalinity-HCO3	370	375	360
Alkalinity-CO3	0	0	0
Alkalinity-OH	0	0	0
Total P	0.7702	0.9645	0.8901
Ortho phosphate (o-P	0.949	1.323	1.43
Reaktive P	0.309	0.431	0.466
NH4-N	<0.01	<0.01	<0.01
NO3-N	0.948	1.775	2.042
NO2-N	0.379	0.945	1.104
N, organic	6.72	7	4.2
TKN	6.72	7	4.2
Ag	<0.01	<0.01	<0.01
Al	0.0142	<0.01	<0.01
As	<0.01	<0.01	0.0104
B	0.3975	0.4854	0.3417
Ba	0.1234	0.1409	0.128
Be	<0.01	<0.01	<0.01
Bi	<0.01	<0.01	<0.01
Ca	50.62	69.65	47.93
Cd	<0.003	<0.003	<0.003
Co	<0.01	<0.01	<0.01
Cr	<0.01	<0.01	<0.01
Cu	<0.01	<0.01	<0.01
Fe	0.0605	0.0445	0.0246
Hg	<0.001	<0.001	<0.001
K	12.06	14.05	11.19
Li	0.1914	0.1914	0.1809
Mg	47.58	55.23	55.24
Mn	0.0632	0.0614	0.0413
Mo	<0.01	<0.01	<0.01
Na	21.65	24.76	20.89
Ni	0.0118	0.0116	0.0114
P	0.9465	0.9465	1.141
Pb	<0.01	<0.01	<0.01
Sb	<0.005	<0.005	<0.005
Se	<0.005	<0.005	<0.005
Si	7.17	9	9.34
Sr	0.4502	0.4871	0.4821
Sn	<0.05	<0.05	<0.05
Ti	<0.01	<0.01	<0.01
Tl	<0.01	<0.01	<0.01
U	0.002	0.0027	0.0027
V	0.12	0.1279	0.1354
Zn	0.0251	0.0189	<0.01

Parameter	SW-5	SW-6	SW-7
DATE	Oct-16	Oct-16	Oct-16
Total CN	<0.02	<0.02	<0.02
TOC	10.22	7.11	8.88
COD	34	28	10
H2S	<0.1	<0.1	<0.1
Grease&oil	0.1705	0.0587	0.0928
MBAS	<0.01	<0.01	<0.01
Anthracene	<0.00002	0.000034	<0.00002
Fluoranthene	0.000021	<0.00002	<0.00002
Naphthalene	0.000046	0.000034	0.000023
Benzo(a)pyrene	0.000039	<0.00002	<0.00002
Benzo(b)fluoranthene	0.000032	<0.00002	<0.00002
Benzo(k)fluoranthene	<0.00002	<0.00002	<0.00002
Benzo(g,h,i)perylene	<0.00002	<0.00002	<0.00002
Indeno(1,2,3-cd) pyrene	0.0001	0.000113	0.000035
Atrazin	<0.000005	<0.000005	<0.000005
Chlorfenvinphos	<0.00008	<0.00008	<0.00008
chlorpyrifos-ethyl	<0.00008	<0.00008	<0.00008
Simazine	<0.000005	<0.000005	<0.000005
Alachlor	<0.000005	<0.000005	<0.000005
Endosulfan	0.00000193	0.00000291	<0.000001
Hexachlorobenzene	<0.000001	<0.000001	<0.000001
Trifluralin	<0.000005	<0.000005	<0.000005
Hexachlorocyclohexane	0.00000658	0.00000548	0.00000439
Benzene	<0.005	<0.005	<0.005
1,2-Dichloroethane	<0.005	<0.005	<0.005
Dichloromethane	<0.02	<0.02	<0.02
Hexachlorobutadiene	<0.00002	<0.00002	<0.00002
Trichloromethane	<0.005	<0.005	<0.005
Trichlorobenzenes	<0.001	<0.001	<0.001
Di(2-ethylhexyl)phthalate	0.00000324	0.00000133	0.00000292
Pentachlorobenzene	<0.000005	<0.000005	<0.000005
Diuron	0.000007	0.000009	0.000008
Isoproturon	<0.000005	<0.000005	<0.000005
Nonylphenols	<0.001	<0.001	<0.001
octylphenols	<0.0005	<0.0005	<0.0005
Pentachlorophenol	<0.00004	<0.00004	<0.00004
Tributyltin	<0.00002	<0.00002	<0.00002
Bromodiphenylethers	<0.00001	<0.00001	<0.00001
Pentabromodiphenylether	<0.00001	<0.00001	<0.00001
C10-13 Chloroalkanes	<0.0004	<0.0004	<0.0004
pp-DDT	<0.000001	<0.000001	<0.000001
BOD5	5.65	4.95	6
Fecal Coliform	>100000	üremedi	üremedi
Total Coliform	>100000	>100000	>100000
Fecal Streptecoc	85	üremedi	6
Escherichia Coli	>100000	>100000	>100000

(Unit: mg/l, alkalinity as CaCO3, color: pt/co, radioactivity Bq/L, bacteriological: cfu/100 mL, temperature oC)

The distribution of major ion concentrations is similar as shown in Schoeller graph (Figure 5.7). Sulfate concentrations increase from upstream to downstream. Chloride, bicarbonate, calcium and sodium concentrations, on the other hand, increase between SW-5 and SW-6 locations but decrease afterwards.

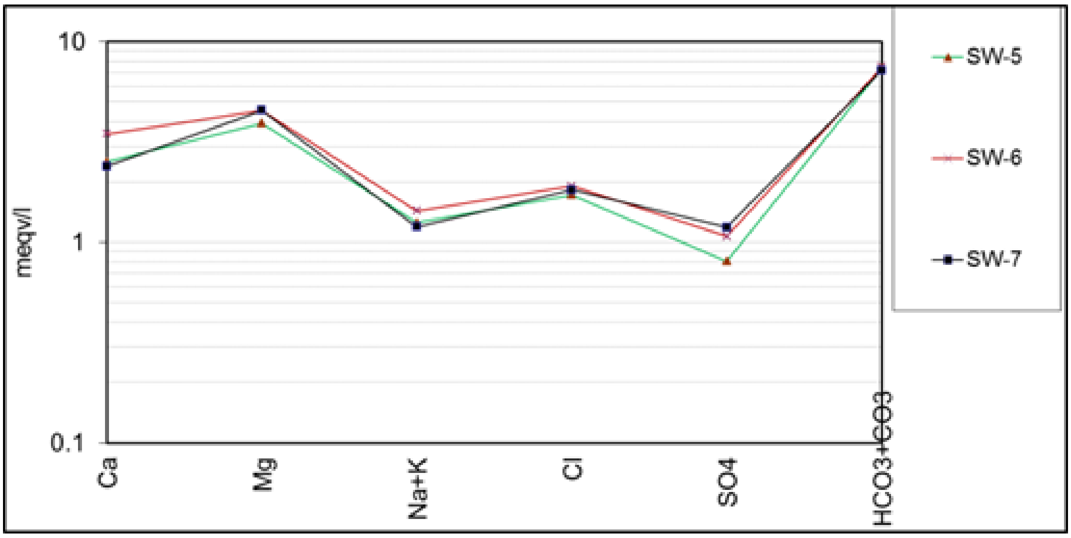

Figure 5.7. Major ion oncentration distribution in Porsuk Stream waters on Schoeller graph (Yazıcıgil et al., 2017).

The comparison of parameter concentrations (which are greater than the detection limits) measured in the Porsuk stream monitoring locations is shown in Figure 5.8. Concentrations of Ag, Be, Bi, Cd, Co, CN, Cr, Cu, Hg, H2S, Mo, NH4, Pb, Sb, Se, Sn, Ti and Tl parameters are below the detection limits in all monitoring locations. From upstream to downstream; Mg, N-NO3, N-NO2, P reactive, Si and SO4 concentrations slightly increase and Al, B, Fe, Mn and Zn values slightly decrease. Among the organic parameters, which are not shown on the figure, above detection limit values were measured at locations of SW-5, SW-6 and SW-7; in concentrations of polyaromatic hycdrocarbons (respectively, 0.238, 0.181, 0.058 µg/), endosulfan (respectively, 0.00193, 0.00291, <0.001 µg/l), hexachlorocyclohexane (respectively, 0.00658, 0.00548, 0.00439 µg/l), Di(2-ethylhexyl) phthalate (respectively, 0.00324, 0.00133, 0.00292 µg/l) and diuron (respectively, 0.007, 0.009, 0.008 µg/l).

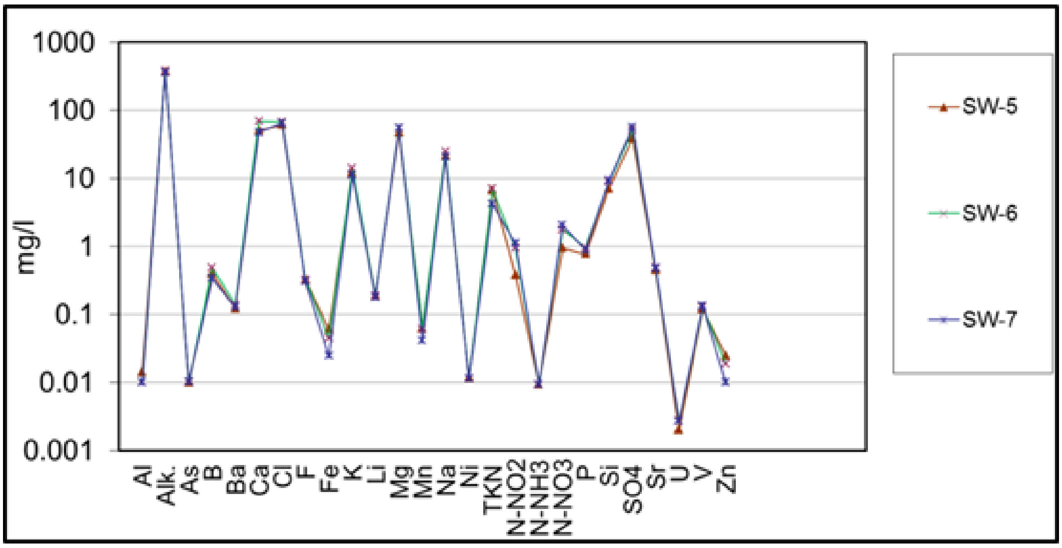

Figure 5.8. Ion concentration distribution in Porsuk Stream waters (Yazıcıgil et al., 2017).

5.2.3. Sediment Chemistry

The results of detailed chemical analyses measured in Porsuk stream sediment sample from upstream (SW5) location are given in Table 5.5. Majority of the measured organic parameters in sediments has below detection limit values. Above detection limit values are measured for parameters of total organic carbon (3.3%), organic nitrogen (8550 mg/kg), naphthalene (0.13 mg/kg), Phenanthrene (0.116 mg/kg), and semi-volatile organics (18.657 mg/kg).

The comparison of average metal concentrations in sediments to those of average upper crustal concentrations (Rudnick and Gao, 2003) is shown as a ratio in Figure 5.9. Porsuk stream sediments have higher Ag, As, B, Bi, Ca, Cd, Cr, Cu, Hg, Li, Mg, Ni, P, Sb, Sn and Zn concentrations than the upper crustal average in SW-5 location.

Table 5.5. Values of parameters measured in upstream sample of Porsuk Stream sediments (Yazıcıgil et al., 2017).

Metals	SW-5
mg/kg	Eki.16
Ag	0.538
Al	9453.414
As	11.194
B	30.056
Ba	124.619
Be	<0.5
Bi	1.357
Ca	45119.25
Cd	1.494
Co	13.789
Cr	106.995
Cu	37.553
Fe	17679.026
Hg	0.115
K	1491.384
Li	106.774
Mg	16416.583
Mn	308.39
Mo	0.698
Na	214.967
Ni	214.866
P	1794.54
Pb	9.493
Sb	0.588
Se	<0.25
Si	182.142
Sr	137.999
Sn	38.459
Ti	53.933
Tl	<0.5
U	1.2
V	15.572
Zn	438.716

Phenolics (mg/kg)	SW-5
4-Chloro-3-methylphenol	<5
2-Chlorophenol	<0.5
3-Chlorophenol	<0.5
4-Chlorophenol	<0.5
2,3-Dichlorophenol	<0.5
2,4 & 2,5-Dichlorophenol	<0.5
2,6-Dichlorophenol	<0.5
3,4-Dichlorophenol	<0.5
3,5-Dichlorophenol	<0.5
2,4-Dimethylphenol	<0.5
o-Cresol	<5
m-Cresol	<5
p-Cresol	<5
Pentachlorophenol	<0.5
Phenol	<1
2,3,4,5-Tetrachlorophenol	<0.5
2,3,4,6-Tetrachlorophenol	<0.5
2,3,5,6-Tetrachlorophenol	<0.5
2,3,4-Trichlorophenol	-
2,3,5-Trichlorophenol	<0.5
2,3,6-Trichlorophenol	<0.5
2,4,5-Trichlorophenol	<0.5
2,4,6-Trichlorophenol	<0.5
Organic C%	3.314
Organic N (mg/kg)	8550.53

Chlorinated Hydrocarbons (mg/kg)	SW-5
1,2-Dichlorobenzene	<2.5
1,3-Dichlorobenzene	<2.5
1,4-Dichlorobenzene	<2.5
Hexachlorobenzene	<0.002
Hexachlorocyclohexane (t)	<0.002
1,2,4-Trichlorobenzene	<2.5
Semi-Volatile Organics (mg/kg)	**SW-5**
Butylbenzyl Phthalate	<1
Diethyl Phthalate	<1
Dimethyl Phthalate	<1
Di-n-butyl Phthalate	3.947
Di-n-Octyl Phthalate	3.333
bis(2-Ethylhexyl)Phthalate	3.802
Diisobutyl Phthalate	7.575

Polycyclic Aromatic Hydrocarbons (mg/kg)	SW-5
Acenaphthene	<0.1
Acenaphthylene	<0.1
Anthracene	<0.1
Benz(a)anthracene	<0.1
Benzo(a)pyrene	<0.1
Benzo(b)fluoranthene	<0.1
Benzo(g,h,i)perylene	<0.1
Benzo(k)fluoranthene	<0.1
Chrysene	<0.1
Dibenz(a,h)anthracene	<0.1
Fluoranthene	<0.1
Fluorene	<0.1
Indeno(1,2,3-c,d)pyrene	<0.1
Naphthalene	0.13
Phenanthrene	0.116
Pyrene	<0.1

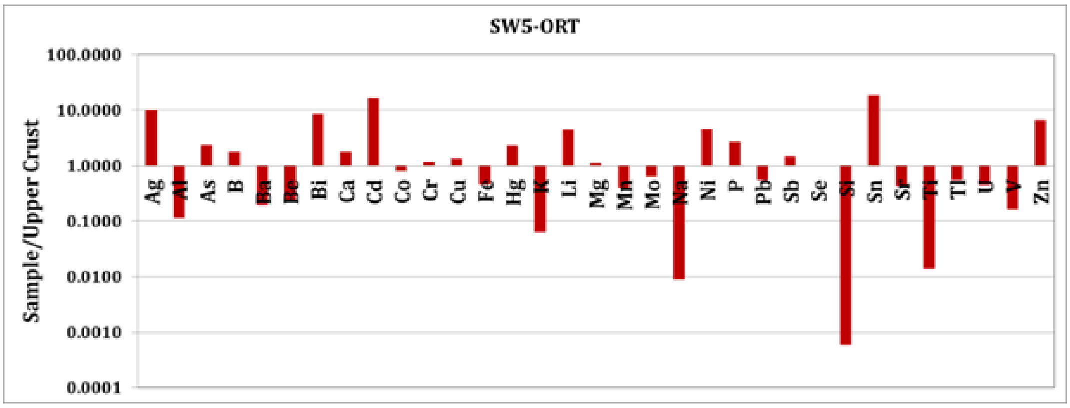

Figure 5.9. Comparison of metal concentrations in Porsuk Stream sediments to those of average upper crustal concentrations (Yazıcıgil et al., 2017).

5.3. Groundwater Hydrochemistry

5.3.1. Well Waters

5.3.1.1. Field Measurements

The results of hydrochemical field parameter measurements and average values together with average deviations for more than one measurement including locations in well waters are listed Table 5.6. Because it was not possible to purge wells during monthly monitoring, only flowing artesian well ESHİD-02P has been monitored monthly. Other measurements were carried out during sampling period.

Table 5.6. Values of hydrochemical field parameters measured in well water monitoring locations (Yazıcıgil et al., 2017).

NO	DATE	T(oC)	pH	ORP (mv)	EC 25oC (µS/cm)	S (ppt)	TDS (mg/l)	DO (mg/l)	DO%
APK-2	02.09.16	16.7	7.67	153	765	0.38	497	2.93	34
APK-3	27.02.17	19.0	7.74	-2	3523	1.75	2287	3.19	38
APK-4	16.02.17	14.1	7.48	143	743	0.37	483	3.31	36
APK-5	01.02.17	20.7	7.75	-134	4683	2.33	3039	4.39	52
APK-6	26.01.17	12.7	7.87	121	1086	0.54	706	4.50	44
APK-7	19.10.16	16.2	7.56	120	700	0.34	455	4.57	51
	02.11.16	14.6	7.94	179	690	0.34	449	5.02	58
	AV(ADEV)	15.4(0.8)	7.75(0.19)	150(30)	695.0(*)	0.3(*)	451.9(*)	4.80(0.23)	54(3.3)
ESHİD-01P	02.09.16	15.1	7.57	166	869	0.43	565	2.49	28
ESHİD-02P	19.11.16	23.0	8.21	-125	11025	5.23	6794	3.40	43
	20.12.16	11.3	8.62	-241	11523	5.50	7145	1.12	12
	26.01.17	12.4	8.92	-204	12366	6.18	8025	2.82	27
	20.02.17	14.2	8.71	-215	12270	6.13	7963	1.61	17
	15.03.17	13.4	8.47	-194	12161	6.07	7892	1.67	21
	AV(ADEV)	14.9(3.3)	8.59(0.20)	-196(29)	11,869(476)	5.93(0.24)	7,703(309)	2.12(0.79)	24(8.9)

AV: average, (ADEV): average deviation and (*): AV is less than the measurement error.

Depth related groundwater temperatures were measured in wells every 6 hours in 550 hours period, in addition to temperature measurements from samples during field parameter monitoring. Average values of these measurements are listed in Table 5.7. The data indicate that groundwater temperatures increase in the range of 14-35 ^{o}C with depth.

Table 5.7. Average groundwater temperatures measured as a function of depth

Unit	Well No	Piezometer Depth (m)	Average Temperature (°C)
Alluvium	ML-3B	16	14.1
Alluvium	ML-3B	30	14.3
Alluvium	ML-1	32	14.6
Pliocene	ML-1	53	15.3
Miocene	ML-1	70	16.4
Miocene	ML-3A	108	18.5
Miocene	ML-3A	163	21.0
Miocene	ML-4A	224.95	23.4
Miocene	ML-4A	307.95	26.6
Shale-coal seam (A)	ML-4B	332.2	28.8
Shale-coal seam (A)	ML-2	375.4	30.6
Sandstone-coal seam (C)	ML-4B	390.2	33.3
Shale-coal seam (D)	ML-2	439.9	34.9

Values (ESHİD-02P and APK-7 are averages) of pH, EC, DO and ORP parameters are shown in Figure 5.10. The electrical conductivity values of well waters are; 743 µS/cm in Alluvium aquifer groundwater (APK-4), 695 µS/cm in Pliocene aquifer groundwater (APK-7), 765 µS/cm in Upper Miocene aquifers groundwater (APK-2) and in the range of 11025-12366 µS/cm in Pliocece + Miocene aquifers groundwater (ESHİD-02P). In groundwater of Alluvium, Pliocene and Pliocene + Miocene aquifers, average values of total dissolved solids are about 483 mg/L, 452 mg/L, 7703 mg/L and salinity are about 0.37 ppt, 0.34 ppt and 5.93 ppt, respectively.

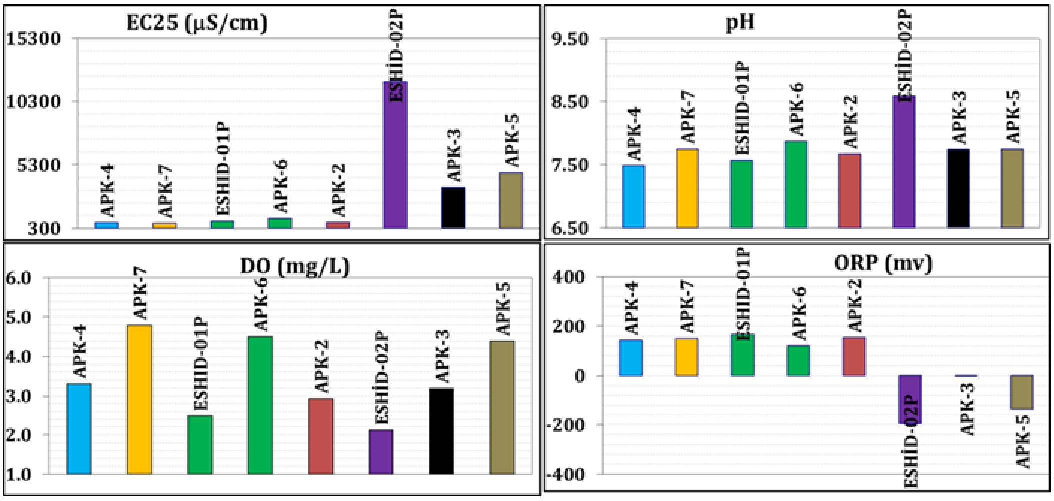

Figure 5.10. pH, EC, DO and ORP values measured in well water monitoring locations. Blue Alluvium aquifer; orange Pliocene aquifer, green Alluvium + Miocene aquifers; claret red Upper Miocene aquifers, purple Pliocene + Miocene aquifers, black Alluvium+ Miocene+ Coal aquifer and gray Miocene+ coal aquifers (Yazıcıgil et al., 2017).

Well waters are in basic character and pH values are 7.48 in Alluvium groundwater, 7.75 in Pliocene groundwater, 7.67 in Pliocene + Upper Miocene groundwater and in the range of 8.21-8.92 in Pliocene + Miocene groundwater. The values in general slightly increase toward deeper aquifer groundwater.

Dissolved oxygen values are 3.31 mg/l in Alluvium groundwater, 4.80 mg/l in Pliocene groundwater, 2.93 mg/l in Pliocene + Upper Miocene groundwater and in the range of 1.12-3.40 mg/l in Pliocene + Miocene groundwater.

Oxidation-Reduction potential values are 143 mV in Alluvium groundwater, 150 mV in Pliocene groundwater and 153 mV in Pliocene + Upper Miocene groundwater with oxidizing character but reducing values in the range of -125 - -241 mV are measured in Pliocene + Miocene groundwater.

Value changes in the field parameters during the monitoring period are calculated for APK-7 ve ESHİD-02P coded well waters as percent average deviation excluding the measurement percent error. The averages of percent average deviations from higher to lower values are determined in dissolved oxygen (36%), temperature (22%), ORP (18%), EC (3.2%) and pH (1.9%) parameters for ESHİD-02P waters and in ORP (16%), temperature (5%), dissolved oxygen (3.5%), pH (2%) and EC (0%) parameters for APK-7 waters. The averages of average deviations for ESHİD-02P well water are about 476 µS/cm in electrical conductivity, 0.20 in pH, 29 mV in ORP and 0.8 mg/l in dissolved oxygen parameters. The averages are for APK-7 well water in the measurement error limit of electrical conductivity, 0.19 in pH, 30 mV in ORP and 0.23 mg/l in dissolved oxygen parameters.

5.3.1.2. Laboratuary Measurements

The results of detailed chemical analyses from well water monitoring locations are given in Table 5.8. Water facies of well waters as determined from relative major ion concentration distributions are shown in Figure 5.11. The field distribution of the facies is given in Figure 5.12. Groundwaters of Alluvium aquifer (composed of sand, clay and gravel) in APK-4 well and Pliocene aquifer (composed of shale, sandstone, siltstone, conglomerate and limestone sequences) in APK-7 well are in Mg-HCO3 facies. Miocene aquifer composed of shale, sandstone and siltstone sequence with gypsum bands includes Mix (Ca,Mg)-SO4 type of groundwater as sampled from ESHİD-02P well which also screens lower Plioecene unit. ESHİD-01 and APK-6 well waters screening Alluvium and Miocene aquifers are Mg-HCO3 type, APK-2 well water screened in Upper Miocene aquifers is Mg-Mix (HCO3) type, APK-3 well water screening Alluvium + Miocene + Coal aquifers is Mg-SO4 type and APK-5 well water screening Miocene + Coal aquifers is (Ca, Mg)-SO4 type.

Table 5.8. Values of laboratory parameters measured in well water monitoring locations (Yazıcıgil et al., 2017).

Parametre	**ESHİD-01P**	**ESHİD-02P**	**APK-2**	**APK-3**	**APK-4**	**APK-5**	**APK-6**	**APK-7**
TARİH	Eylül 16	Aralık 16	Eylül 16	Şubat 17	Şubat 17	Şubat 17	Ocak 17	Kasım 16
Sıcaklık	15.1	23	16.7	19	14.1	20.7	12.7	14.6
pH	7.67	8.08	7.72	7.8	7.48	7.53	7.87	7.94
EC	926	8030	789	3480	581	5290	819	634
DO	4.39	9.14	3.33	4.17	3.31	4	4.45	5.02
DO	45.7	89.9	37.9	49.1	36	47.9	44.4	57.8
Renk	14.329	7.886	14.855	8.408	6.508	9.667	7.767	4.634
TDS	456	5526	382	1726	286	2920	518	308
TSS	<10	<10	16.2	<10	<10	13	<10	<10
Cl	37.28	1015	75.08	319.9	23.61	272.9	36.9	40.41
SO4	95.16	2372.75	68.18	1590.4	55.36	3327	138.82	66.77
F	0.448	<0.02	0.259	0.292	0.266	0.117	0.376	0.34
Alkalinite-Toplam	455	120	145	295	305	255	430	290
Alkalinite-HCO3	455	120	145	295	305	255	430	290
Alkalinite-CO3	10	0	0	0	0	0	0	0
Alkalinite-OH	0	0	0	0	0	0	0	0
Toplam P	0.0208	<0.01	0.0266	0.0158	0.0383	<0.01	0.0136	<0.01
Reaktif P	<0.01	<0.01	<0.01	<0.01	<0.01	<0.01	<0.01	<0.06
N-NH4	<0.01	3.2068	<0.01	1.184	0.0171	0.829	<0.01	<0.01
NO3-N	4.258	0.0535	2.325	2.574	3.748	<0.02	1.323	2.014
NO2-N	0.0398	0.00135	0.031	0.303	<0.001	0.04	<0.001	0.031
N, organik	1.33	2.603	<0.5	<0.5	<0.5	0.151	0.7	<0.5
TKN	1.33	5.81	<0.5	0.56	<0.5	0.98	0.7	<0.5
Ag	<0.01	<0.01	<0.01	<0.01	<0.01	<0.01	<0.01	<0.01
Al	<0.01	0.0253	<0.01	0.0316	0.023	0.03	0.0202	<0.01
As	<0.01	<0.01	0.018	<0.01	<0.01	<0.01	<0.01	0.01
B	0.343	60.02	1.189	12.53	0.6166	48.31	0.8272	0.8368
Ba	0.213	0.0313	0.0475	0.0519	0.133	0.0296	0.1945	0.133
Be	<0.01	<0.01	<0.01	<0.01	<0.01	<0.01	<0.01	<0.01
Bi	<0.01	<0.01	<0.01	<0.01	<0.01	<0.01	<0.01	<0.01
Ca	66.86	763.5	31.12	178.5	50.28	421.5	88.55	50.64
Cd	<0.003	<0.003	<0.003	<0.003	<0.003	<0.003	<0.003	<0.003
Co	<0.01	<0.01	<0.01	<0.01	<0.01	<0.01	<0.01	<0.01
Cr	<0.01	0.0832	<0.01	<0.01	0.01	<0.01	<0.01	0.011
Cu	<0.01	<0.01	<0.01	<0.01	<0.01	<0.01	<0.01	<0.01
Fe	0.0219	0.5936	<0.01	0.6323	0.0247	4.63	0.0103	<0.01
Hg	<0.001	<0.001	<0.001	<0.001	<0.001	<0.001	<0.001	<0.001
K	6.678	14.4	3.6	33.51	3.478	42.11	8.81	1.642
Li	0.1402	4.459	0.3628	0.918	<0.05	1.672	0.0601	0.1259
Mg	65.9	420.9	33.42	163.1	41.99	215.2	82.55	47.58
Mn	<0.01	0.1698	<0.01	0.3696	0.1198	0.236	<0.01	<0.01
Mo	<0.01	0.689	<0.01	<0.01	<0.01	<0.01	<0.01	<0.01
Na	8.06	58.22	15.03	30	2.763	65.46	1.988	2.18
Ni	<0.01	<0.01	<0.01	0.0235	<0.01	<0.01	<0.01	<0.01
P	öy	<0.05	öy	<0.05	<0.05	<0.05	<0.05	<0.05
Pb	<0.01	<0.01	<0.01	0.0142	<0.01	0.0294	<0.01	<0.01
Sb	<0.005	<0.005	<0.005	<0.005	<0.005	<0.005	<0.005	<0.005
Se	<0.005	<0.005	<0.005	<0.005	<0.005	<0.005	<0.005	<0.005
Si	3.721	4.705	3.936	14.63	16.38	8.515	15.85	11.8
Sr	0.8208	9.688	0.9968	3.635	0.4583	6.221	1.704	0.6867
Sn	<0.05	<0.05	<0.05	0.1327	<0.05	<0.05	<0.05	<0.05
Ti	<0.01	<0.01	<0.01	<0.01	<0.01	<0.01	<0.01	<0.01
Tl	<0.05	<0.01	<0.05	<0.05	<0.05	<0.05	<0.05	<0.01
U	0.00814	0.00059	0.00572	0.000002	0.000002	<0.000002	0.000008	0.0014
V	0.1606	0.0445	0.0884	<0.01	<0.01	0.49	0.2045	0.0135
Zn	0.0126	<0.01	0.0346	0.0239	0.0154	0.0101	0.0603	0.0117
Toplam CN	<0.02	<0.02	<0.02	<0.02	<0.02	<0.02	<0.02	<0.02
TOC	<5	<5	<5	<1	<1	1.432	<1	<5
KOİ	37	10	19	22	13	11	10	11
Sülfür	<0.1	<0.1	<0.1	<0.1	<0.1	<0.1	<0.1	<0.1
Yağ ve Gres	<0.1	0.623	<0.1	0.08059	0.07472	0.24769	0.70308	0.13
MBAS	<0.01	<0.01	<0.01	<0.01	<0.01	<0.01	<0.01	<0.01
VOC	<0.01	0.014	<0.01	<0.01	<0.01	<0.01	<0.01	<0.005
Atrazin	<0.00001	öy	<0.00001	<0.00005	<0.00005	<0.000005	<0.000005	öy
Chlorfenvinphos	<0.00008	öy	<0.00008	<0.00008	<0.00008	<0.00008	<0.00008	<0.00008
Chlorpyrifos	<0.00008	öy	<0.00008	<0.00008	<0.00008	<0.00008	<0.00008	<0.00008
Simazine	<0.00001	öy	<0.00001	<0.00005	<0.00005	<0.00005	<0.000005	öy
pp-DDT	<0.000001	öy	<0.000001	<0.000001	<0.000001	<0.000001	<0.000001	<0.000001
Alachlor	<0.000005	öy	<0.000005	<0.00001	<0.00001	<0.00001	<0.00001	öy
Endosulfan	<0.000001	öy	<0.000001	<0.000001	<0.000001	<0.000001	0.00000128	<0.000001
Trifluralin	<0.000005	öy	<0.000005	<0.00001	<0.00001	<0.000001	<0.000001	öy
Diuron	<0.000001	öy	<0.000001	<0.00005	<0.00005	<0.000005	<0.000005	öy
Isoproturon	<0.000001	öy	<0.000001	<0.00005	<0.00005	<0.000005	<0.000005	öy
Trichloroethylene	<0.01	<0.01	<0.01	<0.01	<0.01	<0.01	<0.01	<0.005
Tetrachloroethylene	<0.01	<0.01	<0.01	<0.01	<0.01	<0.01	<0.01	<0.005
Alfa-Rady.	0.11	<0.25	0.08	<0.18	0.05	0.82	0.18	<0.04
Beta-Rady.	0.41	1.63	0.39	<0.6	0.15	0.75	0.54	<0.1
BOİ5	8.55	3.21	3.6	6.07	3.42	2.74	2.39	3.01
Fekal Koliform	0	öy	40	0	0	0	0	öy
Toplam Koliform	7	öy	660	0	10	68	42	öy
Fekal Spreptekok	öy	öy	öy	0	0	0	0	öy
Escherichia Coli	öy	öy	öy	0	0	4	35	öy

(Birim: mg/l, alkalinite as CaCO3, renk: pt/co, radyoaktivite Bq/L, bakteriyolojik: cfu/100 mL, Sıcaklık oC. öy: ölçüm yok)

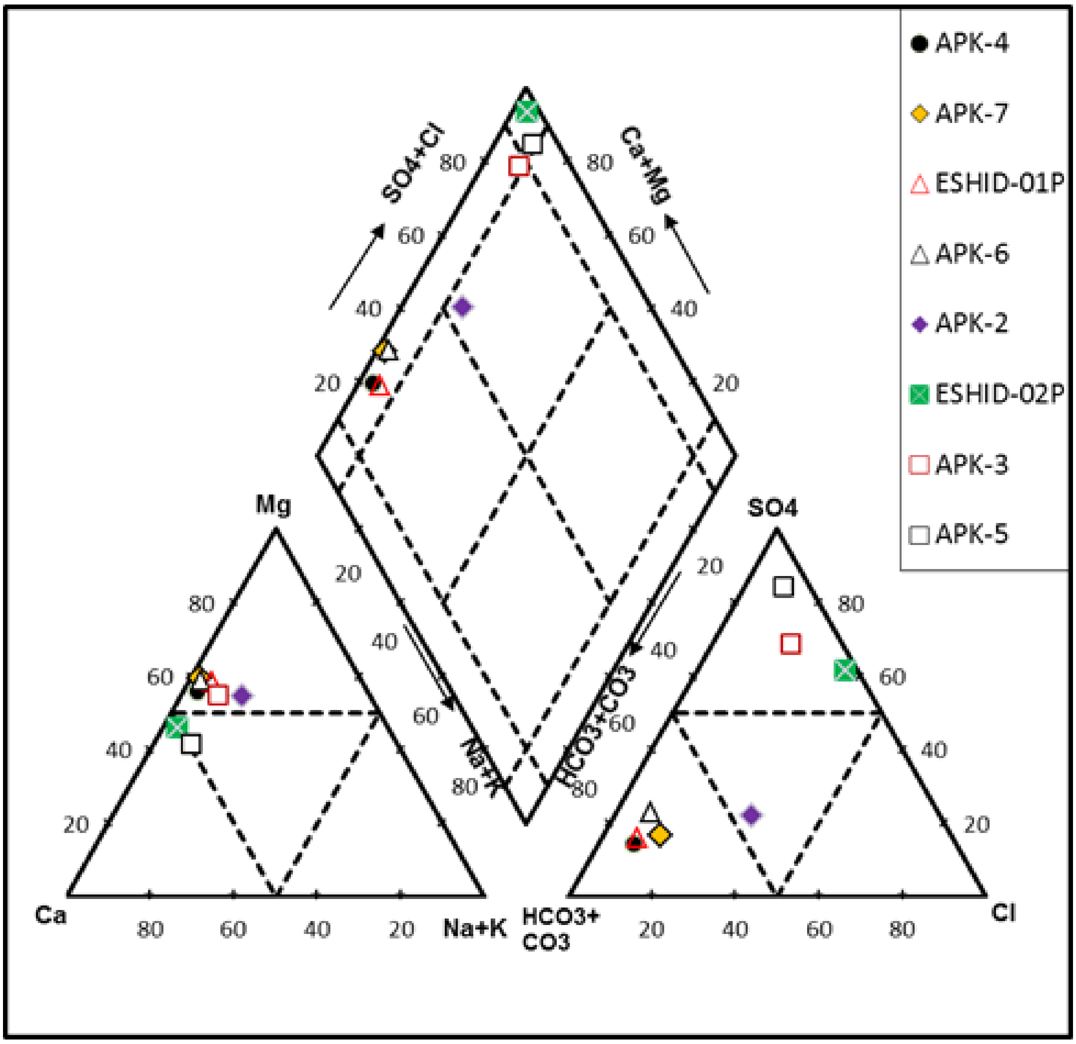

Figure 5.11. Relative major ion concentration distribution in well waters on Piper graph (Yazıcıgil et al., 2017).

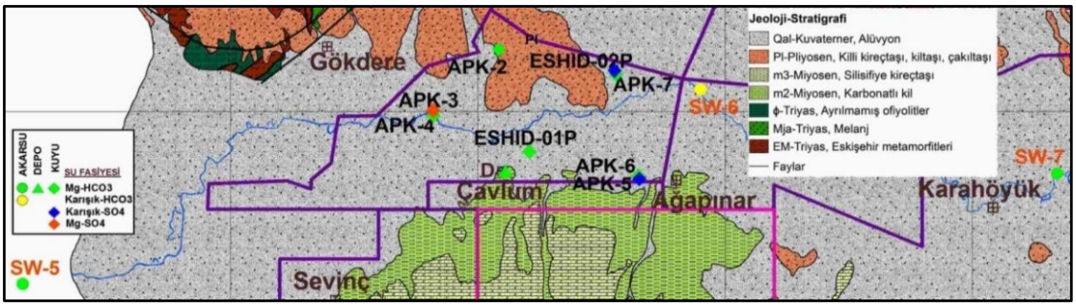

Figure 5.12. Relative major ion concentrations related hydrochemical facies distribution in the monitoring locations (Yazıcıgil et al., 2017).

The differences and similarities of the major ion average concentration distributions are shown in Schoeller graph (Figure 5.13). Miocene aquifer groundwater from deeper levels includes higher ion concentrations. Very high sulfate concentration (about 2000-3000 mg/l) of Miocene groundwater is probably related to the gypsum dissolution.

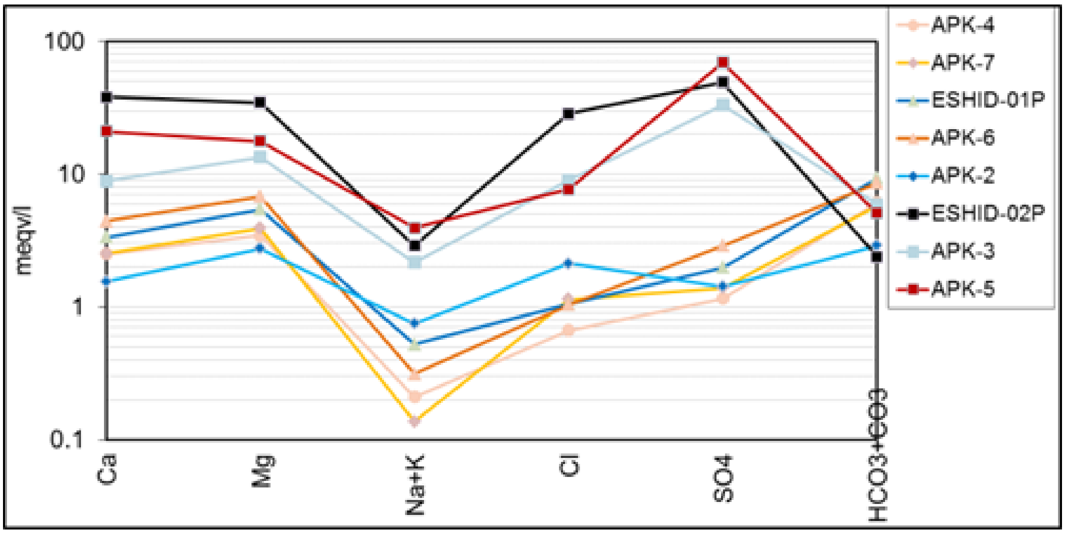

Figure 5.13. Major ion concentration distributions in well waters on Schoeller graph (Yazıcıgil et al., 2017).

A comparison of parameter concentrations (which are greater than the detection limits) in well waters is shown in Figure 5.14. Concentrations of Ag, Be, Bi, Cd, CN, Co, Cu, Hg, P reactive, S, Sb, Se, Ti, Tl and organic parameters [excluding trichloroethylene, tetrachloroethylene, pesticides, volatile organics (except ESHİD-02P 0.014 mg/l) and oil &grease (except in ESHİD-02P, APK-3, APK-4, APK-5, APK-6 and APK-7 waters in mg/l; 0.62, 0.08, 0.07, 0.25, 0.70 and 0.13, respectively)] are below the detection limits in all monitoring locations. In addition to these, As only in Pliocene groundwater; Mo only in Miocene groundwater; Pb, Sn and TOC only in all unit screening (including coal seams) groundwater measured above the detection limits. In addition to major ions, Miocene groundwater includes also much higher B (about sixty times), Sr (about nine times), Li (about four times) and ammonia (about three times) concentrations than the other groundwater.

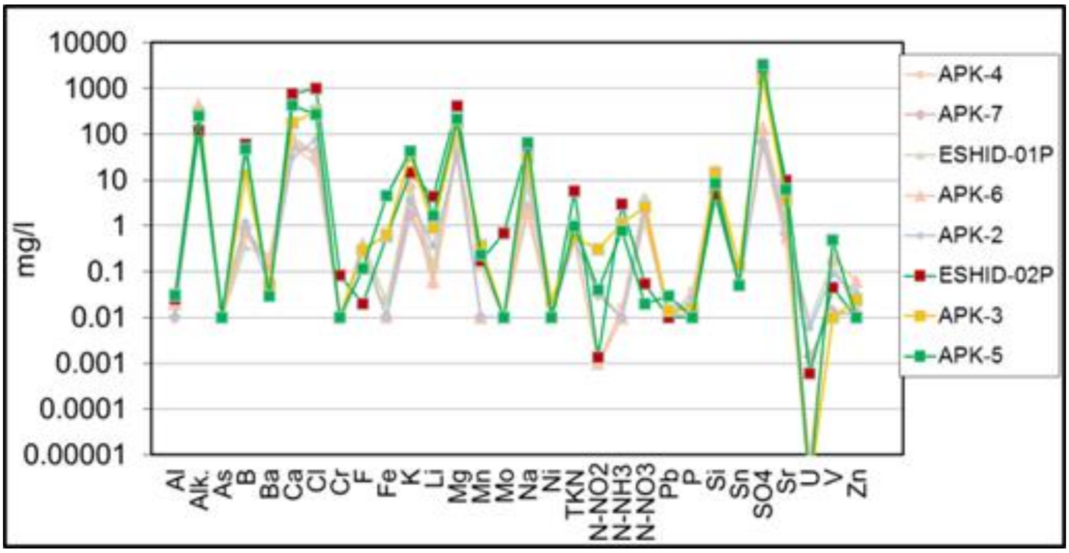

Figure 5.14. Ion concentration distributions in well waters (Yazıcıgil et al., 2017).

Concentration (ESHİD-02P; 3.4 mg/l) of ammonia/ammonium in Pliocene groundwater is much higher than the generally expected values (<0.2 mg/l). This level of ammonia/ammonium is most probably anthropogenic related.

5.3.2. Village Depot Waters

Çavlum village depot water information is summarized below from the report of Yazıcıgil et. al. (2017). Water to the depot is supplied from a captage in silicified limestones within the ESAN coal license area where located at the southeast of Sector-A.

5.3.2.1. Field Measurements

Average electrical conductivity values vary between 342 µS/cm and 389 µS/cm. Average values of total dissolved solids and salinity which are determined using measured EC values, change in the intervals of 223-253 mg/l and 0.16-0.19 ppt, respectively. The depot water is in basic character and average pH values vary in the interval of 7.74 and 8.64; dissolved oxygen average values change in the interval of 6.33-8.29 mg/l. Average values of oxidation-reduction potential are oxidizing and vary in the interval of 111-204 mV.

5.3.2.2. Laboratory Measurements

The results of detailed chemical analyses from Çavlum village water are listed in Table 5.9. The depot water is in Mg-HCO_3 facies. A comparison of parameter average concentrations (which are greater than the detection limits) is shown in Figure 5.15. Concentrations of Ag, Be, Bi, Co, CN, Hg, Mo, Sb, Se, Sn, Ti, TOC and organic parameters are below the detection limits.

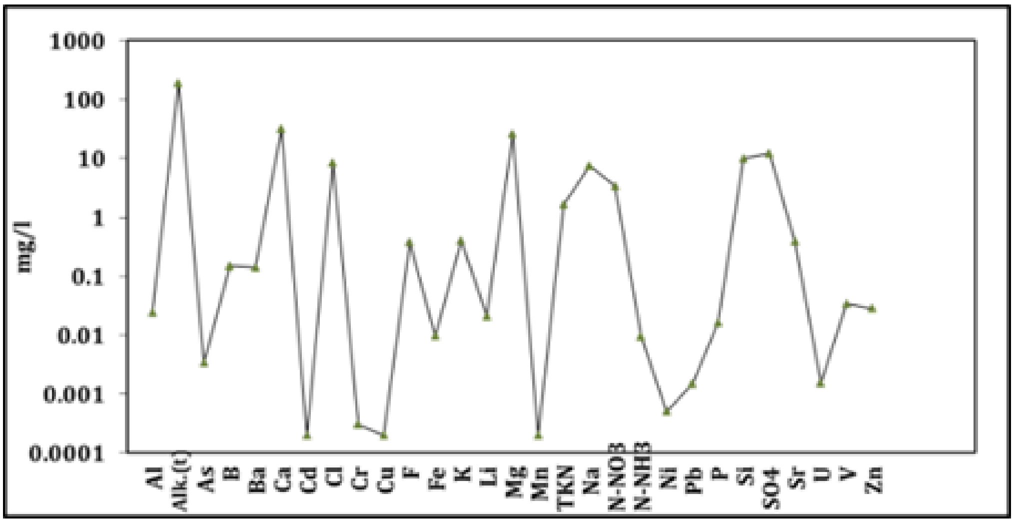

Figure 5.15. Average ion concentration distribution in Çavlum village depot water(Yazıcıgil et al., 2017).

Table 5.9. Average (AV), average deviation (ADEV) values of laboratory parameters measured in Çavlum village depot water (Yazıcıgil et al., 2017).

	Çavlum Depot		Çavlum Depot		Çavlum Depot
Ag	0.0005(*)	**Li**	0.021(*)	**TOC**	1.0(*)
Al	0.024(0.021)	**Mg**	25.60(0.89)	**U**	0.0015(0.0003)
Alk.	190(20)*	**Mn**	0.0002(*)	**V**	0.034(0.030)
As	0.0034(*)	**Mo**	0.001(*)	**Zn**	0.028(0.030)
B	0.148(0.044)	**TKN**	1.63(1.13)	**Trichloroethylene**	0.0008(*)
Ba	0.141(0.023)	**N(Org)**	1.62(1.12)	**Tetrachloroethylene**	0.0008(*)
Be	0.00004(*)	**Na**	7.44(2.22)	**Acrylamid**	0.00005(to)
Bi	0.01(*)	**Ni**	0.0005(*)	**Bromate**	0.01(*)
Ca	31.15(5.51)	**N-NH4**	0.01(*)	**VOC**	0.0034(to)
Cd	0.0002(*)	**N-NO2**	0.013(0.016)	**Benzene**	0.00084(*)
Cl	8.24(0.64)	**N-NH3**	0.01(*)	**1,2-Dichloroethane**	0.0006(*)
CN	0.01(*)	**N-NO3**	3.35(0.46)	**Trihalomethanes**	0.0019(*)
Co	0.0005(*)	**Pb**	0.0015(*)	**Vinyl Chloride**	0.0005(*)
COD	13(5)	**P**	0.016(0.007)	**Tri-tetraCE**	0.0008(*)
Color	5.6(3.4)	**Sb**	0.002(*)	**Benzo(a)pyrene**	0.00005(*)
Cr	0.0003(*)	**Se**	0.005(*)	**Alpha-ac**	0.03(*)
Cu	0.0002(*)	**Si**	9.95(0.80)	**Beta-ac**	0.10(*)
F	0.38(0.03)	**Sn**	0.001(*)	**BOD5**	2.8(1.1)
Fe	0.010(0.005)	**SO4**	12.01(1.49)	**Coli-f**	0(*)
P,reac	0.010(0.000)	**Sr**	0.386(0.030)	**Coli-t**	50000(50000)
Hg	0.00008(*)	**TDS**	160(16)	**f-Streptecoc**	0(*)
K	0.400(0.018)	**Ti**	0.0002(*)	**E-Coli**	50(50)
		Tl	0.062(0.041)	**Enterococ**	0(*)

(*) ADEV less than measurement error

(Unit: mg/l, alkalinity as CaCO3, color: pt/co, radioactivity Bq/L, bacteriological: cfu/100 mL. to: single measurement)

5.4. Water Quality

The surface water classification (YSKYY, 2012, 2015), groundwater classification (SKKY, 2008; YKBKK, 2012), irrigation water classification (AATTUT, 2010), drinking water supply surface water classification (ISYSKY, 2012) and human consumption water limits (ITAS, 2005) are used for the evaluation of water quality. In addition, parameters listed in the surface water monitoring related regulation (YSYSIY, 2014) are taken into consideration.

In the evaluation of water quality, single measurement values are used as characteristic values because existing data covers less than 10 set of measurements in the first three years period as required by the regulations of Surface Water Quality Management (YSKYY, 2012) and Drinking Water Related Surface Water Quality (ISYSKY, 2012).

After the regulation of groundwater protection against contamination and degradation (YKBKK, 2012), previously used groundwater quality determinations related classification limits (SKKY, 2008) are abolished. Because groundwater quality standards and threshold values have not been established yet by Water Management Directorate as required by the forementioned regulation, in the report, previously used quality classification limits (SKKY, 2008) are used by adapting Cd and P limits of YSKYY (2012) and adding parameters (pesticides, tetrachloroethylene, trichloroethylene) of YKBKK (2012).

5.4.1. Surface Waters

Quality of Porsuk stream waters based on the limits of surface water classification, irrigation water classification and drinking water supply surface water classification is given in Table 5.10. In addition, detailed results of the surface water classification are also given in Table 5.11.

Table 5.10. Water quality classifications of Porsuk stream (Yazıcıgil et al., 2017).

	SURFACE WATER CLASSIFICATION	IRRIGATION WATER CLASSIFICATION
SW-5	CLASS IV-TKN, N-NO2, O2, O2%, P, Coli-f, Coli-t	CLASS III-Na(I), V, Coli-f (A), Coli-f (B)
SW-6	CLASS IV-TKN, N-NO2, O2, O2%, P, Coli-t	CLASS III-Na(I), V
SW-7	CLASS IV-N-NO2, P, Coli-t	CLASS III-Na(I), V

	DRINKING WATER SUPPLY SURFACE WATER CLASSIFICATION
SW-5	UNSUITABLE-TKN, O2%, Coli-f, Coli-t
SW-6	UNSUITABLE-TKN, Coli-t
SW-7	UNSUITABLE-TKN, Coli-t

Irrigation water explanation:

(I): Surface water irrigation, (II): Drip irrigation

(A): CLASS A; Good quality irrigation water due to human contact with edible products and plants in park, garden areas. Irrigation of food products that are not commercially processed and irrigation of city park, garden etc.

(B) CLASS B; Low quality irrigation water used for the irrigation of food products that are commercially processed (fruit gardens and vineyards), people restricted areas such as grass growth and agricultural areas and meadow and hay growth areas for range cattle.

Metal parameters are for continuous irrigation of all soil media types.

Concentrations indicate that based on the surface water classification limits, Porsuk stream includes highly contaminated quality (Class IV) water due to high TKN, N-NO2, P, coliform and low O2 values.

According to the drinking water supply surface water limits, Porsuk stream water is in unusable (A4) quality due to high concentrations of TKN and coliform (Table 5.12).

Porsuk stream water is not suitable (hazardous, Class III) for surface water irrigation due to high Na content (Table 5.12). In addition, water includes vanadium concentrations that exceed the limit of continuous irrigation in all soil types. Moreover, stream water at SW-5 location includes f-coliform values greater than the B-level. The irrigation water quality distribution in terms of SAR and EC values and effects on the infiltration rate are shown in Figure 5.16. The stream water as irrigation water does not cause any infiltration rate decrease in soils and includes low sodium (alkali)-high salinity hazard.

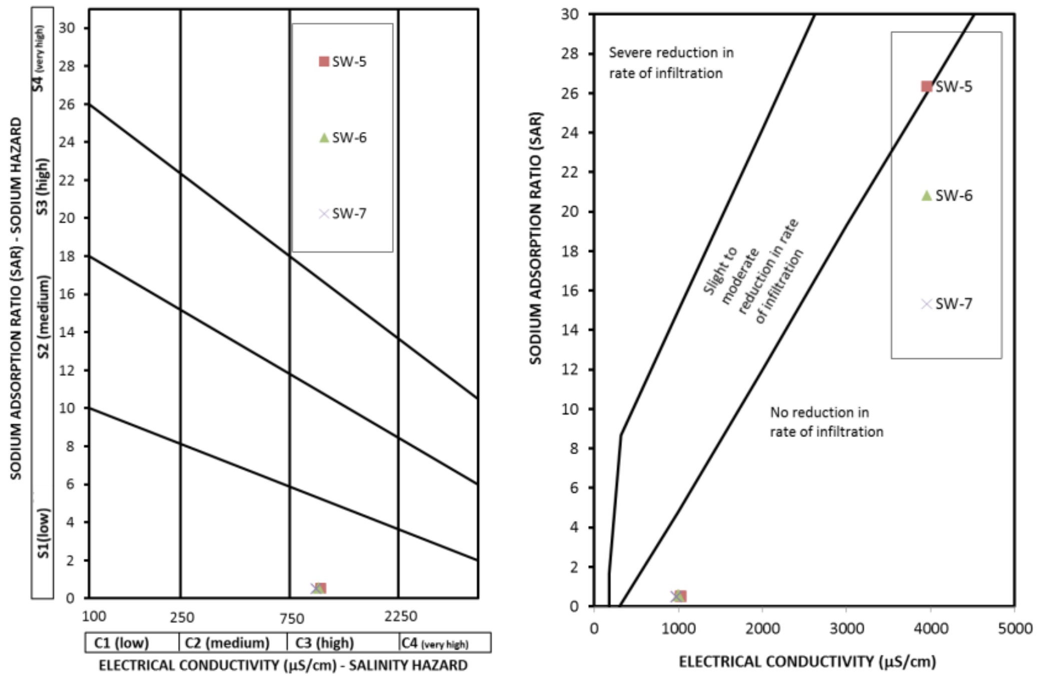

Figure 5.16. According to SAR and electrical conductivity values a) quality distribution and b) effect on the infiltration rate as irrigation water of Porsuk Stream

Table 5.11. Surface water quality classification of Porsuk Stream (Yazıcıgil et al., 2017).

	SURFACE WATER CLASSIFICATION				SW-5	SW-6	SW-7
PARAMETER	**CLASS I**	**CLASS II**	**CLASS III**	**CLASS IV**	**CLASS IV**	**CLASS IV**	**CLASS IV**
Al	0.3	0.3	1	> 1	0.014	-0.010	-0.010
As	0.02	0.05	0.1	> 0.1	-0.010	-0.010	0.010
B	1	1	1	> 1	0.40	0.49	0.34
Ba	1	2	2	> 2	0.12	0.14	0.13
BOD	4	8	20	> 20	5.65	4.95	6
Cd	0.002	0.005	0.007	> 0.007	-0.0030	-0.0030	-0.0030
CN	0.01	0.05	0.1	> 0.1	-0.0200	-0.0200	-0.0200
Co	0.01	0.02	0.2	> 0.2	-0.0100	-0.0100	-0.0100
COD	25	50	70	> 70	34	28	10
Cr	0.02	0.05	0.2	> 0.2	-0.010	-0.010	-0.010
Cu	0.02	0.05	0.2	> 0.2	-0.010	-0.010	-0.010
EC	400	1000	3000	>3000	1030.8	1007.1	980.9
F	1	1.5	2	> 2	0.33	0.33	0.31
Fe	0.3	1	5	> 5	0.061	0.045	0.025
Hg	0.0001	0.0005	0.002	> 0.002	-0.00100	-0.00100	-0.00100
Mn	0.1	0.5	3	> 3	0.063	0.061	0.041
TKN	0.5	1.5	5	> 5	6.72	7	4.2
N-NH4	0.2	1	2	> 2	-0.01	-0.01	-0.01
N-NO2	0.01	0.06	0.12	> 0.3	0.3790	0.9450	1.1040
N-NO3	5	10	20	> 20	0.95	1.78	2.04
Ni	0.02	0.05	0.2	> 0.2	0.0118	0.0116	0.0114
O2	8	6	3	< 3	1.84	2.87	4.28
O2%	90	70	40	< 40	28.90	39.70	55.90
P,t	0.03	0.16	0.65	> 0.65	0.770	0.965	0.890
Pb	0.01	0.02	0.05	> 0.05	-0.0100	-0.0100	-0.0100
pH	6.5-8.5	6.5-8.5	6.0-9.0	<6.0 ->9.0	8.10	8.16	8.29
Color**	5	50	300	>300	27	41	26
S-2	0.002	0.002	0.01	>0.01	-0.100	-0.100	-0.100
Se	0.01	0.01	0.02	> 0.02	-0.0050	-0.0050	-0.0050
Zn	0.2	0.5	2	> 2	0.025	0.019	-0.010
Coli-f	10	200	2000	> 2000	>100000	0	0
Coli-t	100	20000	100000	> 100000	>100000	>100000	>100000

(Detection limits are shown as minus. Unit: mg/l, EC: uS/cm, Coliform: cfu/100 mL.

** Color limits are changed for pt-co scale)

Table 5.12. Drinking and irrigation water quality classifications of Porsuk Stream (Yazıcıgil et al., 2017).

SURFACE WATER	DRINKING WATER SUPPLY SURFACE WATER CLASSIFICATION				SW-5	SW-6	SW-7
PARAMETER	A1	A2	A3	A4	A4	A4	A4
Al	0.3	0.3	1	>1	0.014	-0.010	-0.010
As	0.05	0.05	0.1	>0.1	-0.010	-0.010	0.010
B	1	1	1	>1	0.40	0.49	0.34
Ba	0.1	1	1	>1	0.12	0.14	0.13
BOD	3	5	7	>7	5.65	4.95	6
Cd	0.005	0.005	0.005	>0.005	-0.0030	-0.0030	-0.0030
Cl	200	200	200	>200	61.0	67.6	64.6
CN	0.05	0.05	0.05	>0.05	-0.0200	-0.0200	-0.0200
Co	0.01	0.02	0.2	>0.2	-0.0100	-0.0100	-0.0100
COD	15	30	40	>40	34	28	10
Cr	0.05	0.05	0.05	>0.05	-0.010	-0.010	-0.010
Cu	0.05	0.05	1	>1	-0.010	-0.010	-0.010
EC*	1111	1111	1111	>1111	1030.8	1007.1	980.9
F	1.5	0.7	1.7	>1.7	0.33	0.33	0.31
Fe	0.3	2	2	>2	0.061	0.045	0.025
Hg	0.001	0.001	0.001	>0.001	-0.00100	-0.00100	-0.00100
Mn	0.05	0.1	1	>1	0.063	0.061	0.041
TKN	1	2	3	>3	6.72	7	4.2
N-NH3	0.05	1.5	4	>4	-0.01	-0.01	-0.01
NO3	50	50	50	>50	4.20	7.86	9.05
Ni	0.02	0.05	0.2	>0.2	0.0118	0.0116	0.0114
O2%	70	50	30	<30	28.90	39.70	55.90
P,reac	0.4	0.7	0.7	>0.7	0.309	0.431	0.466
Pb	0.05	0.05	0.05	>0.05	-0.0100	-0.0100	-0.0100
pH	6.5- 8.5	..5.5-9	<5.5 ->9	<5.5 ->9	8.10	8.16	8.29
Color	20	100	200	>200	27	41	26
Se	0.01	0.01	0.01	>0.01	-0.0050	-0.0050	-0.0050
Temperature	25	25	25	>25	17.2	15.7	17.0
SO4	250	250	250	>250	38.68	51.26	57.15
TSS	25	>25			-10	-10	-10
TOC	5	8	12	>12	10	7	9
Zn	3	5	5	>5	0.025	0.019	-0.010
Pesticides,t	0.001	0.0025	0.005	>0.005	-0.00008	-0.00008	-0.00008
Phenolics	0.001	0.005	0.1	>0.1	-0.00004	-0.00004	-0.00004
PAH	0.05	0.2	1	>1	0.0002	0.0002	0.0001
PSAH	0.0002	0.0002	0.001	>.001	0.000	0.000	0.000
MBAS	0.2	0.2	0.5	>0.5	-0.010	-0.010	-0.010
Coli-f	20	2000	20000	>20000	>100000	0	0
Coli-t	50	5000	50000	>50000	>100000	>100000	>100000
f-Spreptecoc	20	1000	10000	>10000	85	0	6

Table 5.12 Cont.

	IRRIGATION WATER CLASSIFICATION			SW-5	SW-6	SW-7
PARAMETER	CLASS I	CLASS II	CLASS III	CLASS III	CLASS III	CLASS III
B	0.7	3	>3	0.3975	0.4854	0.3417
BOD(A)	20		>20	5.65	4.95	6
BOD(B)	30		>30	5.65	4.95	6.00
Cl(I)	140	350	>350	61.0	67.6	64.6
Cl(II)	100		>100	61.0	67.6	64.6
EC	700	3000	>3000	1031	1007	981
Na(I)	3	9	>9	21.65	24.76	20.89
Na(II)	70		>70	21.65	24.76	20.89
pH	6.0-9.0		<6->9	8.10	8.16	8.29
SAR-EC (infiltration)				I	I	I
TDS	500	2000	>2000	506	508	484
TSS(A)	5		>5	-10	-10	-10
TSS(B)	30		>30	-10	-10	-10
Al	5		>5	0.014	-0.010	-0.010
As	0.1		>0.1	-0.010	-0.010	0.010
Be	0.1		>0.1	-0.01000	-0.01000	-0.01000
Cd	0.01		>0.01	-0.0030	-0.0030	-0.0030
Co	0.05		>0.05	-0.010	-0.010	-0.010
Cr	0.1		>0.1	-0.010	-0.010	-0.010
Cu	0.2		>0.2	-0.010	-0.010	-0.010
F	1		>1	0.33	0.33	0.31
Fe	5		>5	0.06	0.04	0.02
Li	2.5		>2.5	0.191	0.191	0.181
Mn	0.2		>0.2	0.063	0.061	0.041
Mo	0.01		>0.01	-0.010	-0.010	-0.010
Ni	0.2		>0.2	0.012	0.012	0.011
Pb	5		>5	-0.010	-0.010	-0.010
Se	0.02		>0.02	-0.005	-0.005	-0.005
V	0.1		>0.1	0.120	0.128	0.135
Zn	2		>2	0.025	0.019	-0.010
Coli-f(A)	0		>0	100000	0	0
Coli-f(B)	200		>200	100000	0	0

(Detection limits are shown as minus. Unit: mg/l, color: pt/co, bacteriological: cfu/100 mL, temperature ºC, for (I), (II), (A) and (B) explanations see foot note of Table 5.10).

5.4.2. Well Waters

The quality of well waters based on the groundwater classification, irrigation water classification and human consumption limits is given in Table 5.13. In addition, detailed results of groundwater classification are given in Table 5.14 and the distribution of quality is shown in Figure 5.17.

Based on the groundwater classification limits, concentrations indicate that all well waters include low quality (Class III) groundwater. Parameters causing low quality in each well are listed in Table 5.13.

Well waters except that of APK-7 are not suitable for human consumption due to high average values of As/B/Cr/Ni/Pb/Alpha activity/Beta activity. The indicator parameters which are the above limits are listed in Table 5.13 and detailed in Table 5.14. APK-4 water is suitable for human consumption if bacteriological parameters are ignored.

Table 5.13. Water quality classifications of well waters (For irrigation water classification explanations see foot note of Table 5.10) (Yazıcıgil et al., 2017).

	GROUNDWATER CLASSIFICATION	IRRIGATION WATER CLASSIFICATION	HUMAN CONSUMPTION	INDICATOR PARAMETERS
ESHID01	CLASS III-BOD5, O2, O2%	CLASS III-V	Coli-t, Alfa-ak	O2
ESHID02	CLASS III-B, Cl, Cr, EC, TKN, N-NH4, O2, O2%, SO4, TDS, VOC, Oil&grease	CLASS III-B, Cl(I), Cl(II), EC, Li, Mo, Na(I), TDS	B, Cr, Beta-ak	Cl, EC, Fe, Mn, O2, NH4, SO4
APK-2	CLASS III-B, O2, O2%	CLASS III-Na(I), TSS(A), Coli-f (A)	As, B, Coli-t	O2
APK-3	CLASS III-B, Cl, EC, N-NH4, N-NO2, O2, O2%, SO4, TDS	CLASS III-B, Cl(II), EC, Mn, Na(I)	B, Ni, NO2, Pb	Cl, EC, Fe, Mn, O2, NH4, SO4
APK-4	CLASS III-O2, O2%	CLASS II-EC	Coli-t	Mn, O2
APK-5	CLASS III-B, Cl, EC, Fe, O2, O2%, Pb, SO4, TDS	CLASS III-B, Cl(II), EC, Mn, Na(I), TDS, TSS(A), V	B, Pb, Coli-t, E-Coli, Alfa-ak	Cl, EC, Fe, Mn, O2, NH4, SO4
APK-6	CLASS III-EC, O2, O2%, Oil&grease	CLASS III-V	Coli-t, E-Coli, Alpha-ac	O2
APK-7	CLASS III-O2, O2%	CLASS II-B, SAR-EC		

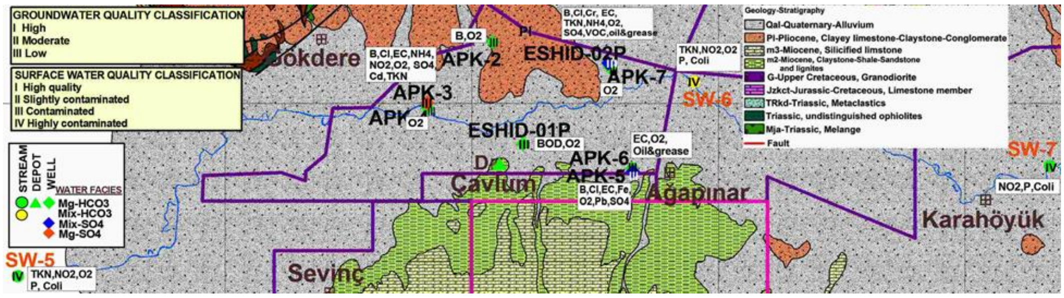

Figure 5.17. Distribution of quality classification in waters

Table 5.14. Groundwater quality classification of well waters and suitability for human consumption (Yazıcıgil et al., 2017).

	GROUNDWATER CLASSIFICATION			HUMAN CONSUMPTION YAS	APK-2	APK-3	APK-4	APK-5	APK-6	APK-7	ESHID-01P	ESHID-02P
PARAMETER	CLASS I	CLASS II	CLASS III	ove limit valu	CLASS III	CLASS III	CLASS III	CLASS III	CLASS III	CLASS III	CLASS III	CLASS III
As	0.02	0.05	>0.05	0.01	0.018	-0.010	-0.010	-0.010	-0.010	0.010	-0.010	-0.010
B	1	1	>1	1	1.19	12.53	0.62	48.31	0.83	0.84	0.34	60.02
Ba	1	2	>2	0.7	0.05	0.05	0.13	0.03	0.19	0.13	0.21	0.03
BOD	4	8	>8		3.6	6.07	3.42	2.74	2.39	3.01	8.55	3.21
Cd	0.002	0.005	>0.005	0.005	-0.0030	-0.0030	-0.0030	-0.0030	-0.0030	-0.0030	-0.0030	-0.0030
CN	0.01	0.05	>0.05	0.05	-0.0200	-0.0200	-0.0200	-0.0200	-0.0200	-0.0200	-0.0200	-0.0200
Co	0.01	0.02	>0.02		-0.0100	-0.0100	-0.0100	-0.0100	-0.0100	-0.0100	-0.0100	-0.0100
COD	25	50	>50		19	22	13	11	10	11	37	10
Cr	0.02	0.05	>0.05	0.05	-0.0100	-0.0100	0.0100	-0.0100	-0.0100	0.0110	-0.0100	0.0832
Cu	0.02	0.05	>0.05	2	-0.0100	-0.0100	-0.0100	-0.0100	-0.0100	-0.0100	-0.0100	-0.0100
F	1	1.5	>1.5	1.5	0.26	0.29	0.27	0.12	0.38	0.34	0.45	-0.02
Hg	0.0001	0.0005	> 0.0005	0.001	-0.001	-0.001	-0.001	-0.001	-0.001	-0.001	-0.001	-0.001
TKN	0.5	1.5	>1.5		-0.5	0.6	-0.5	1.0	0.7	-0.5	1.3	5.8
N-NO2	0.01	0.06	>0.01	0.15	0.031	0.303	-0.001	0.040	-0.001	0.031	0.040	0.001
N-NO3	5	10	>10	11.5	2.3	2.6	3.7	0.0	1.3	2.0	4.3	0.1
Ni	0.02	0.05	>0.05	0.02	-0.0100	0.0235	-0.0100	-0.0100	-0.0100	-0.0100	-0.0100	-0.0100
P,t	0.03	0.16	>0.16		0.027	0.016	0.038	-0.010	0.014	-0.010	0.021	-0.010
Pb	0.01	0.02	>0.02	0.01	-0.0100	0.0142	-0.0100	0.0294	-0.0100	-0.0100	-0.0100	-0.0100
S-2	0.002	0.002	>0.002		-0.1	-0.1	-0.1	-0.1	-0.1	-0.1	-0.1	-0.1
Sb				0.005	-0.0050	-0.0050	-0.0050	-0.0050	-0.0050	-0.0050	-0.0050	-0.0050
Se	0.01	0.01	>0.01	0.01	-0.0050	-0.0050	-0.0050	-0.0050	-0.0050	-0.0050	-0.0050	-0.0050
Temperature	25	25	>25		16.7	19.0	14.1	20.7	12.7	14.6	15.1	23.0
TDS	500	1500	>1500		382	1726	286	2920	518	308	456	5526
TOC	5	8	>8		-5	-1	-1	1	-1	-5	-5	-5
Zn	0.2	0.5	>0.5		0.0346	0.0239	0.0154	0.0101	0.0603	0.0117	0.0126	-0.0100
Pesticides,t	0.001	0.01	>0.01	0.0005	-0.00008	-0.00008	-0.00008	-0.00008	-0.00008	-0.00008	-0.00008	nm
Phenolics, (u)*	0.002	0.01	>0.01		-0.0100	-0.0100	-0.0100	-0.0100	-0.0100	-0.0050	-0.0100	0.0140
Tri-tetraCE				0.01	-0.010	-0.010	-0.010	-0.010	-0.010	-0.005	-0.010	-0.010
MBAS	0.05	0.2	>1		-0.010	-0.010	-0.010	-0.010	-0.010	-0.010	-0.010	-0.010
Oil&grease	0.02	0.3	>0.3		-0.1	0.08059	0.07472	0.24769	0.70308	0.13	-0.1	0.623
Coliform-fecal	10	200	>200		40	0	0	0	0	nm	0	nm
Coliform-total	100	20000	> 20000	0	660	0	10	68	42	nm	7	nm
Alpha ac.	0.5	5	>5	0.1	0.08	-0.18	0.05	0.82	0.18	-0.04	0.11	-0.25
Beta ac.	1	10	>10	1	0.39	-0.60	0.15	0.75	0.54	-0.10	0.41	1.63
				INDICATOR PARAMETERS								
Al	0.3	0.3	>0.3	0.2	-0.010	0.032	0.023	0.030	0.020	-0.010	-0.010	0.025
Cl	25	200	>200	250	75.1	319.9	23.6	272.9	36.9	40.4	37.3	1015.0
EC	400	1000	>1000	2500	765.0	3522.7	743.0	4682.7	1086.2	690.0	869.0	11025.0
Fe	0.3	1	>1	0.2	-0.01000	0.63230	0.02470	4.63000	0.01030	-0.01000	0.02190	0.59360
Mn	0.1	0.5	>0.5	0.05	-0.0100	0.3696	0.1198	0.2360	-0.0100	-0.0100	-0.0100	0.1698
Na	125	125	>125	200	15.03	30.00	2.76	65.46	1.99	2.18	8.06	58.22
N-NH4	0.2	1	>1	0.39	-0.01	1.18	0.02	0.83	-0.01	-0.01	-0.01	3.21
O2	8	6	<6	5	2.93	3.19	3.31	4.39	4.50	5.02	2.49	3.40
O2%	90	70	<70		34.00	38.00	36.00	51.80	44.40	57.80	27.50	43.40
pH	6.5-8.5	6.5-8.5	<6.5->8.5	≥ 6.5 ve ≤ 9.5	7.67	7.74	7.48	7.75	7.87	7.94	7.57	8.21
Color	5	50	>300		15	8	7	10	8	5	14	8
SO4	200	200	>200	250	68.18	1590.40	55.36	3327.00	138.82	66.77	95.16	2372.75

(Detection limits are shown as minus. Unit: mg/l, EC: uS/cm, color: pt/co, temperature ºC, Coliform: cfu/100 mL, Alpha and beta act. Bq/L, nm: no measurement,*VOC analysis results are used).

Excluding Class II (low-middle hazardous) quality irrigation waters of APK-4 and APK-7, well waters include hazardous quality (Class III) irrigation water. But Class A level of APK-2 well water is suitable for the drip irrigation. Irrigation water quality distribution in terms of SAR and EC values and effects on the infiltration rate are shown in Figure 5.18. None of the well waters has adverse infiltration effect if used as irrigation water. ESHİD-02P, APK-3 and APK-5P well waters include low sodium – very high salinity hazard, ESHİD-01P, APK-2 and APK-6 well waters include low sodium – high salinity hazard and APK-4 and APK-7 well waters include low sodium – medium salinity hazard as irrigation water.

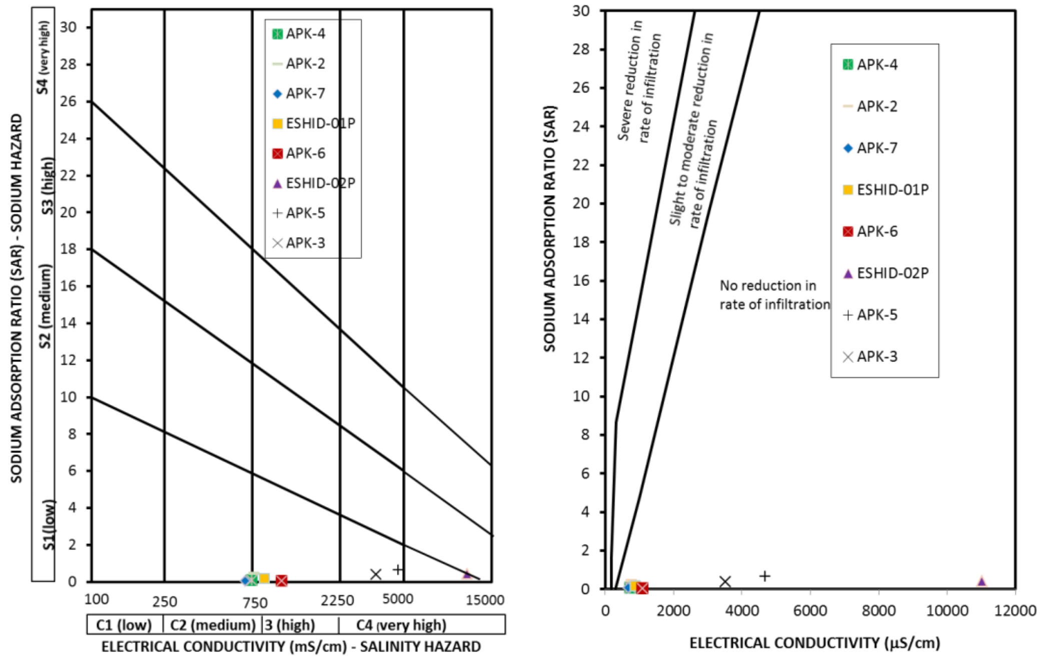

Figure 5.18. According to SAR and electrical conductivity values a) quality distribution and b) effect on infiltration rate as irrigation water of well waters (Yazıcıgil et al., 2017).

5.4.3. Village Depot Waters

The quality of Çavlum village depot water based on the human consumption limits is determined using data of Yazıcıgil et. al. (2017) and listed in Table 5.15.

Table 5.15. Human consumption suitability of Çavlum village depot water (Yazıcıgil et al., 2017).

PARAMETER	HUMAN CONSUMPTION YAS	Çavlum Depot
As	0.01	-0.003
B	1	0.15
Ba	0.7	0.14
Cd	0.005	-0.0002
CN	0.05	-0.0100
Cr	0.05	-0.0003
Cu	2	-0.0002
F	1.5	0.38
Hg	0.001	-0.00008
Ni	0.02	-0.001
NO2	0.5	0.044
NO3	50	14.85
Pb	0.01	-0.0015
Sb	0.005	-0.0020
Se	0.01	-0.0050
Acrylamide	0.0001	-0.00005
Benzene	0.001	-0.00084
Benzo(a)pyrene	0.00001	-0.00005
Bromate	0.01	-0.01
1,2-dichloroethane	0.003	-0.0006
Epikloridin	0.0005	-0.00008
Pesticides,t	0.0001	-0.00005
Tri-tetraCE	0.01	-0.0008
Trihalomethanes	0.1	-0.0019
Vinyl chloride	0.0005	-0.0005
Coli-t	0	50000
E- Coli	0	50
Enterococ	0	0
Alpha ac.	0.1	0.0
Beta ac.	1	-0.1

INDICATOR PARAMETERS	HUMAN CONSUMPTION YAS	Çavlum Depot
Al	0.2	0.024
Cl	250	8.2
EC	2500	361.4
Fe	0.2	0.010
Mn	0.05	-0.0002
Na	200	7.44
NH4	0.5	-0.01
O2	5	6.92
pH	≥ 6.5 ve ≤ 9.5	8.08
SO4	250	12.01

(Detection limits are shown as minus. Unit: mg/l, EC: µS/cm, bacteriological: cfu/100 mL)

Excluding bacteriological parameters, Çavlum depot water is suitable for human consumption. However, according to the values of the bacteriological parameters measured in the dry period, the depot water is not suitable for human consumption.

CHAPTER 6

SUMMARY, CONCLUSIONS AND RECOMMENDATIONS

6.1. Summary and Conclusions

The study area is located in the northwest of the Central Anatolian Region within the Eskişehir graben and it covers the Turkish Coal Enterprises' (TKI) Sector-A license area. The elevation within the study area approximately ranges between 770 and 980 m. The lowest elevation in the study area is observed along the alluvium plain area around the Porsuk Stream (nearly 770-790 m) while the highest elevations within the region are formed by the hills in the north and south of the plain.

In the study area and its surroundings, the basement rocks are represented by Mesozoic units outcropping in the southeastern and northwestern parts of the study area and tectonically in contact with Paleozoic metamorphics form the basement rocks. These basement rocks are unconformably overlaid by coal seam bearing Middle-Upper Miocene deposits. At the bottom of these deposits, there is basal conglomerate (m1) which contains conglomerate, sandstone and claystone. The overlying series is represented from the bottom to the top a sequence of conglomerate, green claystone, coal seam (C), gray sandstone, bituminous shale, coal seam (B), bituminous shale, coal seam (A) and green claystone-sandstone-conglomerate alternation (m2). On this sequence, the Miocene silicified limestone (m3), which outcrops on the high hills at the southwestern part of the study area, is seen. All these Miocene units are unconformably overlain by Pliocene deposits which begins with conglomerates and sandstone strata formed by small granular conglomerates. It is represented by cream, light brown colored, light reddish mudstone and loosely attached multi-type granular conglomerate-sandstone, floating gravelly sandstone. Pliocene deposits outcrop in the northern part of the Sector-A and Quaternary alluvium unconformably overlies this unit. Quaternary unit can be seen in the lower elevations of the study area and around the Porsuk Stream and represented by silt and clay intercalated sand and gravels.

The surface water flow in the region encompassing Sector-A is controlled by irrigation and dewatering channels located around the Porsuk Stream, starting from the Porsuk Dam. The right wing irrigation channel passes through south of Sector-A and left wing irrigation channel passes through the northern part of Sector-A and extents to Yeşildon settlement. The connection between these irrigation channels are provided by ditches and dewatering channels. The amount of water released to these channels is 117×10^6 m^3/year and only 35% of this water is used for irrigation. Moreover, treated waste waters from the Eskişehir city center (ESKİ) and Organized Industrial District are also discharged into the Porsuk stream, causing daily fluctuations in the discharge of the Porsuk stream.

The most important water bearing formations within the study area and its vicinity are Quaternary alluvium and Pliocene limestone, sandstone and conglomerates. The lignite bearing Middle-Upper Miocene age Porsuk Formation is generally composed of claystones, sandstones, conglomerates and bituminous shales display confined to semi-confined aquifer behaviour with relatively low hydraulic conductivity. The Paleozoic metamorphic schists, Mesozoic Ophiolites and the Jurassic-Cretaceous limestones form the basement in Sector-A and its close vicinity. These rocks are generally impervious and semi-pervious and may carry groundwater along fractures that result from faulting.

According to the tests conducted at well clusters the hydraulic conductivity and storage coefficient values of the various lithological units are summarized in Table 6.1.

Table 6.1 Summary table of hyraulic parameters for different units

Tested Unit	Min. Hydraulic Conductivity (m/s)	Max. Hydraulic Conductivity (m/s)	Hydraulic Conductivity-Geomean (m/s)	Min. Storage Coefficient	Max. Storage Coefficient
Alluvium (Quaternary)	5.24E-04	2.03E-03	9.84E-04	1.50E-03	1.95E-01
Pliocene	3.00E-05	4.23E-05	3.44E-05	2.93E-02	4.92E-02
Miocene	5.64E-09	8.92E-07	1.41E-07	8.60E-03	4.20E-02
Quaternary & Miocene	6.82E-06	1.21E-03	4.59E-04	1.67E-02	8.12E-02
Pliocene & Miocene	4.43E-08	4.69E-08	4.58E-08	1.21E-04	2.29E-04

With the help of piezometers the variations in the hydrogeological system and responses during mining activities will be continually monitored and will enable necessary precautions to be taken on time. In addition, knowing the groundwater pressures and temperatures in the coal seams and beneath them will provide important information for the design of panels and necessary support structures. The observed groundwater pressures from installed vibrating wire piezometers below the coal seams are excessive and may cause groundwater inrush into galleries or panels during mining activities. Calculated hydraulic heads from piezometers were also showed the existence of upward vertical hydraulic gradient and groundwater flow takes place from the bottom (Miocene unit) to the upward.

Although the general direction of groundwater flow in Sector-A is from west to the east, there are also groundwater flow from the elevated lands in the north and south toward the Porsuk Stream.

The knowledge, about the interaction between the Alluvium aquifer and the Porsuk Stream running through the middle of sector-A and the hydraulic relation between the alluvium aquifer and the underlying Pliocene and Miocene units, will provide very useful information in several topics including the environmental studies and displacement of the Porsuk Stream bed, in addition to the dewatering and depressurization studies that may be required during mining activities. Therefore, it is of utmost importance to measure the stream stages continuously while measuring the groundwater levels in monitoring wells and vibrating wire piezometers.

All waters in the monitoring stations bear basic and oxidizing characteristics except reducing measurements of Miocene groundwater. The average electrical conductivity values are in the interval of; 944-987 µS/cm in Porsuk Stream, 690-12366 µS/cm in well waters and 342-389 µS/cm in Çavlum village depot water. Dissolved oxygen concentrations are in the interval of; 3.4-4.4 mg/L in Porsuk stream, 1.12-5.02 mg/L in well waters and 6.3-8.3 mg/L in the depot water. Average deviations of field parameter values in the stream waters are 127 S/cm in electrical conductivity; 0.19 in pH; 25 mV in ORP; and 0.75 mg/l in dissolved oxygen parameters.

Porsuk stream have both Mg (Mix)-HCO3 and Mix (Mg)-HCO3 types of water. The stream sediments have higher Ag, As, B, Bi, Ca, Cd, Cr, Cu, Hg, Li, Mg, Ni, P, Sb, Sn and Zn concentrations than the Upper Crustal averages.

Groundwater of Alluvium aquifer and Pliocene aquifer are in Mg-HCO3 facies. Miocene aquifer composed of claystone, sandstone and siltstone sequence with gypsum bands includes Mix (Ca, Mg)-SO4 type of groundwater. Miocene aquifer groundwater from deeper levels includes higher ion concentrations. Very high sulfate concentration (about 2000-3000 mg/l) of Miocene groundwater is probably related to the gypsum dissolution. Concentrations of ammonia/ammonium in Miocene groundwater are much higher than the generally expected values. This level of ammonia/ammonium is most probably not anthropogenic but related to the degradation of natural organic material in the units.

Porsuk stream holds highly contaminated surface water and can be used neither as a drinking water resource nor as irrigation supply water. All well waters include low (Class III) quality groundwater and are not suitable for human consumption (excluding those of APK-4 and APK-7) due to high As/B/Cr/Ni/Pb/Alpha activity/Beta activity. Ignoring bacteriological parameters, depot water of Çavlum village is suitable for human consumption.

6.2. Recommendations

The Porsuk Stream flowing through the center of Sector-A poses an important risk factor for the mining activities. The Porsuk Stream is in interaction with the Quaternary Alluvium deposits which is the most prolific aquifer in the study area. It may be required to divert the the Porsuk Stream to a new canal constructed parallel to the high speed railway, leaving a pillar along the canal route, and lining the canal with an impermeable material to reduce the risk of Porsuk Stream waters which may develop as a result of subsidence during mining activities and afterwards.

The subsidence due to mining activities is expected to be significant and will negatively impact the Porsuk Stream, the alluvium aquifer, and the irrigation channels. The collapse zone that will form due to longwall mining of the coal seams in the Miocene units are expected to increase the hydraulic conductivity of the upper Miocene and Pliocene units. This may cause a reversal in the gradient between the uppermost and permeable alluvium aquifer and the Pliocene aquifer, causing groundwater from the alluvium aquifer and the Porsuk Stream to drain downwards.

These phenomena, which may produce important risks for mining and the environment, should be acknowledged and necessary measures should be taken. In addition, the irrigation channels will also be negatively affected by the surface subsidence. There may be water losses from these channels, unlined at several locations. Currently, irrigated agriculture is the most important activity in Sector-A.

Hydrogeological studies and monitoring activities should be continued to evaluate the negative impacts mentioned above. The data from vibrating wire piezometers should be recorded continuously and evaluated, a groundwater model for operational purposes should be constructed and mine subsidence predictions should be undertaken. However, a basin-wide integrated approach is required to conduct the suggested works as the mining in Sector-A or in the neighboring sectors will impact each other.

Chemical analysis of Porsuk stream should be carried out for the monitoring parameters of alkalinity, total phosphorus, dissolvable reactive phosphorus, total nitrogen, nitrate, nitrite and ammonium.

Mineralogical characteristics of all lithological units should be determined with XRD analysis in order to provide data for detailed evaluations of water-rock interactions (this will also provide data for acid rock drainage studies).

REFERENCES

AATTUT, 2010, Communiqué on Technical Procedures for Wastewater Treatment Plants, Official Gazette No: 27527.

Amer, A.M. and Amer, K.H., 2010, Surface Irrigation Management in Relation to Water Infiltration and Distribution in Soils, Soils & Water Res., 5, 2010 (3): 75-87.

Bayram, A., 2015, Eskişehir – Alpu Coal Field Detailed Hydrogeology Preliminary Report, General Directorate of Mineral Research and Exploration (MTA), Ankara, 85 Pages.

Chow V.T., Maidment, D.R., Mays, L.W., 1988, Applied Hydrology, McGraw Hill Publishing, 572 Pages.

Dönmez, Y., 1979, Umumi Klimatoloji ve İklim Çalışmaları, İst. Uni. Institue of Geography Publications, No:102, İstanbul.

DSİ, 1977, Eskişehir-Alpu Ovası Hidrojeolojik Etüt Raporu, General Directorate of State Hydraulic Works (DSI), 39 Pages.

DSİ, 2010, Eskişehir-Alpu Ovası Revize Hidrojeolojik Etüt Raporu, General Directorate of State Hydraulic Works (DSI), 54 Pages.

Gözler, Z., Cevher, F., Ergül, E. ve Asutay, J.H., (1997) Orta Sakarya ve Güneyinin Jeolojisi, MTA Report No: 9973 (Unpublished), Ankara

HT-TTM, 2016. Eskişehir Alpu Kömür Havzası Yerli Kömür Kaynaklarının Optimum Şekilde Ülke Ekonomisine Kazandırılması Modelinin Oluşturulması Projesi: Hidrojeoloji, Mühendislik Jeolojisi, Jeoteknik ve Kaya Mekaniği Çalışmaları A Sektörü 3. Ara Raporu, 133 Pages, Ankara

İSYSKY, 2012. İçme Suyu Elde Edilen Veya Elde Edilmesi Planlanan Yüzeysel Suların Kalitesine Dair Yönetmelik, Official Gazette No: 28338.

İTAS, 2005. Regulation on Water Intended for Human Consumption, Official Gazette No: 25730.

Koçyiğit, A.,1991. An example of an accretionary forearc basin from northern Central Anatolia and its implications for history of subduction of NeoTethys in Turkey. Geological Society of American Bulletin 103.

MTA, 2005. Turkey Geothermal Resources Inventory. Inventory Series 201, General Directorate of Mineral Research and Exploration (MTA).

MTA-TJVT. Turkey Geological Database. Retrieved July, 2017 from http://www.mta.gov.tr/v3.0/arastirmalar/cografi-bilgi-sistemleri

Palaris Australia Pty Ltd., 2016, Esan Eczacıbaşı Sector A Lignite Scoping Study Report, 135 Pages.

Rudnick, R.L. and Gao, S., 2003. Composition of continentalcrust, Treatise on Geochemistry, V. 3, 1-64.

Siyako, F., Coşar, N., Çokyaman, S. and Coşar, Z., (1991) Bozüyük-İnönü–Eskişehir–Beylikova-Sakarya Çevresinin Tersiyer Jeolojisi ve Kömür Olanakları, General Directorate of Mineral Research and Exploration MTA Report No: 9281 (Unpublished), Ankara.

SKKY, 2008. Regulation Amending the Regulation on Water Pollution Control., Official Gazette No: 26786.

Şengüler, İ., (2013). Eskişehir-Alpu Kömür Havzasının Jeolojisi ve Stratigrafisi, General Directorate of Mineral Research and Exploration (MTA) Natural Resources and Economy Bulletin, Issue 16, p. 89-93, Ankara.

Toprak, S., Sütcü, E.C. and Şengüler, İ., 2015. A fault controlled, newly discovered, Eskişehir Alpu coal basin in Turkey, its petrographical properties and depositional environment. International Journal of Coal Geology, 138 (2015) 127–144.

TÜİK, 2016. Adress based population registration system (ADNKS) database, Population of Eskişehir City and Villages.

Türkiye Petrolleri (TP), 2016, Alpu (TKI) Sismik Veri İşlem ve Yorumlama Raporu, 105 Pages.

Yazıcıgil, H., Çamur, M.Z., Yılmaz, K. K., Çatak, M.O. ve Kılıç, H., 2016. Hydrogeological Investigation and Characterization of ESAN – Alpu Coal Field, Middle East Technical University, Department of Geological Engineering, Project Code. No. 2014-03-09-2-00-29, Final Report, 267 Pages.

Yazıcıgil, H. Çamur, M. Z., Kılıç, H., Düz, T. K. ve Güney, Y. C., 2017. Esan-Alpu Kömür Sahası Yeraltısularının İzlenmesi ve Akım Modelinin Geliştirilmesi. Middle East Technical University, Department of Geological Engineering, Project Code. No. 2016-03-09-2-00-09, Final Raport, 196 Pages.

Yazıcıgil, H. Çamur, M. Z., Kılıç, H., Düz, T. K. ve Güney, Y. C., 2017. Hydrogeological Investigation and Characterization of Alpu A-Sector Coal Field. Middle East Technical University, Department of Geological Engineering, Project Code. No. 2016-03-09-2-00-15, Final Raport, 348 Pages

Yazıcıgil, H. Çamur, M. Z., Rojay F.B., Kılıç, H. ve Güney, Y. C., 2018. Alpu Kömür Havzasinin (A, B, C, D, E, F Sektörleri) Hidrojeolojik Etüdü Ve Karakterizasyonu. Orta Doğu Teknik Üniversitesi, Jeoloji Mühendisliği Bölümü, Proje Kod. No. 2016-03-09-2-00-24, Sonuç Raporu, 497 Pages.

YKBKK, 2012. Regulation on the Protection of Groundwater from Pollution and Degradation, Official Gazette No. 28257.

YSKYY, 2012. Regulation on the Management of Surface Water Quality, Official Gazette No: 28483.

YSKYYD, 2015. Regulation on the Amendment of the Regulation on Management of Surface Water Quality, Official Gazette No: 29327.

YSYSİY, 2014. Regulation on the Monitoring of Surface Waters and Ground Waters, Official Gazette No: 28910.

APPENDICES

APPENDIX-A

WELL LOGS FOR OBSERVATION AND PUMPING WELLS

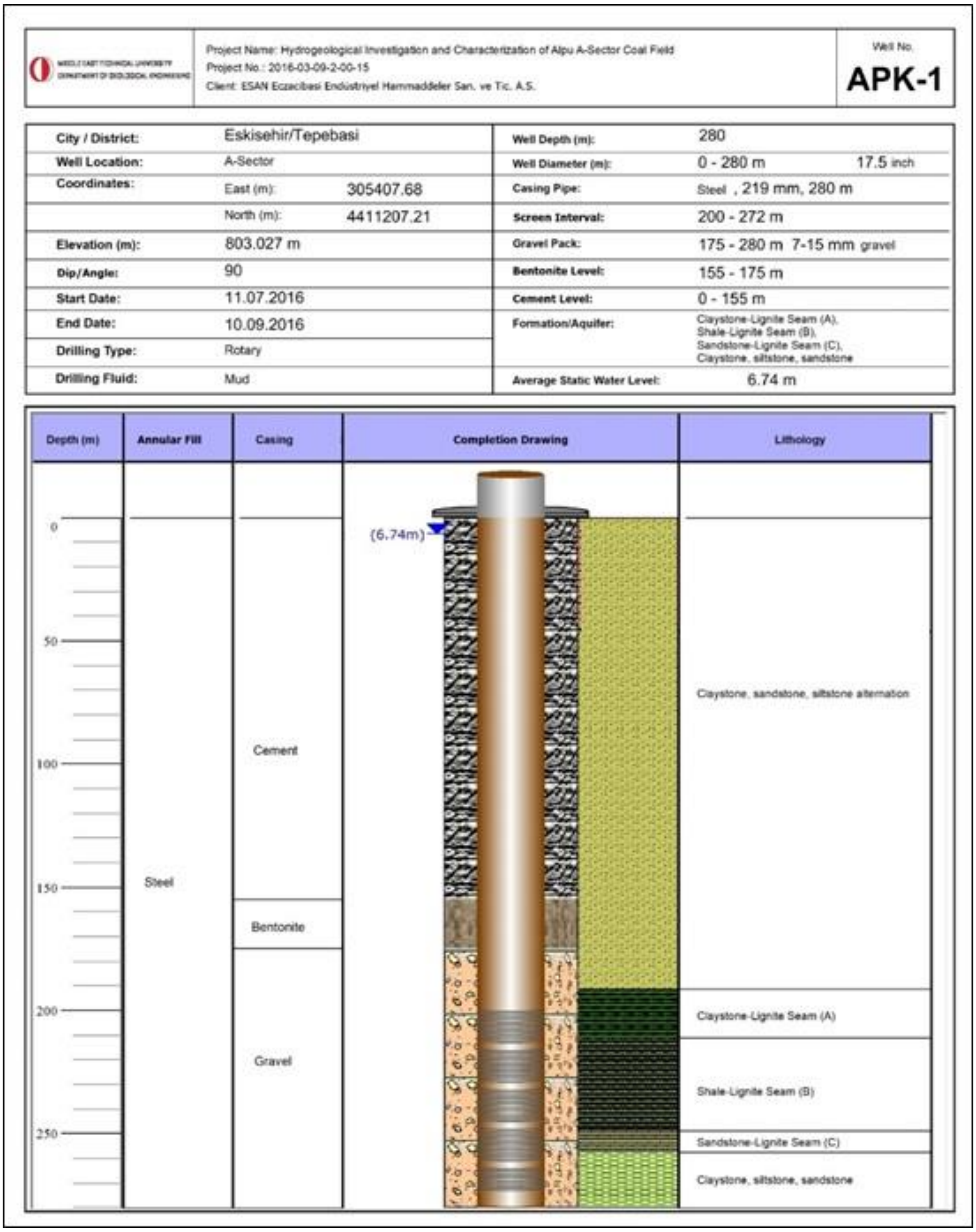

Figure A-1. The well log for APK-1 pumping well (Yazıcıgil et al., 2017).

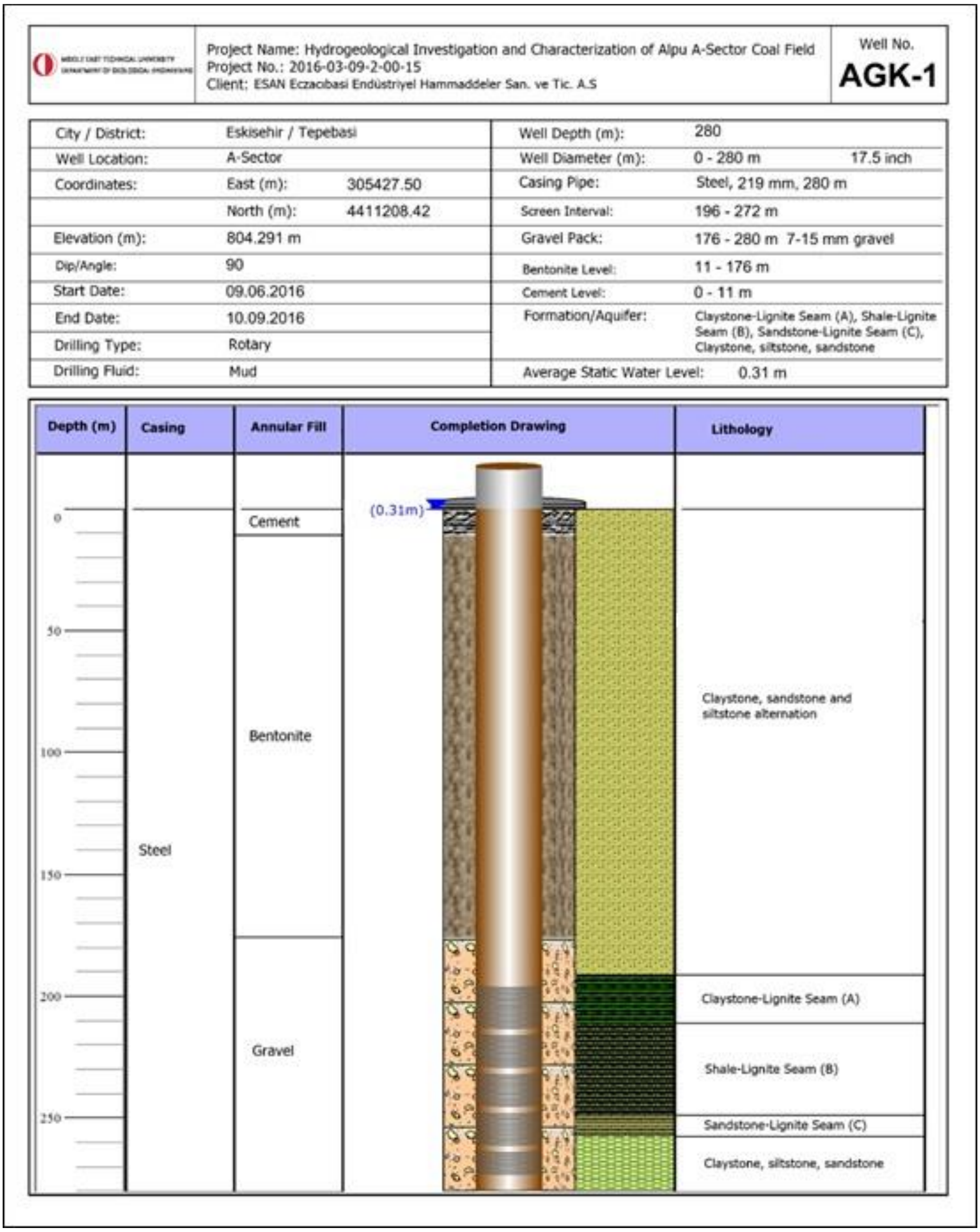

Figure A-2. Well log for AGK-1 observation well (Yazıcıgil et al., 2017).

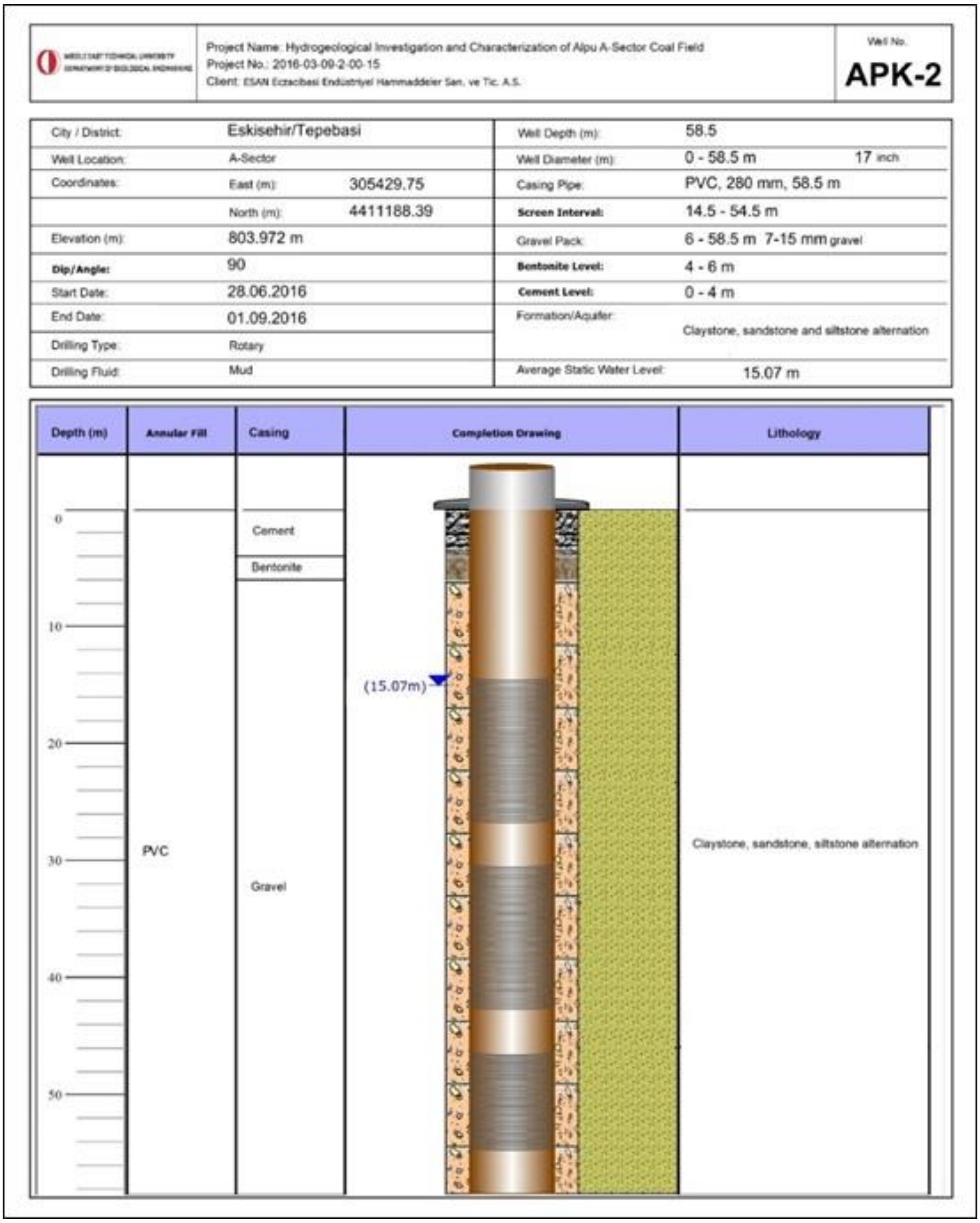

Figure A-3. The well log for APK-2 pumping well (Yazıcıgil et al., 2017).

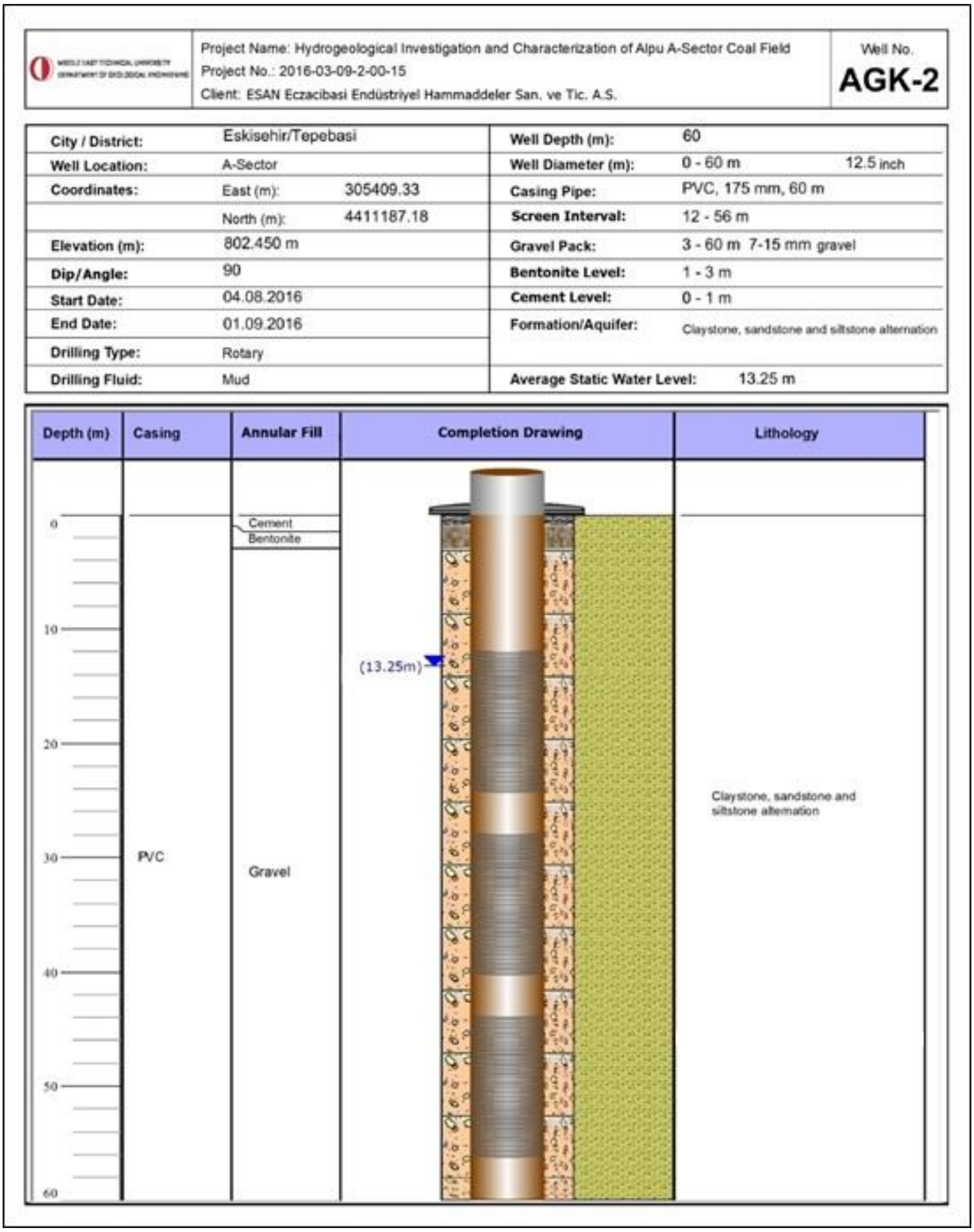

Figure A-4. Well log for AGK-2 observation well (Yazıcıgil et al., 2017).

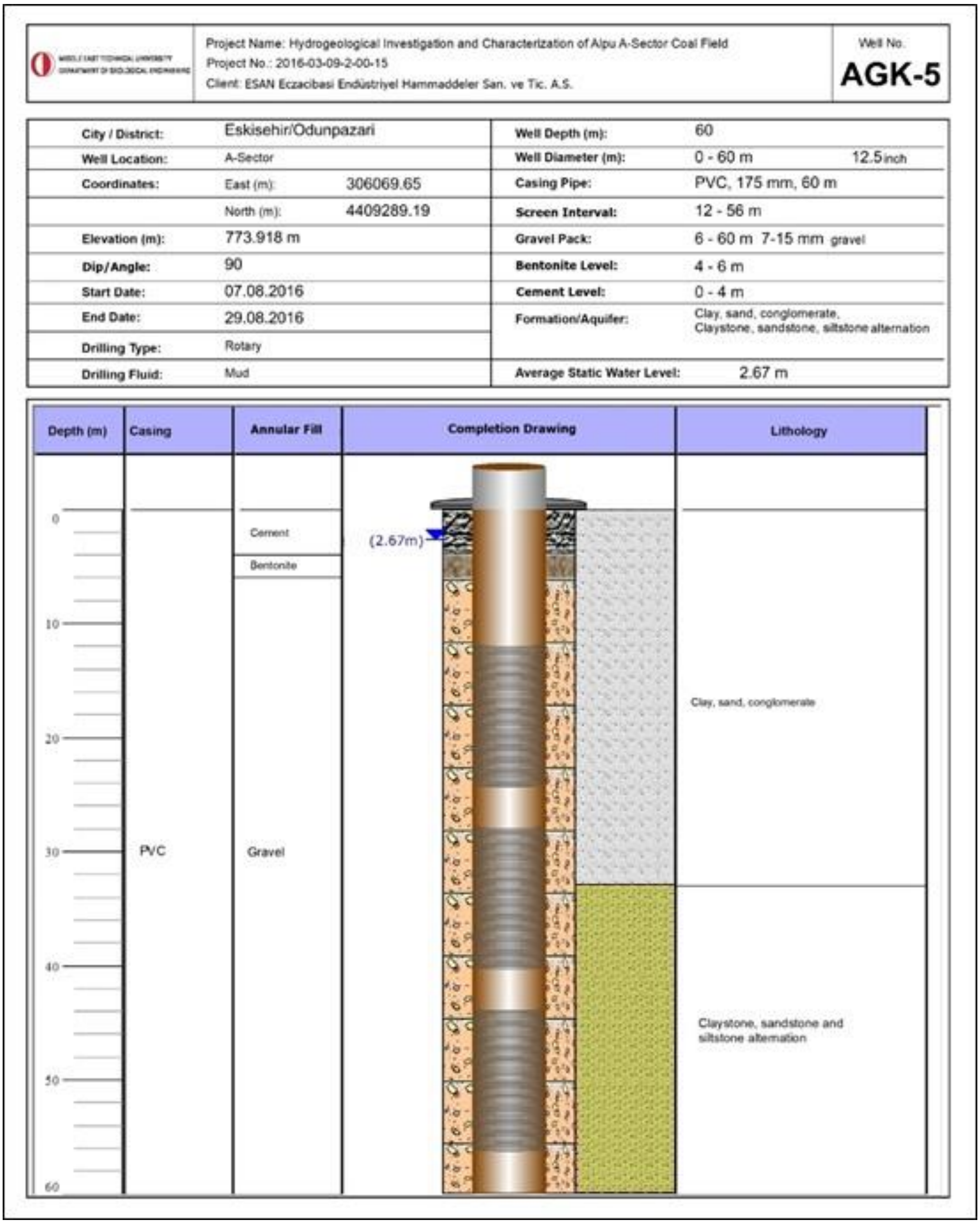

Figure A-5. Well log for AGK-5 observation well (Yazıcıgil et al., 2017).

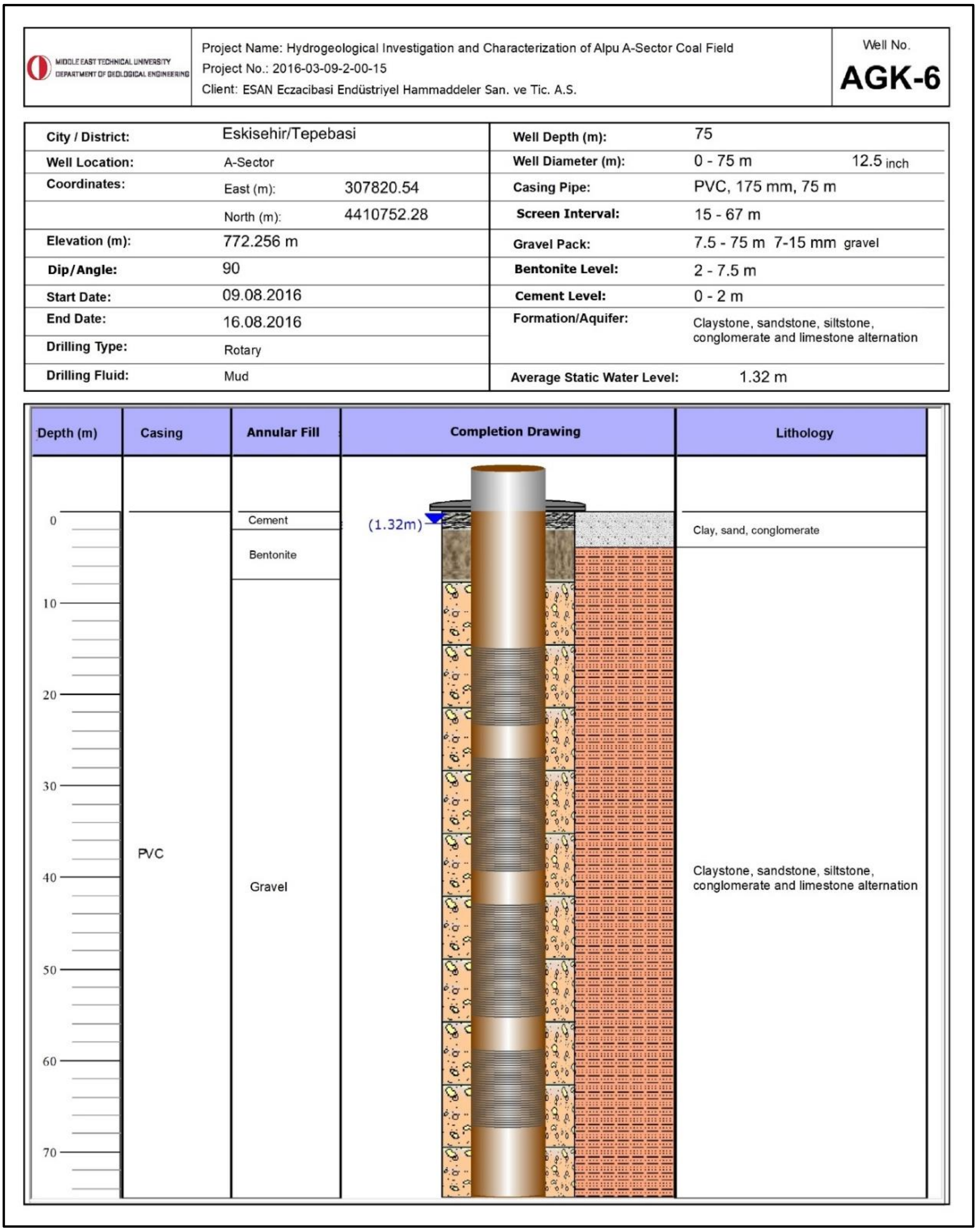

Figure A-6. Well log for AGK-6 observation well (Yazıcıgil et al., 2017).

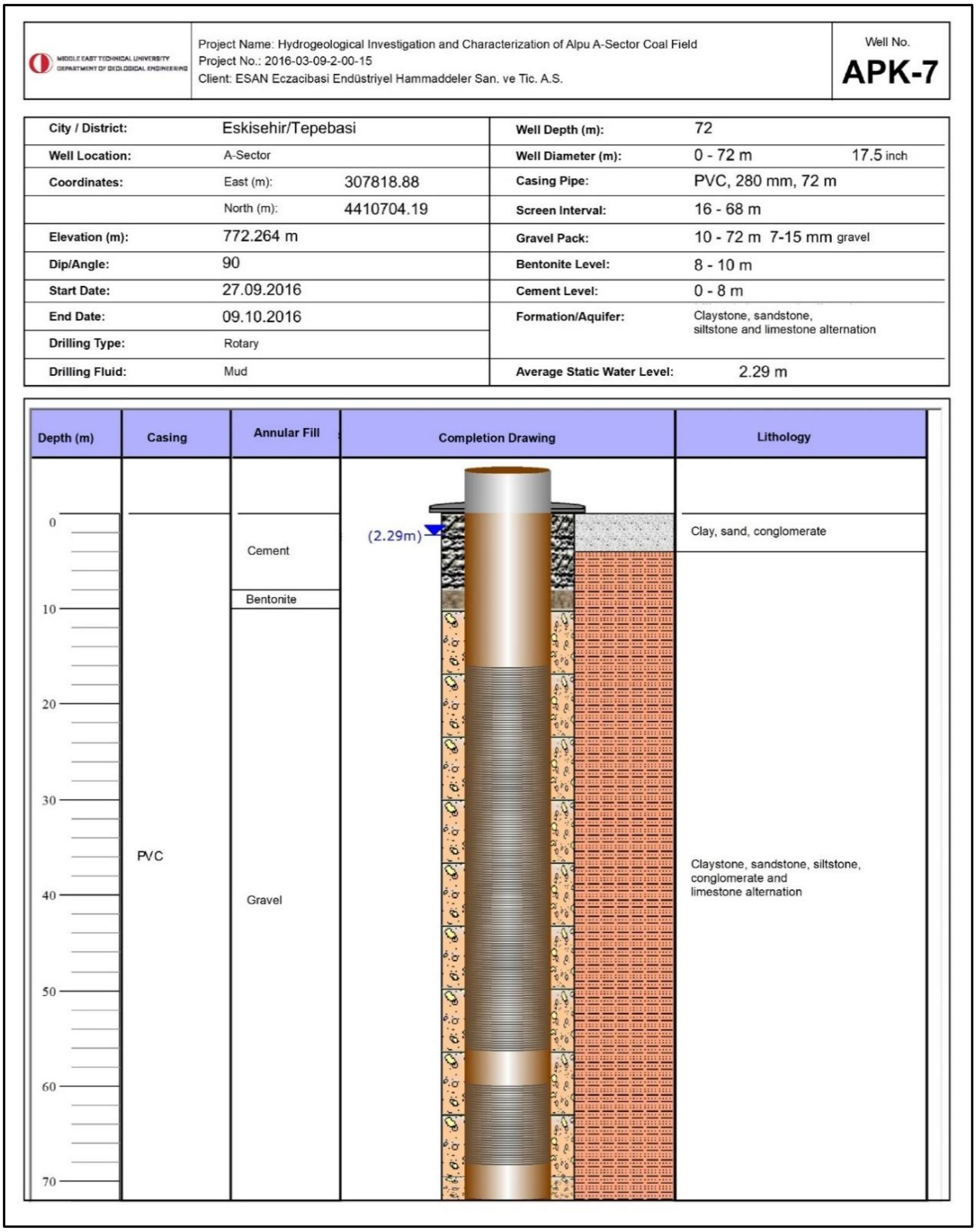

MIDDLE EAST TECHNICAL UNIVERSITY DEPARTMENT OF GEOLOGICAL ENGINEERING	Project Name: Hydrogeological Investigation and Characterization of Alpu A-Sector Coal Field Project No.: 2016-03-09-2-00-15 Client: ESAN Eczacibasi Endüstriyel Hammaddeler San. ve Tic. A.S.	Well No. **APK-7**

City / District:	Eskisehir/Tepebasi		**Well Depth (m):**	72
Well Location:	A-Sector		**Well Diameter (m):**	0 - 72 m 17.5 inch
Coordinates:	East (m):	307818.88	**Casing Pipe:**	PVC, 280 mm, 72 m
	North (m):	4410704.19	**Screen Interval:**	16 - 68 m
Elevation (m):	772.264 m		**Gravel Pack:**	10 - 72 m 7-15 mm gravel
Dip/Angle:	90		**Bentonite Level:**	8 - 10 m
Start Date:	27.09.2016		**Cement Level:**	0 - 8 m
End Date:	09.10.2016		**Formation/Aquifer:**	Claystone, sandstone, siltstone and limestone alternation
Drilling Type:	Rotary			
Drilling Fluid:	Mud		**Average Static Water Level:**	2.29 m

Figure A-7. The well log for APK-7 pumping well (Yazıcıgil et al., 2017).

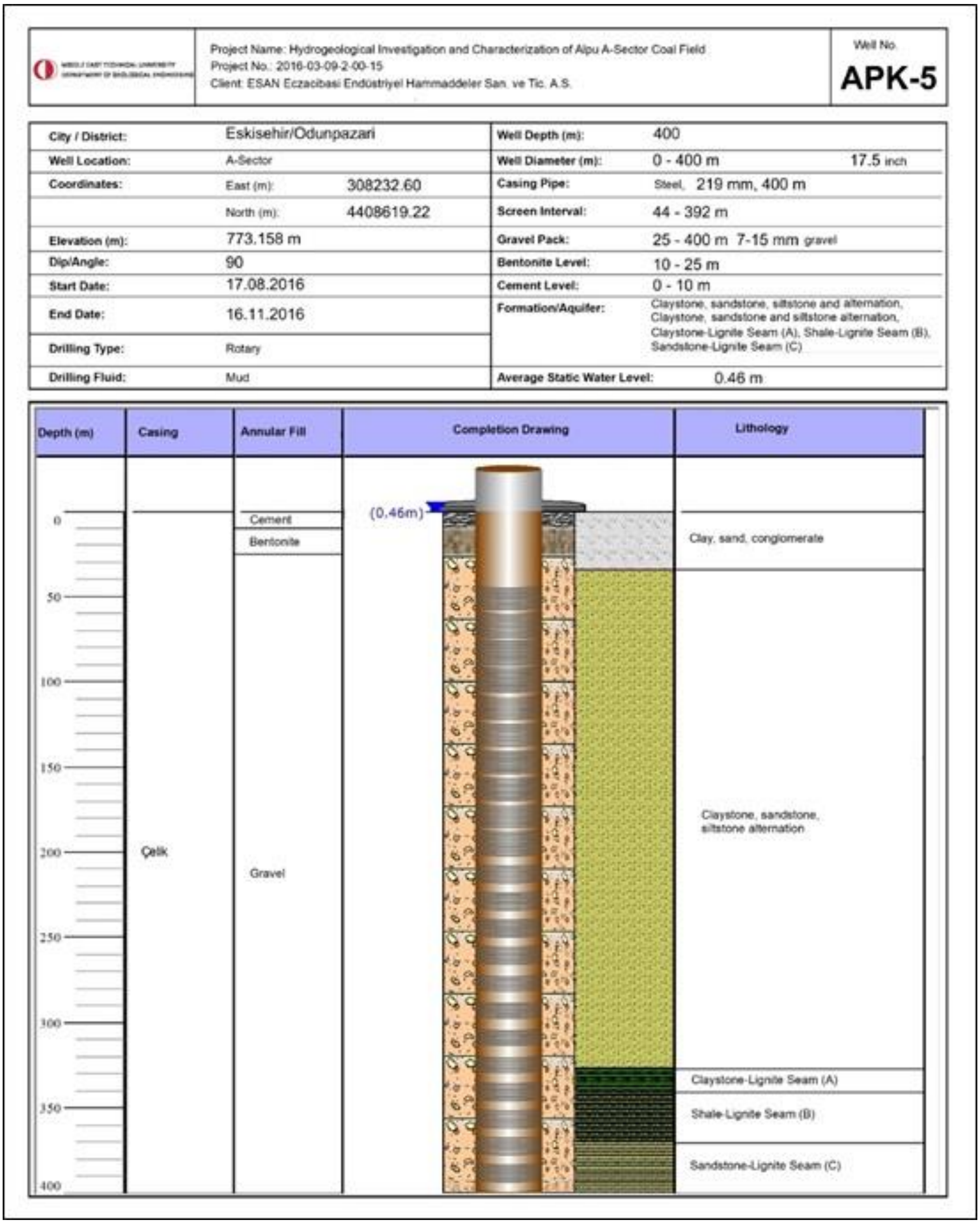

Figure A-8. The well log for APK-5 pumping well (Yazıcıgil et al., 2017).

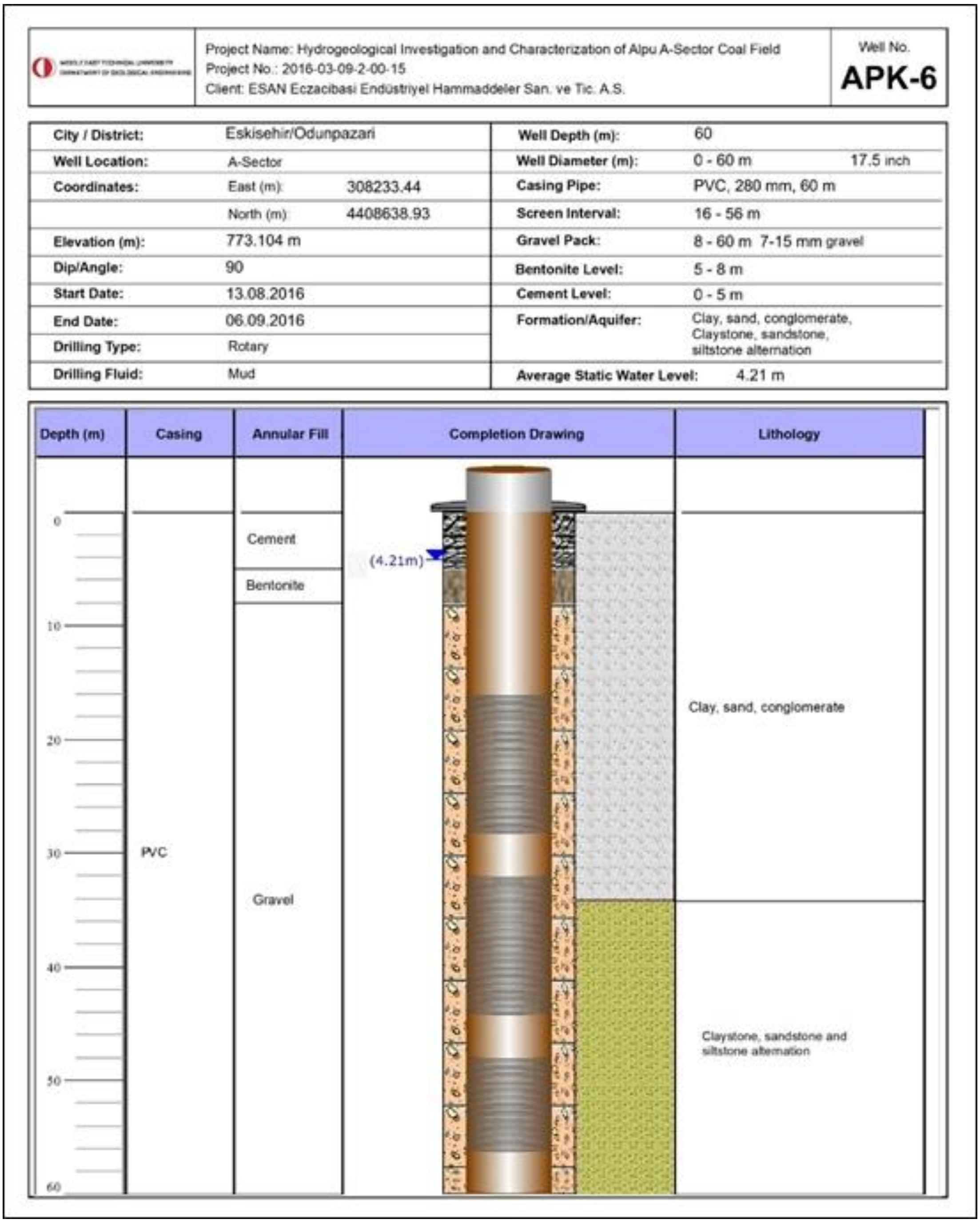

Figure A-9. The well log for APK-6 pumping well (Yazıcıgil et al., 2017).

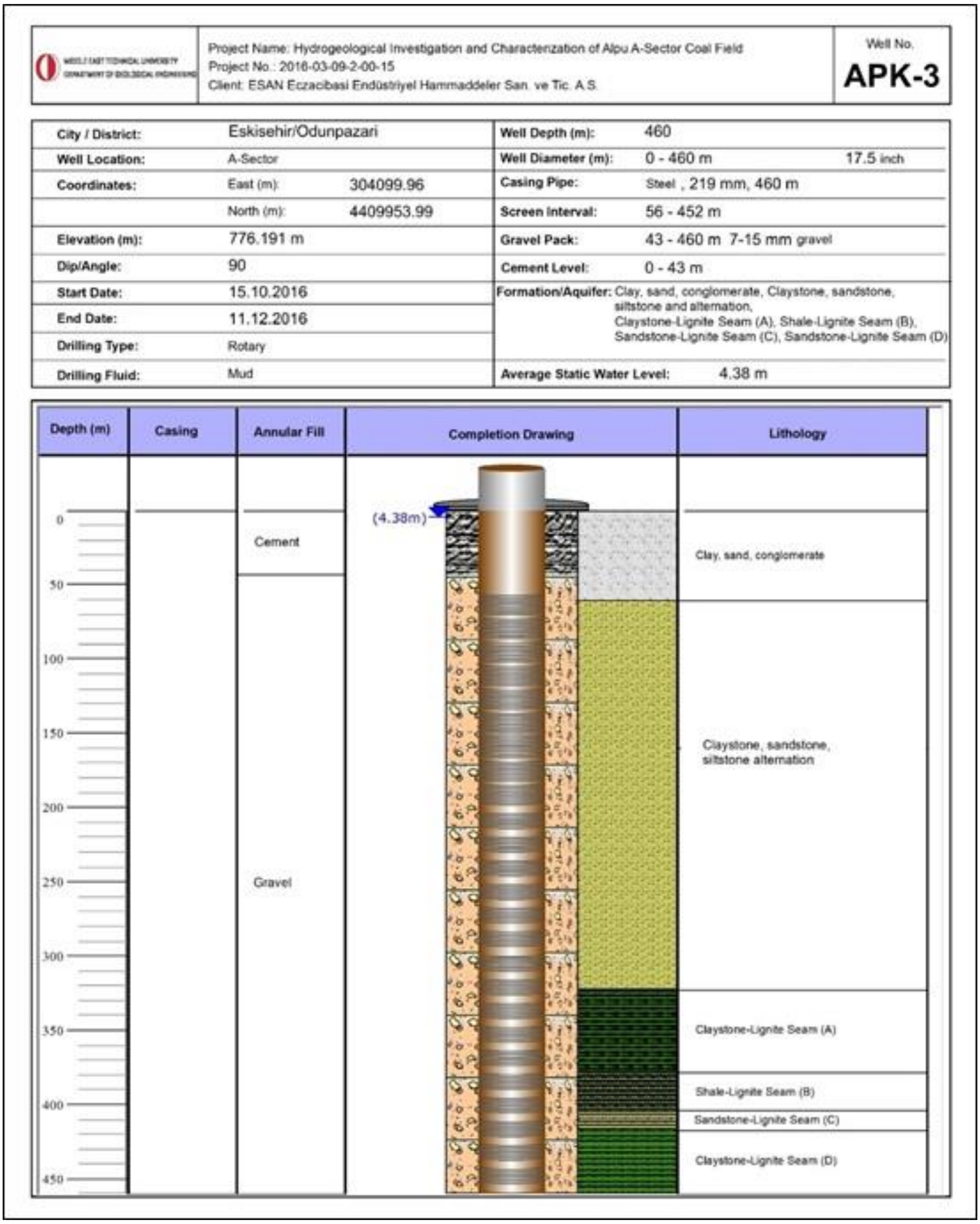

Figure A-10. The well log for APK-3 pumping well (Yazıcıgil et al., 2017).

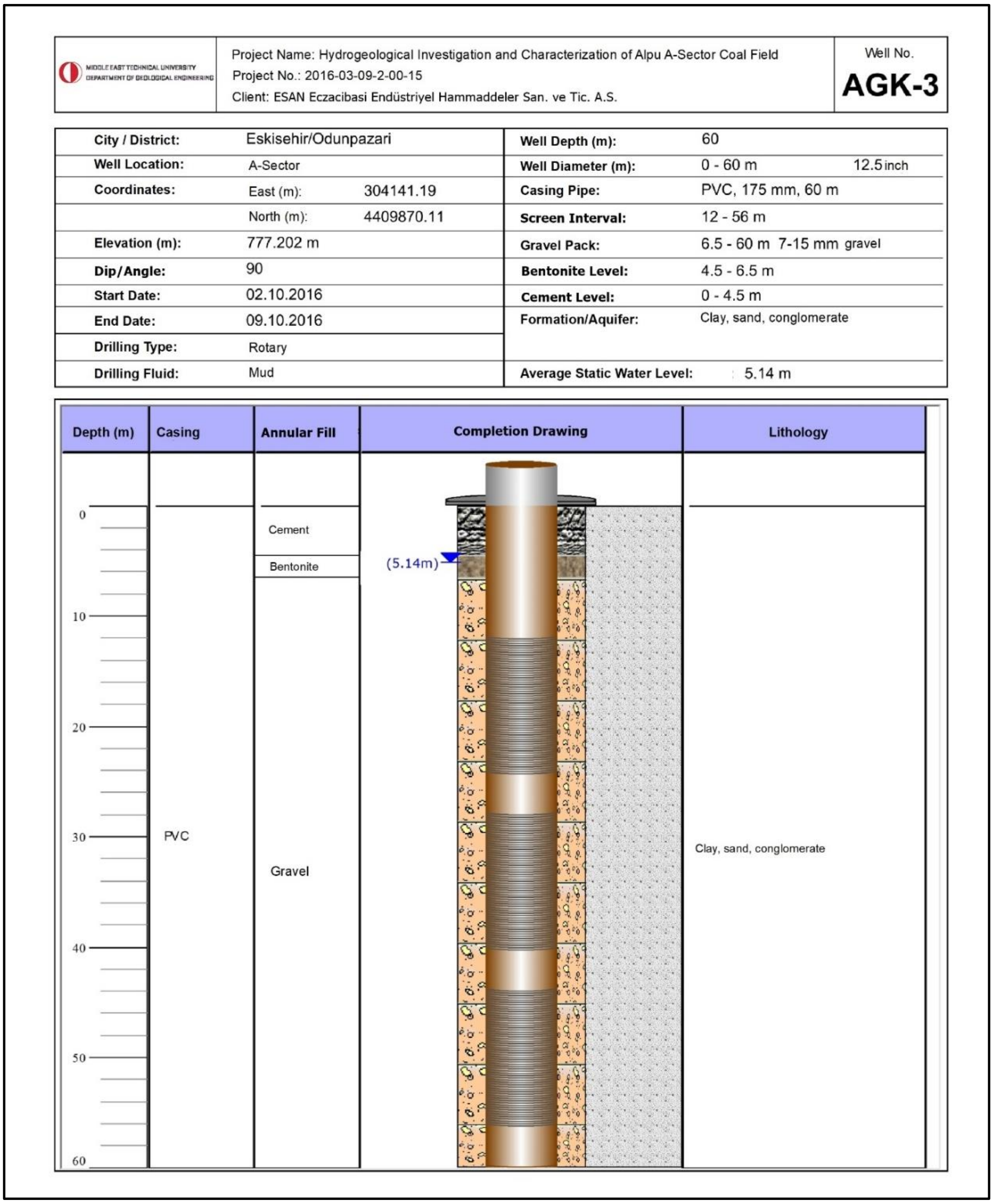

Figure A-11. Well log for AGK-3 observation well (Yazıcıgil et al., 2017).

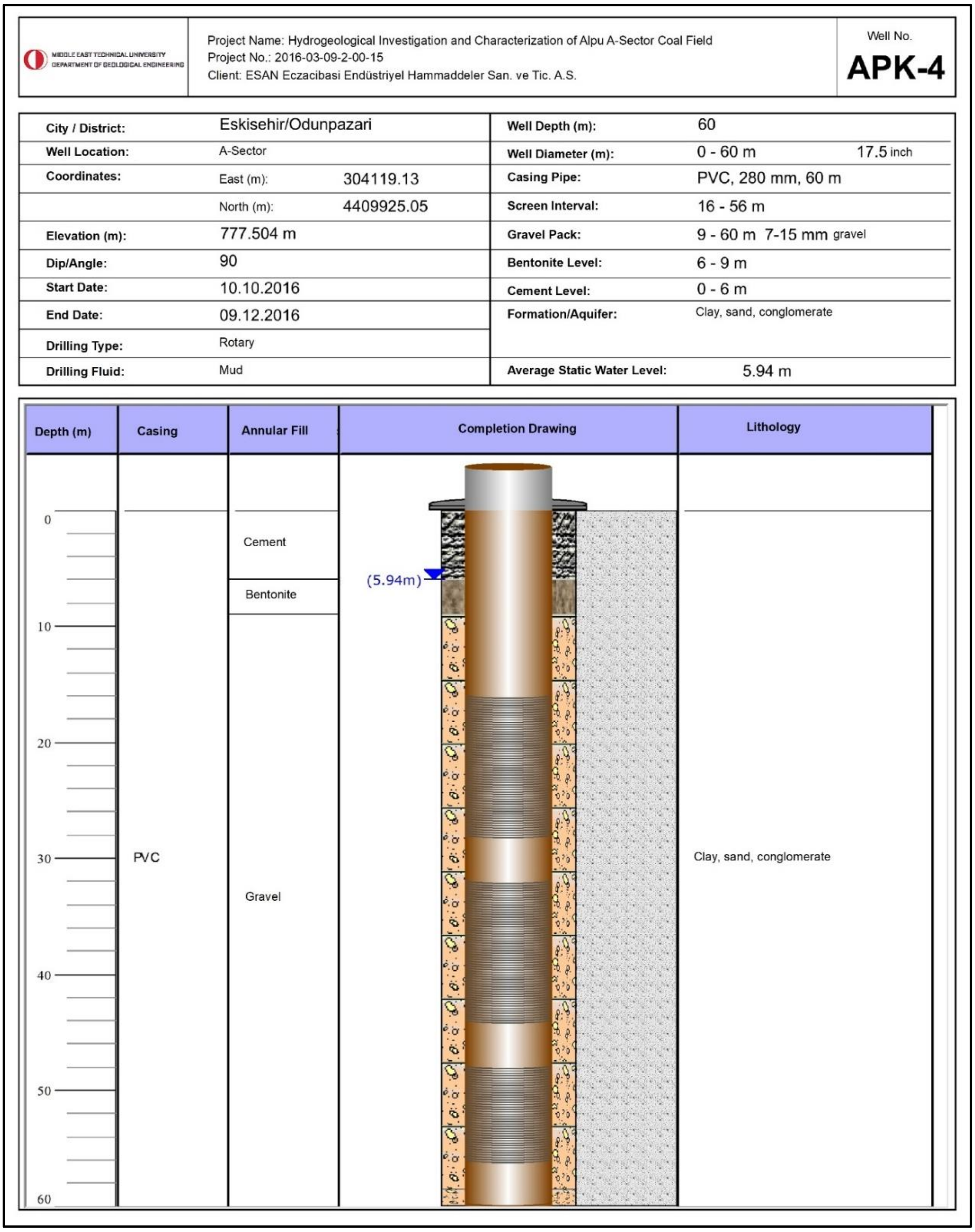

Figure A-12. The well log for APK-4 pumping well (Yazıcıgil et al., 2017).

MIDDLE EAST TECHNICAL UNIVERSITY DEPARTMENT OF GEOLOGICAL ENGINEERING	Project Name: Hydrogeological Investigation and Characterization of Alpu A-Sector Coal Field Project No.: 2016-03-09-2-00-15 Client: ESAN Eczacibasi Endüstriyel Hammaddeler San. ve Tic. A.S.	Well No. **AGK-4**

City / District:	Eskisehir/Odunpazari		**Well Depth (m):**	60	
Well Location:	A-Sector		**Well Diameter (m):**	0 - 60 m	12.5 inch
Coordinates:	East (m):	304132.30	**Casing Pipe:**	PVC, 175 mm, 60 m	
	North (m):	4409930.55	**Screen Interval:**	12 - 56 m	
Elevation (m):	777.369 m		**Gravel Pack:**	7 - 60 m 7-15 mm gravel	
Dip/Angle:	90		**Bentonite Level:**	5 - 7 m	
Start Date:	05.10.2016		**Cement Level:**	0 - 5 m	
End Date:	20.10.2016		**Formation/Aquifer:**	Clay, sand, conglomerate	
Drilling Type:	Rotary				
Drilling Fluid:	Mud		**Average Static Water Level:**	: 5.50 m	

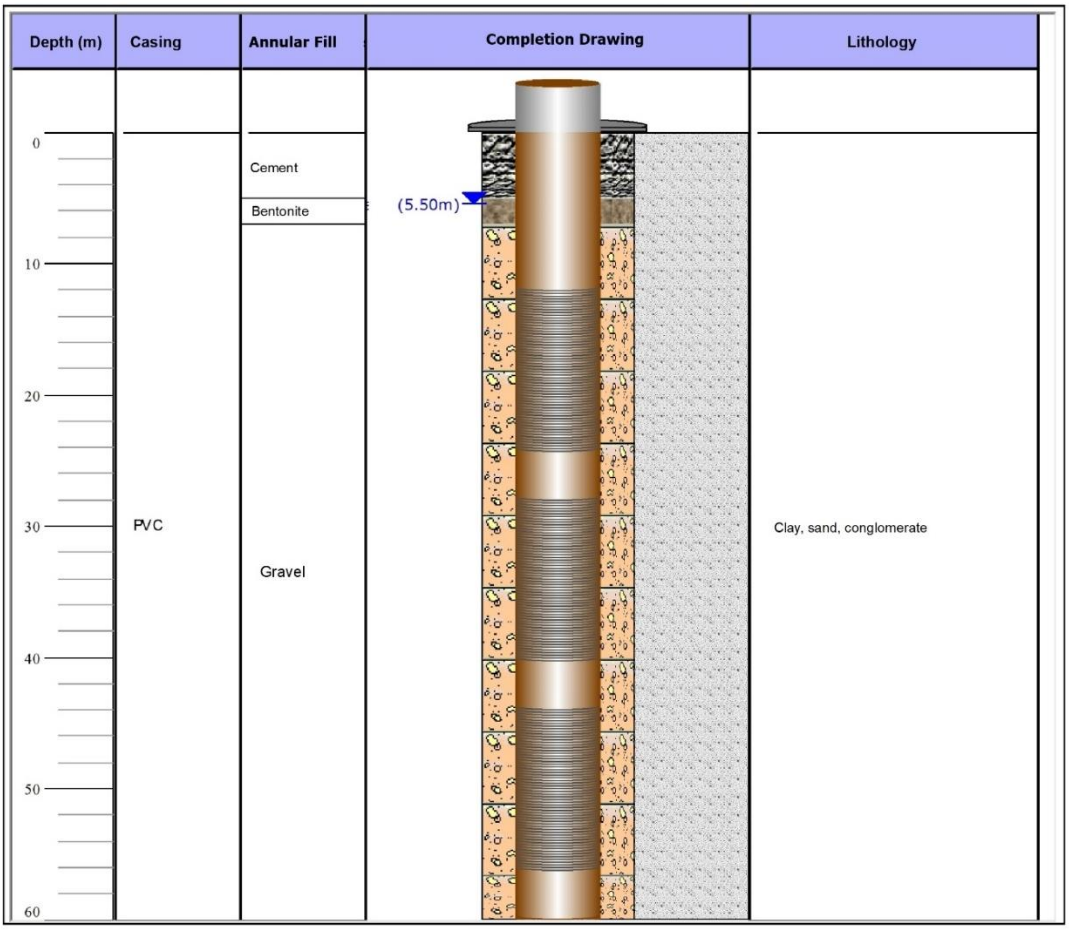

Figure A-13. Well log for AGK-4 observation well (Yazıcıgil et al., 2017).

APPENDIX-B

THE WELL LOGS SHOWING THE INSTALLATION DEPTHS OF VIBRATING WIRE PIEZOMETERS

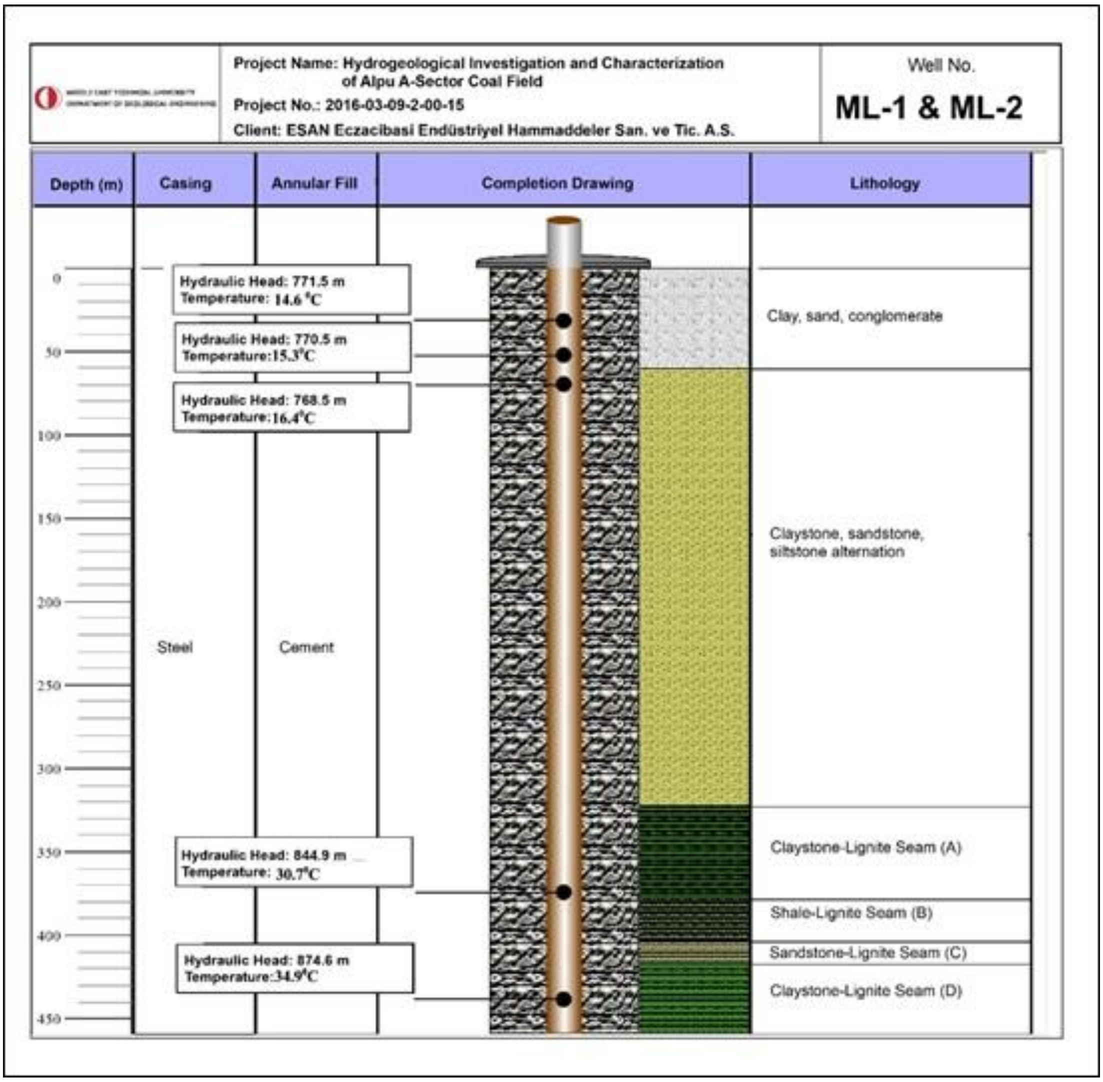

Figure B-1. Well log showing the installation depths of ML-1 and ML-2 vibrating wire piezometers (Yazıcıgil et al., 2017).

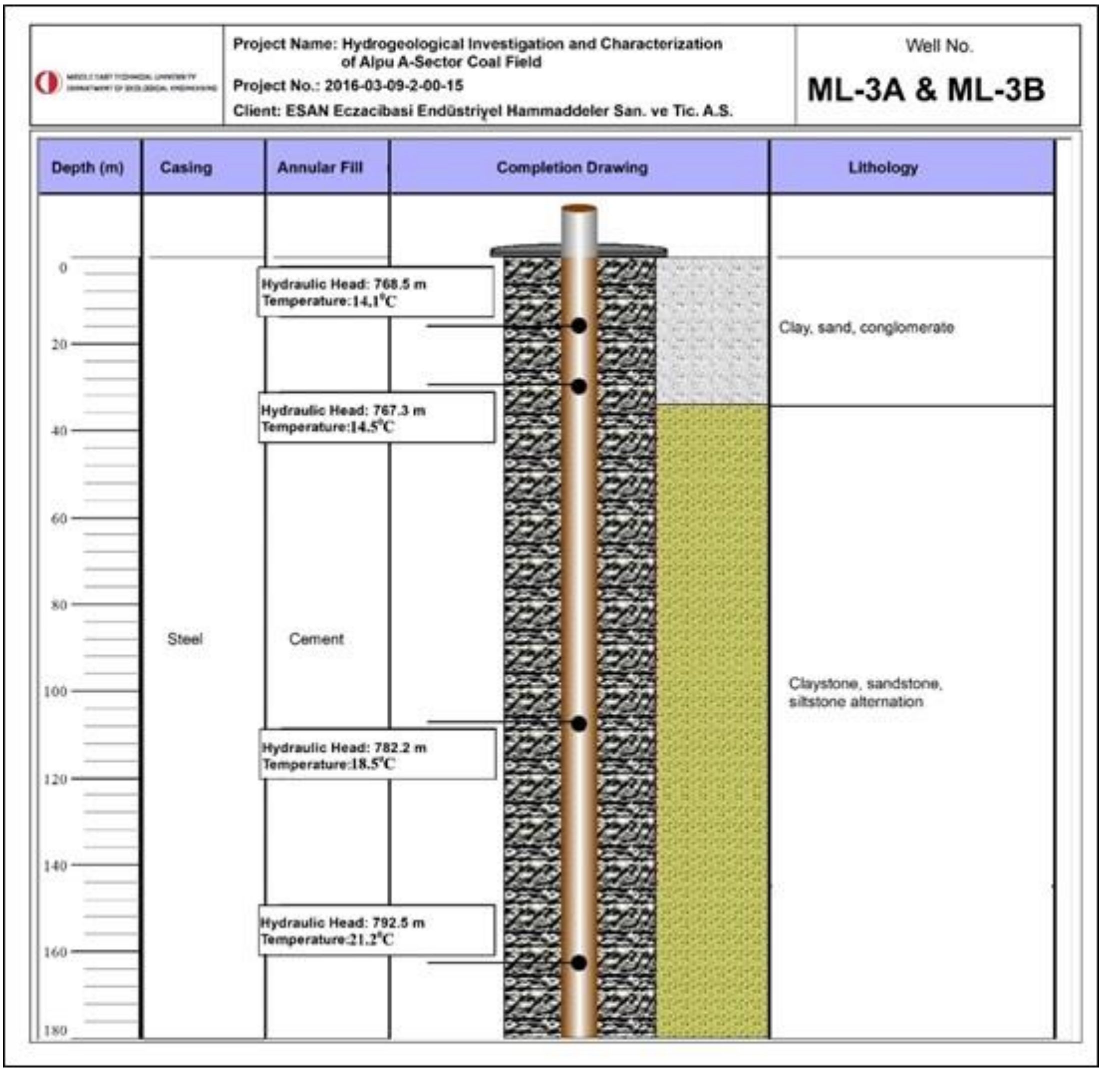

Figure B-2. Well log showing the installation depths of ML-3A and ML-3B vibrating wire piezometers (Yazıcıgil et al., 2017).

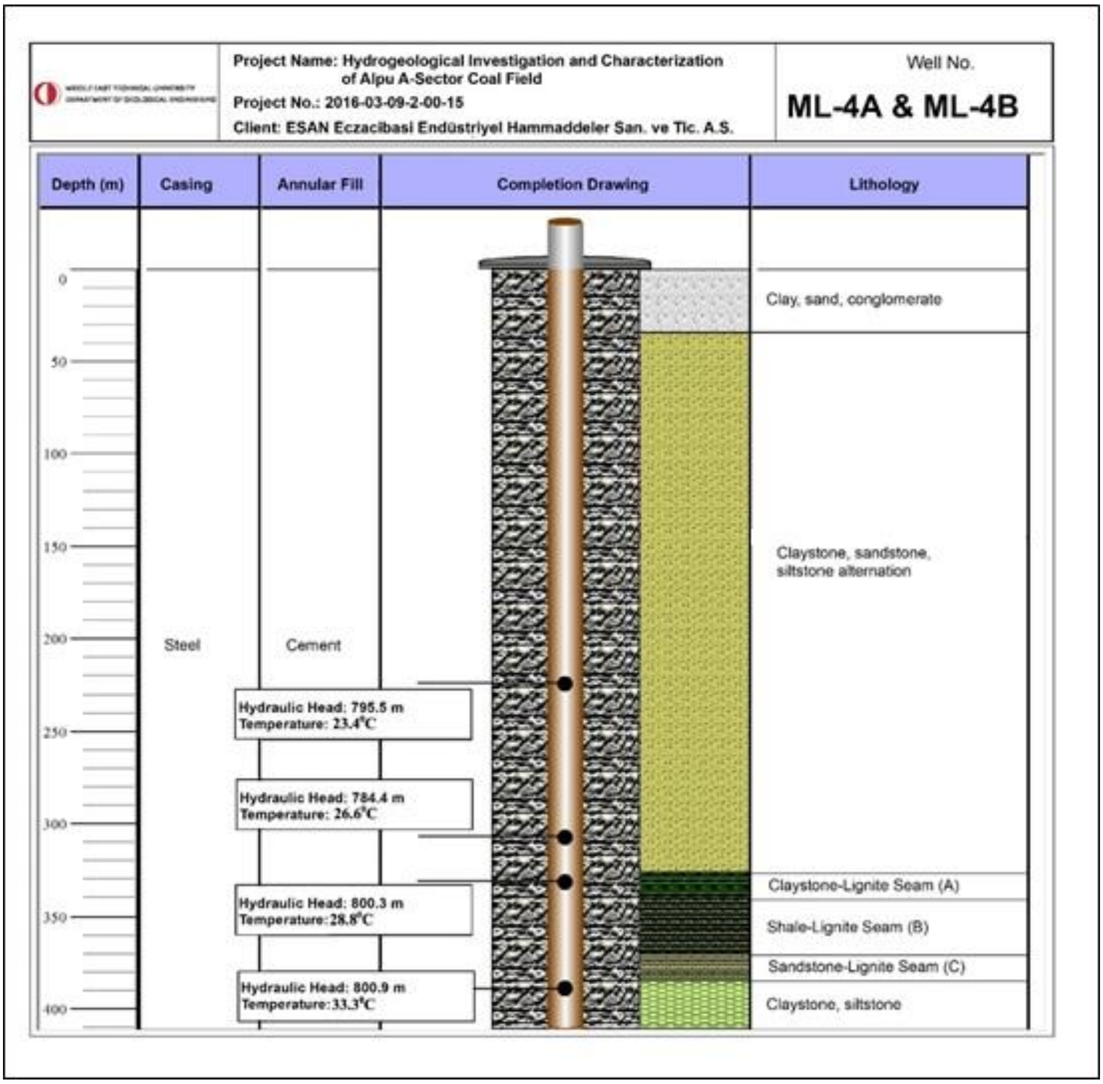

Figure B-3. Well log showing the installation depths of ML-4A and ML-4B vibrating wire piezometers (Yazıcıgil et al., 2017).